

**CHAPTER 12****Methods for Studying and Structure–Function Relationships of Non-Fibrillar Protein Assemblies in Alzheimer's Disease and Related Disorders****Farid Rahimi<sup>1</sup> and Gal Bitan<sup>2,\*</sup>**

<sup>1</sup>*Research School of Biology, Division of Biomedical Science and Biochemistry, College of Medicine, Biology, and Environment, The Australian National University, Canberra, ACT, Australia, and* <sup>2</sup>*Department of Neurology, David Geffen School of Medicine, Brain Research Institute, and Molecular Biology Institute, University of California at Los Angeles, USA*

**Abstract:** Several neurodegenerative diseases, including Alzheimer's, Parkinson's, Huntington's, and prion diseases, are characterized by intra- and/or extracellular deposition of fibrillar proteinaceous aggregates, and by extensive, neuron loss. Related non-neuropathic systemic diseases, *e.g.*, light-chain and senile systemic amyloidoses, and other organ-specific diseases, such as dialysis-related amyloidosis and type-2 diabetes, also are characterized by deposition of aggregated proteins. It is debated whether these hallmark lesions are causative. Substantial evidence suggests that the aggregates are the end state of protein misfolding whereas the actual culprits likely are transient, non-fibrillar assemblies preceding the aggregates. The non-fibrillar, oligomeric assemblies are believed to initiate pathogenesis, leading to synaptic dysfunction, neuron loss, and pathognomonic brain atrophy. It is hypothesized that non-fibrillar assemblies or fibril-derived fragments may promote anatomical progression of pathology, or even disease transmissibility, akin to misfolded prions.

Amyloid  $\beta$ -protein ( $A\beta$ ), which is believed to cause Alzheimer's disease, is considered an archetypal amyloidogenic protein. Intense studies have led to nominal, functional, and structural descriptions of oligomeric  $A\beta$  assemblies. However, the dynamic and metastable nature of  $A\beta$  oligomers renders their study difficult. Different results generated using different methodologies under different experimental settings further complicate this complex area of research and identification of the exact pathogenic assemblies *in vivo* seems daunting.

In this chapter we review structural, functional, and biological experiments used to produce and study non-fibrillar  $A\beta$  assemblies, and highlight similar studies of proteins involved in related diseases. We discuss challenges that contemporary researchers are facing and future research prospects in this demanding, yet highly important, field.

---

**\*Corresponding author Gal Bitan:** David Geffen School of Medicine, University of California at Los Angeles, Neuroscience Research Building 1, Room 451, 635 Charles E. Young Drive South, Los Angeles, CA 90095-7334, USA; Tel: 310-2062082; Fax: 310-2061700; E-mail: gbitan@mednet.ucla.edu

D.K. Lahiri (Ed)

All rights reserved-© 2014 Bentham Science Publishers

**Keywords:** Amyloid, neurodegeneration, Alzheimer's disease, amyloid  $\beta$ -protein, protein misfolding, non-fibrillar assemblies, oligomers, toxicity, prion

## INTRODUCTION

The “amyloid cascade hypothesis” [1], suggesting that amyloid  $\beta$ -protein ( $A\beta$ ) fibril formation and plaque deposition lead to neuronal dysfunction, dementia, and death in Alzheimer's disease (AD), had guided scientific research into discovery of etiologic and pathogenic mechanisms of AD. However, this hypothesis has been contentiously debated because: 1) fibrillar amyloid burden does not correlate well with neurological dysfunction [2], 2) cognitive impairment in transgenic murine models of AD is observed before and/or independently of amyloid plaque formation [3], 3) plaque-independent pathology can be explained by the neurotoxicity of soluble  $A\beta$  assembly intermediates, 4) oligomer-induced memory dysfunction occurs before neuronal death, and 5) brain, plasma, and cerebrospinal fluid (CSF) concentrations of soluble  $A\beta$  oligomers correlate with neurodegeneration better than those of fibrils [4]. These observations have led to a burgeoning yet encompassing alternative paradigm hypothesizing that soluble non-fibrillar protein assemblies, rather than mature fibrillar deposits, act as proximate neurotoxins that cause synaptic dysfunction, neuron loss, dementia, and death [4-11]. This new hypothesis has been supported by discovery of toxic non-fibrillar protein assemblies involved in other protein-misfolding diseases, such as, Parkinson's disease (PD), Huntington's disease (HD), transmissible spongiform encephalopathies (TSEs), amyotrophic lateral sclerosis, polyglutamine diseases, type-2 diabetes mellitus (T2D), and systemic amyloidoses [7, 12-15].

Diversity and sometimes inaccuracy in nominal definitions, and in structural/functional descriptions of soluble non-fibrillar  $A\beta$  assemblies, along with different methodologies to generate and study these assemblies, are confounding factors in this already vast and complex research area. Various forms of soluble non-fibrillar  $A\beta$  assemblies (reviewed in [10, 16-18]) including monomeric  $A\beta$  conformers [19], secreted cell- and brain-derived low-order oligomers [20-25],  $A\beta$ -derived diffusible ligands (ADDLs) [26, 27], protofibrils (PF) [28-30],  $A\beta^{*56}$  [31], paranuclei [32-34], amylospheroids [35], annular assemblies [36], amyloid pores [18, 36, 37], toxic fibrillar oligomers [38], and

$\beta$ amyloid balls [39] have been described Protein Assemblies. However, despite a global concerted scientific effort, the relationships amongst these A $\beta$ -derived assemblies and their relevance to AD pathogenesis are unclear and the fundamental quest for a unanimous pathogenic “equivalent” active in AD-afflicted brain is ongoing [9].

We begin our discussion in the first step of studying non-fibrillar A $\beta$  assemblies—protein preparation.

### SOURCES AND METHODS OF A $\beta$ PREPARATION

The low physiological concentration and the difficulty of procuring highly pure and homogeneous tissue-derived A $\beta$  have precluded its routine use in experimental studies *in vitro*. Therefore, synthetic A $\beta$  preparations have emerged as alternatives. Synthetic A $\beta$  is produced either by standard solid-phase peptide synthesis (SPPS) [40, 41] or by recombinant DNA technology [42-45].

The A $\beta$  sequence is recognized as a “difficult” target for SPPS owing to its high hydrophobicity and innate propensity to aggregate [46-48]. To overcome these issues, various deprotecting agents [46], novel solvent systems for coupling [47], solid-support modifications [49], or microwave-assisted SPPS [50] have been used to augment synthetic yield and improve purity of crude A $\beta$  peptides. Application of an *O*-*N* acyl migration reaction, also called “*O*-acyl isopeptide” chemistry was proposed as an efficient alternative SPPS route for generating A $\beta$  with increased solubility and purity [51, 52].

Similarly, tailored recombinant or semisynthetic expression systems have been used to produce A $\beta$  in high yields. A strategy to increase solubility and facilitate purification is co-expression of A $\beta$  with A $\beta$ -specific affibodies [53] or as fusions with sequences affording high solubility, followed by cleavage of the fusion protein and purification by high-performance liquid chromatography (HPLC) [42-45, 54-56]. A semisynthetic procedure for generating full-length A $\beta$  has been reported, producing 8–10 mg of pure A $\beta$ (1–40) per liter of bacterial culture [57].

Because self-association of A $\beta$  is believed to be central in the pathogenesis of AD, extensive research has been dedicated to developing methodologies to characterize A $\beta$  assemblies structurally and biologically [58]. Multiple studies

have shown that many of the neurotoxic effects of A $\beta$  assemblies can be recapitulated by synthetic A $\beta$  *in vitro* or *in vivo* [59]. However, differences in peptide quality, presence of trace contaminants in A $\beta$  preparations from different sources, and compositional variation of A $\beta$  preparations, even from the same source, have been serious problems leading to irreproducible or discrepant reports and study outcomes [60-62]. For example, under identical conditions, an A $\beta$  oligomer-specific monoclonal antibody was shown to react only with oligomers derived from recombinant A $\beta$  but not those derived from chemically synthesized A $\beta$  [63]. In our hands, Photo-Induced Cross-linking of Unmodified Proteins (PICUP) using A $\beta$  obtained from different sources, but prepared identically, yielded distinct results (Fig. 1).

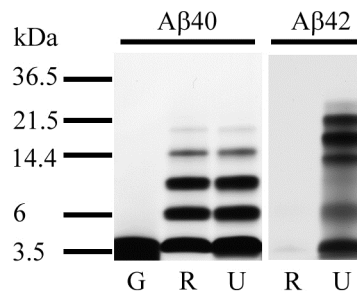


**Figure 1: Comparison of photo-cross-linking using A $\beta$  peptides from different sources.** Synthetic A $\beta$  from Global Peptide (G) and the UCLA Biopolymers Laboratory (U), and recombinant A $\beta$  from rPeptide (R) were prepared in 10 mM sodium phosphate, pH 7.4, at 2 mg/mL nominal concentration and filtered through a 10-kDa molecular-weight cut-off filter [106]. Each filtered peptide was cross-linked using PICUP [98]. The resulting cross-linked oligomers were subjected to SDS-PAGE and silver-staining. The data suggest that A $\beta$ 40 from Global peptide contained contaminants that prevented cross-linking and that A $\beta$ 42 from rPeptide aggregated during the filtration step and was hardly detectable.

Neither SPPS nor recombinant methods can produce 100% pure A $\beta$ . Failure sequences, oxidation of Met<sup>35</sup>, and racemization may occur during various SPPS steps [58]. Similarly, Met<sup>35</sup> oxidation may occur in bacterial inclusion bodies [57]. In recombinant preparations where a fusion protein is enzymatically cleaved to release A $\beta$ , it is important to verify that the cleavage product is not contaminated with the uncleaved fusion protein, the cleaving enzyme, or adventitious proteolytic fragments [58]. Practically, it is important that the researcher verifies chemical purity of the preparation and ensures removal of residual components which could complicate solvation and stock preparation,

potentially alter the biophysical and biological characteristics of the peptide, and render concentration measurements error-prone [58].

## METHODS USED TO STUDY NON-FIBRILLAR A $\beta$ ASSEMBLIES

Important biological functions of oligomeric A $\beta$  assemblies have spurred extensive efforts to characterize them structurally. The non-crystalline nature of the oligomers and their slow tumbling time in aqueous solutions preclude high-resolution structural determination by X-ray crystallography and solution-state NMR [64], respectively. Moreover, the metastable nature of A $\beta$  oligomers and their existence in rapidly changing mixtures have made their structural characterization particularly difficult [65, 66]. To address these issues, multiple low-resolution methods have been used to assess various structural features of non-fibrillar A $\beta$  assemblies. Here, we outline some of the key methods used to provide structural and biophysical information on non-fibrillar A $\beta$  assemblies.

### Atomic-Resolution Techniques

#### *NMR Spectroscopy*

Solution-state NMR is a powerful high-resolution technique for determining peptide and protein structure in solution [67]. Typically, the structure is calculated based on distances and angles obtained through measurements of nuclear Overhauser effect and spin–spin scalar coupling interactions as constraints for computer-generated models. As mentioned above, peak broadening due to slow tumbling times [64] currently precludes solving structures of A $\beta$  assemblies using solution-state NMR. However, multiple NMR studies have assessed structural properties of A $\beta$  monomers. For instance, studies by Lee *et al.* introduced the concept of “plaque competence”, which defines the propensity of near-physiological concentrations of soluble A $\beta$  to deposit onto authentic amyloid plaques *in vitro* [68]. The plaque competence assay identified a central 26-residue fragment (Tyr<sup>10</sup>–Met<sup>35</sup>) which was deemed necessary to mimic plaque-deposition characteristics of the full-length A $\beta$  [68]. Preliminary NMR conformational analyses showed that this 26-residue fragment had a different conformation from a plaque-incompetent fragment (Asp<sup>1</sup>–Lys<sup>28</sup>) [68]. Further NMR studies also

confirmed that the central 26 residues of A $\beta$  were sufficient to mimic amyloidogenic properties of A $\beta$ 40 and A $\beta$ 42 [69]. It was reported that the central hydrophobic cluster of full-length A $\beta$ , and A $\beta$ (10–35), both adopted well-defined, albeit irregular, conformations in solution, whereas the C- and N-terminal flanking regions of the full-length A $\beta$  were partially disordered [69].

NMR studies also have highlighted differences between A $\beta$ 40 and A $\beta$ 42. Solution-phase NMR studies of non-oxidized [70] or Met-oxidized [71, 72] A $\beta$ 40 and A $\beta$ 42 showed that the C-terminus of A $\beta$ 42 is more rigid compared to that of A $\beta$ 40, likely due to the extended hydrophobic C-terminus of A $\beta$ 42. Similarly, a study combining molecular dynamics and NMR experiments, showed that the C-terminus of A $\beta$ 42 is more structured than that of A $\beta$ 40 [73]. NMR studies also revealed that common C-terminal peptide segments within A $\beta$ 40 and A $\beta$ 42 have distinct structures, which may be relevant to the strong disease association of elevated A $\beta$ 42 production [74]. Various types of NMR applications to studying of oligomeric assemblies of amyloid proteins have been reviewed recently by Bemporad *et al.* [75].

### ***X-Ray Crystallography***

X-ray crystallography examines atomic structures of crystals by X-ray diffraction techniques (reviewed in [76]). The signal is intensified by the coherent alignment and repetitive lattice of crystal structures. The wavelength of radiation used in X-ray crystallography is usually  $\sim 1.5$  Å, about the length of a C–C bond. Use of X-rays with this wavelength theoretically allows resolution of individual atoms. Sawaya *et al.* reported that 33 peptide segments derived from 14 different amyloidogenic proteins formed amyloid-like fibrils, microcrystals, or both [77] and used X-ray crystallography to examine the atomic organization of molecules within microcrystals of these peptides. Microcrystals of three A $\beta$  segments were resolved, Gly<sup>37</sup>–Ala<sup>42</sup>, Met<sup>35</sup>–Val<sup>40</sup>, and Val<sup>36</sup>–Ala<sup>42</sup>. The authors suggested that the structural organization of these peptides within the crystals is similar to those of A $\beta$  fibrils and concluded that the fundamental unit of amyloid-like fibrils is a steric zipper arrangement formed by two tightly interdigitated  $\beta$ -sheets [77].

### ***Hydrogen–Deuterium Exchange***

Hydrogen–deuterium exchange is a powerful technique for probing protein structure and dynamics. The method involves studying of exchange rates of labile protons in proteins with deuterons from the solvent, typically D<sub>2</sub>O. Labile protons are those bonded to nitrogen, sulfur, or oxygen. These protons can exchange with solvent hydrogen or deuterium cations. Labile protons that are solvent-exposed and are not involved in hydrogen bonding exchange rapidly, whereas buried or hydrogen-bonded protons exchange at substantially slower rates. This makes hydrogen–deuterium exchange sensitive to structural rearrangements occurring during protein aggregation. Thus, amide protons buried in the core of oligomeric and high-order assemblies or hydrogen-bonded in helices and sheets do not exchange readily with solvent deuterons. The exchange rate is detected using NMR and/or mass spectrometry [67]. For study of rapidly changing assemblies, mass spectrometric detection of exchange may be advantageous because NMR requires longer times (hours) to record the spectra, making the study of short-lived oligomers difficult. In addition, NMR requires prior assignment of protons and generally is limited to proteins smaller than 25 kDa. An additional advantage of mass spectrometric detection of exchange is requirement of substantially smaller amounts of proteins. However, assignment of specific exchanging protons using mass spectrometry requires tandem mass spectrometry and can be a daunting task, whereas for a previously assigned NMR spectrum, identification of exchanging protons is straightforward. Hydrogen–deuterium exchange coupled with mass spectrometry was used to map structural differences in A $\beta$  PF and fibrils [78].

### **Determination of Oligomer Size Distribution**

#### ***Sodium Dodecyl Sulfate–Polyacrylamide Gel Electrophoresis (SDS-PAGE)***

SDS-PAGE is a routine and inexpensive method enabling separation of proteins based on their electrophoretic mobility, which is affected by a combination of primary, secondary, tertiary, and quaternary structures of proteins. In this method, protein mixtures are electrophoresed after treatment with SDS. SDS binds proteins *via* its hydrophobic dodecyl tail, leaving its sulfate group solvent-exposed, thus creating a negatively charged envelope that “coats” protein molecules [79]. SDS binds different polypeptides at an approximately constant

mass ratio—1.4 g SDS per gram of polypeptide (reviewed in [67]). In most cases, SDS binding denatures secondary and non-disulfide-linked tertiary structures, negatively charging proteins approximately uniformly and proportionally to their mass. Under these conditions, electrophoretic migration of proteins through the gel matrix is governed directly by the molecular mass of the protein. Without SDS, different proteins of the same mass may electrophorese distinctly due to differences in overall charge (different isoelectric points) and folding.

It has been shown that at an appropriate protein–SDS molar ratio, SDS readily induces aggregation of diverse proteins at a pH two units below their respective isoelectric points (pI) with no aggregation at a pH two units above pI [80]. Electrostatic interactions were observed to play a leading role in the induction of amyloid under these conditions [80]. Importantly, the effect of SDS on all proteins is not equivalent [81]. Different proteins, different conformations of the same protein [82], or truncated versions of certain proteins [83] may not bind stoichiometric amounts of SDS. In many cases, SDS can induce or stabilize secondary and quaternary structures rather than denaturing them [82, 84, 85]. SDS may cause dissociation of some protein assemblies or conversely induce oligomerization and aggregation [85-88]. A $\beta$ 42-derived “globulomers”, for example, are oligomeric assemblies produced by incubating A $\beta$ 42 with 0.2% SDS [89]. Therefore, resolution of apparently monomeric or low-molecular-weight (LMW) oligomeric components in a protein mixture does not necessarily indicate existence of such components under native conditions, *i.e.*, without SDS. A $\beta$  is an amphipathic protein known to form SDS-stable oligomers [90]. Indeed, SDS-induced assembly of A $\beta$  into insoluble aggregates has been capitalized on to purify A $\beta$  from brain homogenates [91]. When treated with SDS, A $\beta$  assembles rapidly into high-molecular-mass aggregates [63]. Furthermore, circular dichroism (CD) spectroscopy, thioflavin T fluorescence, nuclear magnetic resonance, and Fourier-transform infrared (FTIR) spectroscopy experiments have shown that A $\beta$ 40 undergoes structural transitions when treated with SDS or lithium dodecyl sulfate [92]. In this study, in solutions without SDS, A $\beta$ 40 yielded CD signals consistent with a random coil or a “statistical coil” structure [93], whereas at SDS concentration of ~4 mM (53-fold excess detergent to protein),

this signal disappeared [92]. At 67-fold excess SDS, CD showed a typical  $\beta$ -sheet spectrum. At SDS concentrations of  $>10$  mM (133-fold excess detergent), A $\beta$ 40 secondary structure was mainly  $\alpha$ -helical [92]. Thus, the concept of “SDS stability” [94] in its essence is questionable in view of the fact that SDS has been used as amyloid [80, 92] or as  $\alpha$ -helix inducer [92]. During electrophoresis of A $\beta$ 40, aggregates dissociate completely and only a monomer is observed following detection, whereas electrophoresis of A $\beta$ 42 yields apparent trimeric and tetrameric components [32]. Essentially identical monomer–trimer–tetramer distributions are observed when different preparations of A $\beta$ 42, including “monomeric”, oligomeric, and fibrillar A $\beta$ 42 are analyzed by SDS-PAGE [95]. In a urea-containing SDS-PAGE system, A $\beta$  and truncated versions thereof do not obey the law of mass–mobility relationship, likely because A $\beta$ –SDS binding is proportional to the sum of the hydrophobicity indices, rather than the number, of constituent amino acids [83]. Thus, despite its wide use, SDS-PAGE is not a reliable method for characterization and size determination of non-covalently associated A $\beta$  assemblies (see also [96] for a discussion of other analytical challenges in studying amyloid proteins).

### ***Photo-Induced Cross-Linking of Unmodified Proteins (PICUP)***

PICUP is a method originally developed to study stable protein homo- and hetero-oligomers [97]. PICUP was used by us and others to study oligomer size distribution of A $\beta$  [66] and a variety of other proteins, including amyloidogenic proteins [98]. PICUP generates covalent bonds between closely interacting polypeptide chains within  $\leq 1$  s exposure to visible light without *pre facto* chemical modifications of the native sequence and without using spacers. The cross-linking is induced by rapid photolysis of a tris-bipyridyl Ru(II) complex in the presence of an electron acceptor. Illumination causes generation of a Ru(III) ion, which subsequently abstracts an electron from, and produces a carbon radical within, the polypeptide. The radical reacts rapidly with adjacent susceptible groups and forms covalent bonds. Therefore, PICUP stabilizes oligomer populations by covalent cross-linking, and “freezes” molecular interactions that exist before cross-linking. The mechanism, protocol, and limitations of PICUP were discussed in detail elsewhere [97-100]. Recently, a continuous-flow reactor,

an “oligomerator”, has been used to produce large-scale PICUP-stabilized amyloid oligomer mixtures [101]; however, purification of large quantities of single-order oligomers stabilized by PICUP still is a laborious and costly process.

### ***Size-Exclusion Chromatography (SEC)***

SEC (gel-permeation or gel-filtration chromatography) fractionates solutes based on their Stokes (hydrodynamic) radii, *i.e.*, hydrodynamic volumes (which can be correlated with molar mass) [102]. SEC is used to determine molar mass averages and molar mass distributions of solutes. SEC separation is achieved using a stationary phase comprising a porous matrix. When solutes of different sizes pass through a SEC column packed with porous material, larger molecules spend less time interacting with the solid phase and elute faster, whereas smaller molecules diffuse into the pores and therefore spend more time interacting with the solid phase and elute later. SEC affords an SDS-independent separation mechanism and covers a molecular mass range of  $\sim 10^3$ – $10^6$  Da. However, SEC provides lower resolution than SDS-PAGE and estimations of polypeptide molecular masses may be inaccurate because the elution profiles are sensitive to protein conformation. SEC analysis of A $\beta$  assemblies does not resolve LMW assemblies but can distinguish between PF and small oligomers [90]. At this resolution, SEC may be useful for studying the kinetics involved in conversion of LMW A $\beta$  to PF (or dissociation of PF into LMW A $\beta$ ). In addition to its use as an analytical method [39], SEC has been used extensively to purify fractions of particular A $\beta$  assemblies [30, 32, 37, 103-105]. Description of the basic instrumentation and utilization of SEC for preparation of aggregate-free A $\beta$  was published previously [106].

### ***Analytical Ultracentrifugation***

Analytical ultracentrifugation is a versatile technique used extensively to characterize the hydrodynamic and thermodynamic properties of proteins or macromolecules (reviewed in [67]). Conceptually, this method allows real-time quantitative analysis of spatial redistribution of soluble analytes under a high centrifugal force field. Unlabeled and unmodified proteins can be analyzed by this method in various excipients, obviating analyte–matrix interactions such as those occurring during SEC. Because molecular frictional forces oppose the centrifugal force, sedimentation depends, in addition to other parameters, on the hydrodynamic

properties of the molecules, providing low-resolution information on the structure of protein complexes, thus enabling detection of conformational alterations.

This technique combines an ultracentrifuge, a multicompartamental rotor, and an optical detection system for measuring analyte concentration inside the centrifuge cell during sedimentation. The optical detection system is triggered by the revolution of the rotor, allowing data acquisition only during the extremely short intervals when a particular sample assembly aligns within the optical path. Coupled with data-analysis software, analytical ultracentrifugation can determine sample purity and molecular mass in the native state, measure sedimentation and diffusion coefficients, characterize assembly–disassembly mechanisms of complex analytes, determine subunit stoichiometry, detect and characterize macromolecular conformational changes, and measure equilibrium constants and thermodynamic parameters for homo- or hetero-associating assemblies. Two types of experiments are commonly performed using ultracentrifugation—sedimentation velocity [107, 108] and sedimentation equilibrium [109]. Typically, sedimentation-velocity experiments are conducted at relatively high rotor speeds. Under these conditions, each protein species in a mixture forms a unique boundary and sediments at a characteristic speed governed by its molecular mass, size, and shape. The velocity and shape of the moving concentration boundary is used to estimate the sedimentation coefficient, diffusion coefficient, molecular mass, and equilibrium constants of interacting species. In contrast, sedimentation-equilibrium experiments are performed at relatively low rotor speeds. The sedimentation of proteins under lower centrifugal forces than in sedimentation-velocity experiments is opposed by the diffusion, and eventually when equilibrium is reached, a time-invariant exponential concentration gradient is established throughout the centrifuge cell. The concentration gradient of proteins at equilibrium has been used widely to determine the molecular weight, stoichiometry, binding affinity, and virial coefficient of hetero-interacting or self-associating systems. Sedimentation-equilibrium experiments can analyze a mixture of moieties of different molecular masses. After each analyte reaches its equilibrium, high-molecular-mass species locate towards the cell bottom, whereas low-molecular-mass species dominate at the top. The equilibrium data can be fitted to calculated models for solute distribution. Using this type of analysis,

Huang *et al.* have reported that A $\beta$ 40 existed as an equilibrium mixture of monomers, dimers, and tetramers at neutral pH [110]. However, other equilibria, including monomer–dimer, monomer–trimer, or monomer–tetramer, produced equivalent residuals [110], hindering precise determination of the oligomerization state of the peptide. ADDLs, which are soluble, A $\beta$ 42-derived, non-fibrillar neurotoxic assemblies, have been shown to contain a high-molecular-mass component with an estimated mass of 175 kDa by sedimentation-velocity and 120–540 kDa by sedimentation-equilibrium experiments [95].

### ***Dynamic Light Scattering (DLS) Spectroscopy***

DLS, also known as quasielastic light scattering, intensity-fluctuation spectroscopy, or photon-correlation spectroscopy, is a non-invasive, nondestructive, quantitative, optical analytical method for determining diffusion coefficients of particles (0.1–3000-nm size range [111]) undergoing Brownian motion in solution (reviewed in [67]). DLS measures the temporal dependence of light scattering emanated from an analyte in solution over  $10^{-7}$ –1 s. Temporal fluctuations in intensity of the scattered light relate to rate of the Brownian motion which is correlated to the diffusion coefficients,  $D$ , and radii of particles according to the Stokes–Einstein equation [112, 113]:

$$D = \frac{K_B T}{6\pi\eta R_h} = \frac{K_B T}{3\pi\eta D_h},$$

where  $K_B$  is Boltzmann's constant,  $T$  is the absolute temperature,  $\eta$  is the viscosity of the suspending liquid, and  $R_h$  and  $D_h$  are the hydrodynamic radius and diameter, respectively. Knowledge of diffusion coefficients of molecules allows determination of molecular features, including size and flexibility. Temporal changes in these parameters provide information about the kinetics and structural transitions occurring, *e.g.*, during protein assembly–disassembly processes. In a polydisperse mixture, a distribution of diffusion coefficients is obtained.

DLS is intrinsically biased for large aggregates because the intensity of the scattered light is proportional to the square of the particle mass [114]. Therefore, DLS is suited well to measure minute amounts of protein aggregates (<0.01% by weight) on the background of monomers and small oligomers. For large or extended proteins (rod-like/unfolded), scattering varies significantly with angle [115]. Determining scattering at additional angles by multi-angle laser-light scattering (MALLS) allows direct

measurements of masses up to MDA ranges. Because the light-scattering signal is directly proportional to protein concentration and molecular mass, a combination of DLS signal and concentration measurements using refractive indexes or absorbance, allows calculation of the molecular mass of each component when proteins are fractionated chromatographically. DLS can resolve the monomeric and dimeric state of a protein if the shape of the protein is known, but it cannot distinguish among small oligomers when their hydrodynamic radii differ by less than a factor of 2 [116] or between, for example, a compact dimer and an extended monomer. Consequently, DLS is less useful for analyzing individual small oligomers than SEC-MALLS, PICUP coupled with SDS-PAGE, or sedimentation-velocity analytical ultracentrifugation. Because DLS allows monitoring protein assembly without analyte manipulation or consumption, it has been used widely to study A $\beta$  aggregation and assembly processes [32, 104, 117-121]. Solution state and size distribution of ADDLs have been assessed by Hepler *et al.* using SEC coupled with MALLS [95]. Walsh *et al.* reported studies using DLS and other techniques examining early stages of A $\beta$  oligomerization and characterization of A $\beta$  intermediates during fibrillogenesis [90]. Detailed accounts of the theory and practice of DLS and its application to study of A $\beta$  were given by Lomakin *et al.* [114, 122, 123].

### ***Ion-Mobility Spectroscopy–Mass Spectrometry (IMS–MS)***

IMS–MS is a mass-spectrometric method that can resolve molecules of identical mass-to-charge ( $m/z$ ) values differing by collision cross-section, which in turn correlates with assembly state or conformation [124]. An IMS–MS instrument performs five basic processes: sample introduction, compound ionization, ion-mobility separation, mass separation, and ion detection [125]. Four types of IMS are used: drift-time, aspiration, differential, and traveling-wave IMS. Drift-time IMS is operated under either ambient pressure or reduced pressure. Aspiration and differential IMS are operated under ambient pressure, whereas traveling-wave IMS is performed under reduced-pressure conditions. Each of these IMS setups can be interfaced with a variety of mass spectrometers, including time-of-flight, quadrupole, ion-trap, ion-cyclotron, or magnetic-sector mass spectrometers.

In traditional drift-time IMS–MS, ions are carried by a weak, uniform electric field through a drift cell. In the drift cell, the analytes collide at low velocity with a low-

pressure inert gas (typically helium) such that the collision thermal energy due to the buffer gas is greater than the energy the ions obtain from the electric field. Under this principal condition, ions have energies similar to that of the buffer gas so that they undergo a directional diffusion process. Under these low-field conditions, the drift velocity of ions is directly proportional to the electric field but inversely proportional to their collision cross-section. This proportionality is defined by the ion-mobility constant,  $K$ , which is related to the ionic cross-section by

$$K = \left(\frac{3q}{16N}\right) \sqrt{\left(\frac{2\pi}{kT}\right)} \sqrt{\left(\frac{m+M}{mM}\right)} \left(\frac{1}{\Omega}\right),$$

where  $q$  is the ion charge,  $N$  is the number density of the buffer gas,  $k$  is Boltzmann's constant,  $T$  is the absolute temperature,  $m$  is the mass of the buffer gas,  $M$  is the mass of the ion, and  $\Omega$  is the collision cross-section of the ion [124]. Under low-velocity, low-pressure conditions, the analyte ions quickly reach equilibrium resulting in a constant drift velocity. Because at equilibrium ion mobility is inversely proportional to collisional cross-section, in the case of a mixture of protein assemblies, conformers/ions with compact structures and smaller cross-section have higher mobility and drift faster through the cell than ions with larger cross-sections. The ions exit the drift cell, pass through a mass filter, and are detected as a function of time, producing a temporal arrival distribution. The traditional drift-time IMS is the only type allowing measurement of collision cross-section of ions.

Protein oligomers often have identical  $m/z$  ratio (*i.e.*, a singly charged monomer would have the same  $m/z$  as a doubly charged dimer, triply charged trimer, *etc.*). IMS-MS analysis can resolve these species yielding an assembly size distribution. IMS-MS studies of A $\beta$  have shown that freshly prepared low-molecular-mass A $\beta$ 40 contained monomers, dimers, trimers, and tetramers, whereas similarly prepared solutions of A $\beta$ 42 comprised oligomers up to a dodecamer [126]. These results accord with earlier observations of distinct oligomer size distributions of A $\beta$ 40 and A $\beta$ 42 by PICUP [32] and may explain differences in neurotoxic effects of the two A $\beta$  alloforms.

Utilization of gas-phase approaches such as IMS has led to accumulation of extensive evidence that ESI [and to some extent matrix-assisted laser desorption

ionization (MALDI)] can produce ions that retain key structural aspects of proteins in solution [127]. In particular, the dependence of protein conformation on solution conditions, *e.g.*, pH and excipient composition, in IMS and field-asymmetric ion-mobility spectrometry (FAIMS) shows that gas-phase measurements can concord with protein conformations in solution [127]. Furthermore, 2D FAIMS–IMS separations coupled with MS can reveal many more protein conformations, including low-abundance conformations, than either FAIMS or IMS [127], suggesting that IMS–MS and IMS–IMS–MS offer great potential in the dissection of protein conformational dynamics, a feat currently unachievable by other biophysical techniques.

### **Analysis of Secondary Structure**

#### ***Circular Dichroism (CD) Spectroscopy***

CD is the change in the absorption of circularly polarized light as a function of wavelength exhibited by optically active molecules. Because secondary structural elements such as  $\alpha$ -helices,  $\beta$ -strands,  $\beta$ -turns, and disordered regions display characteristic wavelength-dependent dichroism, CD is a useful method to determine secondary structure of proteins. Secondary structure analysis of peptides and proteins by CD spectroscopy uses “far-UV” spectra (180–250 nm), in which the chromophores are peptide bonds due to the effect of the dihedral angle of peptide bonds on the absorption of the chiral center at the  $\alpha$ -carbon. In contrast, near-UV CD spectra (250–350 nm) reflect contributions of aromatic side-chains and disulfide bonds and provide information about polypeptide tertiary structure [128].

Samples for CD spectroscopy typically are dissolved in aqueous buffers with or without co-solvents. Because most of the structural information of proteins is obtained in the far-UV range, the buffer and co-solvent choices are critical. Several chemical bonds have strong absorption in this range. Hence, buffers with minimal absorption in the far-UV range should be chosen. A typical buffer used in CD experiments is 10 mM sodium phosphate [128].

The CD signal reflects an average of the entire ensemble of molecular structures. Quantitative assessment of secondary structures can be achieved by deconvolution

of experimental spectra using libraries of existing known structures [129]. Therefore, CD can only determine the overall proportion of secondary structural elements, but not the amino acid residues involved or the fraction of molecules with a particular conformation. Thus, on the basis of CD data alone, it is impossible to distinguish, for example, between a situation in which part of a protein monomer is  $\alpha$ -helical and another in  $\beta$ -sheet conformation, and a heterogeneous population in which a portion of the monomers are purely helical and another portion entirely in a  $\beta$ -sheet conformation.

CD has been used extensively to investigate secondary structures of A $\beta$  peptides and to monitor structural transitions of A $\beta$  during its oligomerization and aggregation [30, 130-133].

### ***Fourier-Transform Infrared (FTIR) Spectroscopy***

Complementary to CD, FTIR enables determination of the secondary structure of protein samples as thin films, as solids, or in solution. Characteristic bands in IR spectra of proteins and polypeptides include predominantly amide I and amide II. The amide-I band corresponds to the absorption in the vibrational spectrum of the C=O component of the amide bond ( $1600\text{--}1700\text{ cm}^{-1}$ ), whereas C–N stretching and C–N–H bending vibrations give rise to absorption bands at  $1550\text{ cm}^{-1}$  (amide II) and  $1250\text{ cm}^{-1}$  (amide III), which are useful for assigning secondary structures. Because C=O and N–H bonds are involved in hydrogen bonding, the absorption wavelength of both amide-I and amide-II bands are sensitive to the secondary structure content of proteins. In many cases, instead of a series of well-resolved peaks for each type of secondary structure, one broad peak is observed. However, for proteins that cannot be studied by high-resolution methods, FTIR provides useful structural information. It is thought that FTIR is more sensitive to  $\beta$ -sheet content whereas CD measurements generally tend to underestimate  $\beta$ -sheet relative to  $\alpha$ -helix content [134]. The main bands of interest in the amide-I region for detection of  $\beta$ -strand alignments are at  $1626$  and  $1632\text{ cm}^{-1}$  for parallel  $\beta$ -sheet and at  $1690\text{ cm}^{-1}$  for antiparallel  $\beta$ -sheet structures. The signature of statistical coil [93] (extended, irregular structure with distinct spectroscopic features) is a band at  $1644\text{ cm}^{-1}$  and that of  $\alpha$ -helix is a band at  $1654\text{ cm}^{-1}$ . However,  $\alpha$ -helical conformations also contribute to band intensities at  $1644$  and  $1662\text{ cm}^{-1}$ , making distinction from statistical coil difficult. Non- $\alpha$  and non- $\beta$  structures appear at  $<1660\text{ cm}^{-1}$ . Although strong signals corresponding to particular secondary structures exist in this region, information in IR spectra obtained in aqueous

buffers is masked by a strong signal at  $1630\text{ cm}^{-1}$  due to water bending vibrations. Hence, alternative strategies have been adopted to probe the secondary structure of proteins in general, and amyloidogenic proteins in particular, with IR spectroscopy. Isotopic substitution has far-reaching effects on IR absorption. The peak positions of  $^{13}\text{C}=\text{O}$  and  $\text{C}=\text{}^{18}\text{O}$  stretching bands shift to lower frequency relative to  $^{12}\text{C}=\text{}^{16}\text{O}$  bands. Isotopic labeling thus allows assignment of secondary structures at a single-residue level. For example, for  $\alpha$ -helix, the  $^{13}\text{C}=\text{O}$  appears at  $1600\text{ cm}^{-1}$ , whereas  $^{13}\text{C}=\text{O}$   $\beta$ -sheet bands are at  $1586\text{ cm}^{-1}$  (parallel) and  $1595\text{ cm}^{-1}$  (antiparallel). Another isotopic labeling strategy is changing the solvent from  $\text{H}_2\text{O}$  to  $\text{D}_2\text{O}$ . This shifts the water bending vibration peak from  $1630$  to  $1290\text{ cm}^{-1}$  facilitating measurement in the amide-I region. FTIR has been used extensively to study the conformational changes of  $\text{A}\beta$  during assembly [135-139].

By two-dimensional IR and isotope labeling,  $\text{A}\beta_{40}$ -derived amyloid fibrils were shown to contain significant amount of mobile water molecules trapped within the inter-sheet space in the fibril structures [140]. Woys *et al.* reported novel quantitative structural parameters for measuring parallel  $\beta$ -sheet vibrational couplings by two-dimensional IR [141]. Recently, isotope labeling and kinetic two-dimensional infrared spectroscopy were used to obtain residue-specific structural information in a complex of human islet amyloid polypeptide (IAPP, also called amylin) with rat IAPP, which inhibits the aggregation of human IAPP [142]. It was revealed that significant structural rearrangements continued to occur after the system had apparently reached equilibrium assessed by a thioflavin T (ThT) fluorescence assay. Rat IAPP was found to block *N*-terminal, rather than *C*-terminal,  $\beta$ -sheet formation at 8 h after mixing with human IAPP, whereas at 24 h, rat IAPP formed its own  $\beta$ -sheet fibrils without blocking human IAPP  $\beta$ -sheet formation [142]. These exemplary studies indicate that FTIR and 2D IR spectroscopic studies are important quantitative tools for elucidating amyloid structures or amyloid-inhibitor interactions.

## Morphological Analysis

### *Transmission Electron Microscopy (TEM)*

TEM uses a cathode-ray source that emits and accelerates a high-voltage electron beam focused by electrostatic and electromagnetic lenses. When the electron beam passes through a thin, electron-transparent specimen, it carries information about the

inner structure of the sample as it reaches the TEM imaging system. There, the spatial variation in this information, which creates the image, is magnified by a series of electromagnetic lenses and detected by a fluorescent screen, photographic plate, or a light-sensitive sensor, *e.g.*, a charge-coupled device or a camera. Macromolecular specimens are applied typically onto a fine, metallic grid support coated by a thin, electron-transparent carbon film. Because biological macromolecules have nearly identical density to that of the carbon film, unstained macromolecules have intrinsically low contrast when viewed by TEM. To enhance contrast and reduce image noise, several strategies, including negative staining [143, 144], rotary shadowing [145], and cryo-EM [146], are used. In negative staining, the stain circumscribes the macromolecule, the shape of which is deduced from distribution of the stain, which scatters most of the electrons. In shadowing experiments, heavy metals are applied by evaporation to form a thin coating on specimens and enhance contrast. Metals may be evaporated unidirectionally either onto a static or a rotating specimen while shadowing takes place. In cryo-EM, the hydrated specimen is preserved in a thin vitreous film of ice maintained at  $-180^{\circ}\text{C}$  preventing both its sublimation and crystallization. Cryo-EM also circumvents the need for staining. Examples for using TEM to characterize various assembly states of A $\beta$  include LMW A $\beta$  [32, 33], small A $\beta$  oligomers [147-150], paranuclei [32, 33], PF [30, 104, 105, 121], and fibrils [90, 121, 151]. Cryo-EM was used to resolve the structure of A $\beta$ 42 fibrils, which comprised regularly spaced ( $\sim 45$  Å) protofilaments that twist regularly along the fibril axis [152].

### ***Scanning Transmission Electron Microscopy (STEM)***

In STEM, a high-energy (100 kV) electron beam scans the specimen and scattered electrons are collected by various types of detectors located behind the specimen. Commonly, the detectors include electron-energy-loss spectrometers, X-ray emission spectrometers, and cathodoluminescence spectrometers (reviewed in [67]). The specimen image is generated as the focused beam moves step by step over the specimen. In a thin proteinaceous specimen, the image intensity is directly proportional to the mass of the irradiated region. Therefore, following background subtraction and calibration, the protein mass and mass-per-length unit (MPL) can be determined quantitatively [153]. Of note, other biophysical techniques, including DLS and analytical ultracentrifugation can monitor

quaternary structural alterations during amyloid fibril formation and enable measuring average molecular masses reflecting the distribution of an ensemble of quaternary structures in solution. However, the size and morphological heterogeneity of the intermediate structures during fibrillogenesis preclude assignment of molecular mass averages to a particular quaternary structural element. In contrast, STEM captures images of isolated and unstained specimens, allowing for accurate, quantitative mass determination of individual molecules or macromolecular assemblies [154].

STEM is an excellent tool for characterizing the homogeneity and structural properties of transient quaternary structure intermediates in amyloid fibril-formation pathways. STEM has been used to characterize the MPL ratios of A $\beta$  fibrils and PF [155-157]. A brief history of STEM, description of STEM mass mapping, and advantages and limitations of STEM have been reviewed by Wall *et al.* [158].

### ***Atomic-Force Microscopy (AFM)***

AFM captures high-resolution ( $\leq 1$  nm) topography of a sample adsorbed on an atomically flat smooth surface, typically mica. A cantilever tip samples the surface contour of a specimen and when the tip contacts a spot on the adsorbed sample, an ionic repulsive force (pN–nN range) bends the cantilever upwards. The extent of bending, measured by a laser, is translated to force units by a photodetector. By keeping the force constant while scanning across the surface, the vertical movement of the tip generates the surface contour, which is recorded as a topographic map of the sample. AFM has been modified for specific applications and can be used in different modes. In “tapping mode” (also dubbed “intermittent-contact” or “dynamic-force mode”), a stiff cantilever oscillates close to the sample. Part of the oscillation extends into the repulsive regime so that the tip intermittently touches, or taps, the surface. This mode provides good resolution of soft samples and thus is useful for investigation of non-fibrillar A $\beta$  species.

An advantage of AFM over TEM is that it allows continuous monitoring of the growth of A $\beta$  oligomers [159]. Multiple studies on the structure of soluble oligomers have used conventional tapping-mode AFM [26, 30, 90, 160-163]. Individual A $\beta$ 42 oligomers have been studied by AFM following dilution of the sample to concentrations that practically arrest oligomer growth. The smallest size

of individual oligomers that could be observed by AFM corresponded to a height of ~1–4 nm and were interpreted as folded monomers [139, 164].

### ***Scanning Tunneling Microscopy (STM)***

STM is a non-optical microscopic technique based on principles of quantum mechanics. The electron cloud of atoms in a sample extends a minute distance above the sample surface. An  $x$ - $y$ - $z$  piezoelectric translator controls the movement of the tip in three dimensions. When a probe, with a tip as sharp as a single atom, is brought sufficiently close to such a surface and a small voltage is applied, a strong interaction occurs between the electron cloud on the surface and the tip, leading to an electric tunneling current. The magnitude of the current depends exponentially on the distance between the probe and the surface. The tunneling current rapidly increases as the distance between the tip and the surface decreases. This rapid alteration in the current due to changes in distance results in construction of an atomically resolved image when the tip scans the structure. The feedback signal, applied to a piezoelectric element provides a measure of molecular surface contours. The principles and applications of STM in technology and biology have been reviewed by Hansma *et al.* [165]. Initial low-resolution STM studies of A $\beta$  showed the ribbon-like filamentous nature of A $\beta$  fibrils [166]. Later studies showed that A $\beta$  fibrils contained laterally associated filaments that exhibited a right-handed twist [163]. STM was used to examine the structure of A $\beta$ 40 monomers, dimers, and oligomers on a surface of atomically flat gold [167]. At low concentrations (0.5  $\mu$ M) small globular structures were observed. High-resolution STM measurements of A $\beta$  samples, both immediately following preparation and after 24-h aging, found structures of ~3–4 nm in diameter corresponding to oligomeric A $\beta$ . These results suggested that oligomer formation could potentially proceed through a mechanism involving linear association of monomers [167].

### **STRUCTURAL AND BIOLOGICAL STUDIES OF NON-FIBRILLAR A $\beta$ ASSEMBLIES**

The use of proper terminology to describe soluble non-fibrillar A $\beta$  assemblies is crucial to forming consensus in the literature. However, achieving this goal is difficult because various *in vitro* oligomeric entities of A $\beta$  have been described structurally, functionally, or both and the relationship or kinship amongst them are unclear [65]. Although all these structures are oligomeric, the use of the term

“oligomer” to describe all the assemblies may be misleading for at least three reasons, as discussed before: 1) the structure of each assembly is unique; 2) the pathways leading to the formation of the assemblies or the ultimate path they may take towards fibrillization may differ; 3) the biological activities of each assembly may differ or similar activities may be mediated through different mechanisms [63]; and 4) methods used to study and determine the oligomeric state may differ. Adding to this complexity is the fact that no single oligomeric species remain structurally unique under test conditions because of the metastable nature of oligomers [65]. Furthermore, detection of oligomeric state has to be strictly defined and distinguished contextually—whether they have been studied or shown *in vitro* or *in vivo*. In the following section, we describe non-fibrillar A $\beta$  species ranging from monomers to PF (Table 1). In most cases, we begin with structural characterization of each species followed by discussion of its biological activity.

**Table 1:** Summary of structural and biological characteristics of non-fibrillar A $\beta$  assemblies.

Assembly	Structural Characteristics/Production	Biological Activity
“Activated monomeric conformer” of A $\beta$	<ul style="list-style-type: none"> <li>Produced during aggregation of A<math>\beta</math>40 by constant rotary shaking.</li> <li>Measured by turbidity assay and HPLC.</li> <li>Postulated to be an oxidative or hydrolytic derivative of A<math>\beta</math> [19, 168].</li> <li>The monomeric nature of these conformers is not confirmed unambiguously.</li> </ul>	<ul style="list-style-type: none"> <li>Forms 2–3-fold more complexes with apoE4 than apoE2 or apoE3 [168].</li> <li>Enhances toxicity and apoptotic activity in neurons [19].</li> <li>Inhibits action potential by blocking fast, inward tetrodotoxin-sensitive Na<sup>+</sup> channels [169]</li> </ul>
Natural cell-derived A $\beta$ oligomers	<ul style="list-style-type: none"> <li>Predominantly dimers, trimers, and tetramers, produced by CHO cells transfected with mutated or wild-type APP [23, 170].</li> <li>Resistant to SDS denaturation (see our discussions about “SDS stability” under “Determination of Oligomer Size Distribution”) and to cleavage by insulin degrading enzyme [24].</li> </ul>	<ul style="list-style-type: none"> <li>Inhibit LTP <i>in vivo</i> [24].</li> <li>Enhance LTD by mGluR or NMDAR activity [171].</li> <li>Impair short-term memory in rats [172].</li> <li>Cause dendritic spine loss [173].</li> <li>Affect synaptic structure and function.</li> <li>Cognitive impairment in mice [94].</li> <li>It was suggested that apparent toxic effects mediated by dimers were attributable to relatively stable, dimer-derived PF [174].</li> </ul>
A $\beta$ -derived diffusible ligands (ADDLs)	<ul style="list-style-type: none"> <li>Synthetic species formed in the presence of apolipoprotein J [175], in F-12 media [176], or in PBS [177].</li> <li>Small globules 3–8 nm in diameter</li> </ul>	<ul style="list-style-type: none"> <li>Highly neurotoxic [26, 179].</li> <li>Inhibit LTP [26].</li> <li>Bind to neuronal surfaces [59] co-localizing with neuronal proteins at</li> </ul>

Assembly	Structural Characteristics/Production	Biological Activity
	<p>measured by AFM [178].</p> <ul style="list-style-type: none"> <li>• Polydisperse mixtures of 150–1,000 kDa determined by MALLS [95].</li> <li>• A11-positive [65].</li> </ul>	<p>postsynaptic punctate sites [180, 181] and NR1 and NR2B subunits of NMDAR [180, 181].</p> <ul style="list-style-type: none"> <li>• Promote oxidative stress and increased <math>[Ca^{2+}]_i</math> [182].</li> <li>• Induce <math>\tau</math> phosphorylation [177] and misfolding [183].</li> <li>• Induce IL-1<math>\beta</math>, iNOS, NO and TNF-<math>\alpha</math> in astrocytes [184].</li> <li>• Abnormal mitochondrial distribution in neurites caused by impaired <math>\tau</math>-dependent axonal transport [183, 185]</li> </ul>
Protofibrils (PF)	<ul style="list-style-type: none"> <li>• Curvilinear fibril-like structures 6–8 nm in diameter and <math>\leq 200</math> nm long by TEM [90]; a periodicity of 20 nm and diameter of 4.3 nm were determined by AFM [161].</li> <li>• Rich in <math>\beta</math>-sheet structure.</li> <li>• Bind Congo red and thioflavin T [10].</li> <li>• A<math>\beta</math>40Ser26Cys dimers stabilized by disulfide bonding form stable PF (comprising ~100–450 monomers), which do not readily sediment unlike typical amyloid fibrils [174].</li> <li>• These species were relatively stable because PF persisted even after a one-month-long incubation period in certain samples at 37°C [174].</li> </ul>	<ul style="list-style-type: none"> <li>• Increase EPSCs [29], and cause cell death [29, 30].</li> <li>• May activate NMDAR in contrast to fibrils which activate non-NMDA glutamate receptors [186].</li> <li>• Patch-clamping using A<math>\beta</math>42 PF induces reversible, <math>Ca^{2+}</math>-dependent increase in spontaneous action potentials and membrane depolarizations.</li> <li>• Can inhibit the A- and D-type <math>K^+</math> currents, but not other outward/inward rectifying <math>K^+</math> channels.</li> <li>• PF-induced membrane activity increases <math>[Ca^{2+}]_i</math> spikes [187].</li> <li>• A<math>\beta</math>40 containing the E22G substitution forms PF faster and in larger quantities than wild-type A<math>\beta</math> <i>in vitro</i>, suggesting that PF may be the main disease-causing agents in carriers of the Arctic mutation [188].</li> <li>• Stable, dimer-derived PF inhibit LTP [174].</li> </ul>
A $\beta$ *56	<ul style="list-style-type: none"> <li>• Extracted from brains of <i>Tg2576</i> mice and isolated by immunoaffinity and SEC [31].</li> </ul>	<ul style="list-style-type: none"> <li>• Concentration correlates with degree of cognitive deficits.</li> <li>• Cause defects in long-term spatial memory in rats (micromolar concentrations) [31, 94].</li> <li>• NMDAR-dependent synaptotoxicity, but no cytotoxicity (reviewed in [65]).</li> <li>• Concentration-dependent cognitive deficits in rats by an Alternating Lever Cyclic Ratio (ALCR) cognitive assay [94]</li> </ul>

Assembly	Structural Characteristics/Production	Biological Activity
Amyloid pores	<ul style="list-style-type: none"> <li>Channel-like structures of synthetic A<math>\beta</math>, having outer diameter of 8–12 nm and inner diameter of 2–2.5 nm, associated with artificial membrane bilayers [18, 36].</li> </ul>	<ul style="list-style-type: none"> <li>Pore- and channel-forming capacity that may lead to membrane leakage and increased [Ca<sup>2+</sup>]<sub>i</sub>; [18, 36].</li> </ul>
Toxic fibrillar oligomers of A $\beta$ (TABFOs)	<ul style="list-style-type: none"> <li>A<math>\beta</math>42-derived fibrillar conformation or lattice reactive with OC, but not A11, antibody [38, 189, 190].</li> <li>Can seed formation of additional fibrillar oligomers, but not fibrils [191].</li> <li>M<sub>r</sub> = 80,000 ± 20,000; <math>\beta</math>-sheet-rich; <math>\alpha</math>-helix-poor [190].</li> </ul>	<ul style="list-style-type: none"> <li>Cytotoxicity likely mediated by pore-forming capacity predicted by modeling studies [190]</li> </ul>
Double-cysteine mutant A $\beta$ 42 PF	<ul style="list-style-type: none"> <li>Stabilized by intramolecular disulfide bonds, which forms a <math>\beta</math>-sheet-rich structure that does not form fibrils [192].</li> <li>Weak reactivity with A11 [192].</li> </ul>	<ul style="list-style-type: none"> <li>Synaptotoxicity [65].</li> <li>Caspase activation in human neuroblastoma cells [192]</li> </ul>
“SDS-stable” brain-derived dimers and synthetic dimers (A $\beta$ 40Ser26Cys)	<ul style="list-style-type: none"> <li>8–12 kDa assemblies.</li> <li>3–4 nm height.</li> <li>No detectable secondary structure.</li> <li>For a discussion on the concept of “SDS-stability” refer to “Determination of Oligomer Size Distribution”.</li> </ul>	<ul style="list-style-type: none"> <li>LTP impairment [193].</li> <li><math>\tau</math> phosphorylation in primary neurons [194].</li> <li>Not cytotoxic to primary neurons (micromolar concentration), but toxic to neurons co-cultured with microglia [149].</li> <li>It was suggested that the A<math>\beta</math>40Ser26Cys dimers were not cytotoxic and the initial toxicity described for these dimers [193, 195] was attributed to PF, which may have formed during frozen storage of the A<math>\beta</math>40Ser26Cys samples [174].</li> </ul>
Annular A $\beta$ 42-derived protofibrils (APF)	<ul style="list-style-type: none"> <li>Off-path A<math>\beta</math>42 assemblies arranged as hexamers [196].</li> <li>Weakly reactive with A11 [197].</li> <li>Form pores with outer diameter of 11–14 nm and inner diameter of 2.5–4 nm [196].</li> <li>Highly reactive with an anti-serum raised against APF (<math>\alpha</math>APF), which was shown to react also with fibrils and oligomeric assemblies of A<math>\beta</math>42 [197].</li> </ul>	<ul style="list-style-type: none"> <li>Postulated to cause Ca<sup>2+</sup> overload and cytotoxicity [196].</li> <li>Immunoreactivity of <math>\alpha</math>APF was observed in tissues from AD brains leading to the conclusion that annular amyloid pores are present in AD brain tissues [196]; however, the same antibody was shown to react with oligomeric and fibrillar assemblies of A<math>\beta</math>42 [197].</li> </ul>
Amylospheroids	<ul style="list-style-type: none"> <li>10–15-nm spherical A<math>\beta</math>40- or A<math>\beta</math>42-derived assemblies [35] which are A11-negative (reviewed in [65])</li> </ul>	<ul style="list-style-type: none"> <li><math>\tau</math> protein kinase 1/GSK-3<math>\beta</math> activation [35].</li> <li>NMDAR-independent cytotoxicity in neurons at high picomolar to low nanomolar concentrations [198, 199].</li> </ul>

## **“Activated Monomeric Conformer” of A $\beta$**

### ***Structural Characterization***

Monomer activation denotes a conformational change preceding A $\beta$  self-assembly that may render monomers toxic, or cause their nucleation and further aggregation, or both. Based on concepts taken from actin polymerization [200] and a kinetic model of A $\beta$  aggregation induced by constant rotary shaking, Taylor *et al.* introduced the idea of “activated monomeric conformers” of A $\beta$ 40 [19], also called “intermediate aggregated species” [168]. It was postulated that this moiety was an oxidative or hydrolytic derivative or a slowly folding conformer of intact A $\beta$ 40 [19, 168]. It was proposed that the “inactive” monomer slowly converted into the “activated” monomeric conformer, several of which may cooperate to form growing nuclei for oligomerization and progression of aggregation [19]. In these studies, the presence of the active monomeric A $\beta$  conformer was tested by HPLC using acetonitrile and trifluoroacetic acid, which might have caused structural alterations in A $\beta$  sequence by increasing its  $\beta$ -sheet content [201]. Lee *et al.* have provided evidence that A $\beta$  aggregation intermediates and final structures formed under slowly agitated or quiescent conditions at 37°C differed in their toxicity, stability to denaturants, and apparent morphologies [202], emphasizing that parametrical consideration of methods used to prepare A $\beta$  for structural or biological studies and proper methods to assess the assembly state of the resulting preparations are paramount [58]. Similarly, NMR studies emphasize the importance of performing structural studies under physiological conditions [71] rather than “structure-inducing” milieus as reported by Taylor *et al.* [19].

Other studies also have shown presence of A $\beta$  intermediates; however, the assembly states of these were not determined unambiguously. A study by Chimon *et al.* described A $\beta$ 40 intermediates that contained a  $\beta$ -sheet-rich character and were thought to originate from a monomeric state, preceding PF and fibril formation [203]. Filtration experiments showed that these intermediates were not monomeric but were likely larger than decamers, indicating that unambiguous determination of the assembly intermediates is difficult. By electron microscopy, these intermediates had a spherical morphology similar to ADDLs [178], amylospheroids [35], and  $\beta$ amy balls [39]. NMR studies showed that the intermediate species were well-ordered in the hydrophobic core and the C-

terminal region [203]. A $\beta$ 40 was used in this study at higher concentrations than those found in biological specimens and the possibility that the intermediates could have undergone fibril formation during preparation for NMR studies was not excluded. Similarly, Lim *et al.* provided evidence for presence of monomeric intermediates using CD and NMR studies of A $\beta$ 40 and A $\beta$ 42 under both non-amyloidogenic (<5°C) and amyloid-promoting conditions (>5°C) at physiological pH [132]. CD studies suggested that the initially unfolded A $\beta$  peptides at low temperature gradually transformed to  $\beta$ -sheet-containing monomeric intermediates at stronger amyloidogenic conditions (higher temperatures) [132]. However, exclusive presence of monomers after dialysis of 1,1,1,3,3,3-hexafluoro-2-isopropanol (HFIP)-treated A $\beta$  species against phosphate buffer was not confirmed [132]. Providing formal proof for the presence of A $\beta$  monomers exclusively is difficult and has not been achieved unambiguously in the studies mentioned above. Therefore, whether a critical conformational change in the monomer occurs before self-assembly, or the conformational change and the assembly occur concurrently and co-dependently remains an open question.

### **Biological Activity**

In cell biological studies, toxicity and apoptotic activity were enhanced when the concentration of the “activated monomeric conformer” described by Taylor *et al.* was maximal during the aggregation continuum [19]. Similarly, in electrophysiologic experiments, A $\beta$  species described as monomeric conformers obtained between ~60–120 min during rotary-shaken aggregation inhibited neuronal action potentials [169]. This neurotoxicity was attributed only to the “active” monomeric conformers detected at 60 min after the initiation of aggregation but not to inactive monomers or fully formed aggregates [19, 168, 169]. In these studies, the kinetics of aggregation was monitored by turbidity and the loss of the starting low-molecular-mass material was monitored by HPLC [19]. The sensitivity of turbidity measurements for detection of small particles is substantially lower than that of DLS and it is thus unlikely that the method can distinguish monomers from small oligomers. Also of note is that biological activities similar to those obtained by Taylor *et al.* [19] have been described for A $\beta$  oligomers [59], thus it is unclear that these toxicity data can be ascribed to monomeric A $\beta$ .

## Brain- and Cell-Derived Low-Order A $\beta$ Oligomers

### *Structural Characterization*

Dimeric and trimeric assemblies of A $\beta$  have been isolated from amyloid plaque cores [20], CSF [22], and human cortical homogenates [21], and produced by cells transfected with amyloid  $\beta$ -protein precursor (APP) [23]. Dimeric and trimeric A $\beta$  (apparent SDS-PAGE mobility corresponding to ~9 and ~13.5 kDa) purified from neuritic plaques and leptomeningeal mural amyloid, were characterized by SEC, AFM, and electron microscopy [149]. MALDI mass spectrometry was used to determine the mass of the “dimeric” components [149]. However, to extract A $\beta$  from tissue sources, SDS was included in extraction buffers and the possibility that these A $\beta$  species could form during the extraction process, *ex vivo*, was not excluded. In fact, SDS has been shown to be a useful amyloid inducer under certain pH and protein–SDS stoichiometric conditions [80]. Immunoaffinity purification, HPLC, and MALDI analyses of CSF from patients suffering from meningitides and other neurological conditions, including dementia, revealed A $\beta$  species of various length, including two truncated trimer species—(Asp<sup>1</sup>–Met<sup>35</sup>)<sub>3</sub> and (His<sup>6</sup>–Ala<sup>42</sup>)<sub>3</sub>— and an A $\beta$ 40 dimer, (Asp<sup>1</sup>–Val<sup>40</sup>)<sub>2</sub> [22]. A $\beta$  in CSF was shown to be associated with high-density-lipoprotein particles in an apparently monomeric form detected by SDS-PAGE [204, 205]. Similarly, 24% and 27% of brain A $\beta$ 40 and A $\beta$ 42, respectively, were shown to be concentrated in lipid-raft extracts as dimers determined by SDS-PAGE in the *Tg2576* murine model of AD [206]. However, as discussed previously, SDS-PAGE is not a reliable method for A $\beta$  size determination [63] and presence of SDS in buffers used to extract A $\beta$  species makes assessment of these *ex vivo* findings questionable [63, 65] in relation to what is actually present *in vivo*.

Walsh *et al.* have reported “natural” A $\beta$  oligomers that are “SDS-stable”, low-order oligomers (dimers, trimers, and tetramers) detected in the conditioned media and/or lysates of cells [23, 25, 170, 207, 208]. These oligomers are produced by Chinese hamster ovarian cells that express human mutant (V717F, V717I, or E693Q, cells referred to as 7PA2), or wild-type APP [23, 209]. Low-abundance species of masses ~10, 14, and sometimes 16 kDa, which were reactive with antibodies against A $\beta$  also were detected in the culture media of these cells [23]. The nature of these low-order oligomers is not fully understood but the

observation that they are not disassembled by several types of denaturants suggests that they may be covalently linked [25].

### **Biological Activity**

Initially, biological effects of oligomeric A $\beta$  fractions purified from neuritic plaques and leptomenigeal mural deposits were investigated in an *ex vivo* astroglial–neuronal co-culture system believed to approximate *in vivo* conditions [149]. Neuronal viability was compromised by AD-derived A $\beta$  only when microglial cells were co-cultured, indicating that toxicity was mediated through a microglia-dependent mechanism [149].

Ease of maintenance and fast growth-rate of 7PA2 cells facilitated investigations of the biological activities of “natural”, cell-derived A $\beta$  oligomers. Intracerebroventricular microinjection of small volumes (~1.5  $\mu$ L containing ~3 ng/mL A $\beta$ ) of SEC-fractionated cell-culture media to anesthetized wild-type rats was shown to inhibit hippocampal long-term potentiation (LTP) [24, 210]. This inhibition was predominantly mediated by A $\beta$  trimers in wild-type murine hippocampal brain slices, whereas dimers and tetramers had intermediate potencies, and monomers were apparently ineffective [208]. Cell-derived oligomers were shown to interfere primarily with LTP induction, but not its expression, once the signaling cascades responsible for LTP were initiated [208]. These results suggested that cell-derived oligomeric A $\beta$  assemblies altered certain aspects of hippocampal synaptic plasticity both *in vivo* and *in vitro* (reviewed in [211]).

The validity of LTP as an electrophysiological paradigm for learning and memory composition has been debated [212]. To test the effect of the “natural A $\beta$  oligomers” in a non-LTP paradigm, Cleary *et al.* used an *in vivo* behavioral model in rats that were injected with cell-conditioned media containing A $\beta$  assemblies into the dorsal lateral cerebral ventricles. This treatment was found to transiently interrupt pre-learned behaviors [172]. This was attributed to A $\beta$  oligomers because SEC fractions containing oligomers caused the deficits, whereas monomer-containing fractions were ineffective [172].

Actin-based cytoskeletal network dynamics is critical for regulation of neuronal spine morphology and function [213]. Alterations in spine morphology and actin-

regulatory mechanisms recently have emerged as sensitive measures of early neuronal functional deficits and neurotoxicity [180, 214, 215]. Because loss of synaptic termini strongly correlates with the severity of dementia, Shankar *et al.* assessed the effect of cell-derived soluble oligomers on synapses [173]. They showed that the density of dendritic spines decreased substantially in neurons treated with sub-nanomolar levels of cell-derived A $\beta$  oligomers [173]. This effect was shown to be specific to A $\beta$  oligomers, *i.e.*, SEC monomer fractions alone were ineffective. The decrease in spine density was reversed by monoclonal immunodepletion of A $\beta$ , by transfer of cells back into the control media, and by *scyllo*-inositol [173], a molecule thought to stabilize synthetic A $\beta$  as nontoxic species, possibly preventing A $\beta$  interaction with neuronal target proteins [216, 217].

In cultures of dissociated cortical neurons, synthetic A $\beta$  was shown to activate nicotinic acetylcholine receptors (nAChRs) and trigger internalization of *N*-methyl-D-aspartate (NMDA) receptors (NMDARs) [218]. However, Shankar *et al.* found that an irreversible nAChR antagonist did not affect A $\beta$ -oligomer-mediated spine loss, indicating that nAChR activity was unnecessary for this effect [173]. Signaling cascades involving NMDARs, cofilin, and calcineurin were found to be involved in A $\beta$ -induced spine loss as determined by inhibition studies [173]. Together, these data demonstrated that cell-derived low-order A $\beta$  oligomers could cause reduction of synapse density and loss of electrophysiologically active synapses in hippocampal pyramidal neurons, suggesting that their deleterious effects may be important mechanistic contributors to synaptic dysfunction in AD *in vivo* [211].

### **A $\beta$ -Derived Diffusible Ligands (ADDLs)**

#### ***Structural Characterization***

ADDLs are exclusively A $\beta$ 42-derived soluble non-fibrillar assemblies that morphologically appear as 3–8-nm globules by AFM [26, 178] and have estimated masses between 17–42 kDa [26] (reviewed in [176]). It was first observed that apolipoprotein J (also called clusterin, a ubiquitous multifunctional glycoprotein co-localizing with fibrillar deposits in systemic/localized amyloid disorders [219]) partially inhibited A $\beta$  aggregation and caused formation of “slowly precipitating” A $\beta$ 42 complexes of >200 kDa [175]. Follow-up studies showed that ADDLs with the same biochemical and neurotoxic characteristics could be produced in clusterin-free solutions by incubating aggregate-free A $\beta$ 42 in phenol-red-free F-12 medium at

4–8°C for 24 h, in clusterin-free brain-slice culture media at 37°C for 24 h [26, 176], or even in phosphate-buffered saline [177].

By SEC, ADDL preparations contained two distinct peaks—an early-eluting high-mass component, which exhibited punctate binding to primary neurons, and a late-eluting low-mass component (13 kDa), which lacked this property [178]. These peaks are similar to those reported by Walsh *et al.* for protofibrillar and LMW preparations of A $\beta$ , respectively (see below) [90]. However, Walsh *et al.* showed by TEM that the early-eluting peak contained abundant PF whereas the late-eluting peak was reported later to contain a mixture of monomer and small oligomers detected using PICUP [103]. When SEC coupled with MALLS and analytical ultracentrifugation was used to determine the size distribution of ADDLs, the SEC peaks corresponding to 75 and 13 kDa showed oligomer masses ranging from 150–1,000 kDa, and a monomeric component of 4.5 kDa by MALLS [95]. This study suggested that previous reports identifying low-molecular-mass components as a composite of low-number oligomers were misrepresentations of what might actually be a monomeric A $\beta$ 42 fraction [95]. ADDLs found in the early-eluting peak were shown to be in a dynamic equilibrium comprising a polydisperse population of oligomers [95]. Multiple parameters such as peptide concentration, temperature, pH, storage duration, and excipient addition were shown to affect this equilibrium dramatically [220].

Importantly, A $\beta$ 40 does not form ADDLs [95]. NMR studies have shown that the C-terminus of A $\beta$ 42 is more rigid compared to that of A $\beta$ 40 [70–72] potentially due to the extended hydrophobic C-terminus of A $\beta$ 42. This C-terminal difference and potentially the different monomeric A $\beta$ 42 conformers generated due to this structural difference may account for the increased toxicity and plaque competence of A $\beta$ 42 compared to A $\beta$ 40 [70, 71]. Indeed, some oligomeric moieties (ADDLs, paranuclei, and globulomers, see below) were shown to form by A $\beta$ 42 only. In fact, the exclusive A $\beta$ 42 derivation of ADDLs and paranuclei, and the fact that ADDLs and paranuclei are indistinguishable morphologically (compare [26, 178] with [32]), suggests that ADDLs and paranuclei may be related to each other or even be the same species obtained under different conditions [26, 32].

ADDLs have been shown to resist dissociation by low SDS concentrations (0.01%) [175]. However, when supramicellar SDS concentrations were used, ADDLs and fibrils migrated with the same electrophoretic profile yielding monomeric, trimeric, and tetrameric moieties [95]. A similar profile was observed for LMW A $\beta$ 42 [32] produced by SEC or filtration [106]. At submicellar concentrations of SDS, oligomers were detected both by denaturing electrophoresis and SEC [95]. When A $\beta$ 42 was electrophoresed in the presence of submicellar or supramicellar concentrations of SDS, high-molecular-mass aggregates and intermediate-sized assemblies formed, respectively [63]. During SDS-PAGE, these aggregates may partially dissociate as diffuse A $\beta$ 42 trimer/tetramer components [63] as observed for ADDLs [95]. These observations re-emphasize that visualization of SDS-stable oligomeric A $\beta$  likely misrepresent the actual assembly state.

### ***Biological Activity***

Initial clusterin-induced ADDL preparations (0.34 mg/mL) were neurotoxic [175]. Later studies showed that ADDLs selectively targeted the principal neurons in the hippocampal *strata pyramidale* and *granulosum* in organotypic murine brain slices [26] and inhibited LTP in rat hippocampal brain slices [221, 222]. ADDLs also were shown to augment the negative synaptic plasticity of long-term depression (LTD) [223]. Prolonged maintenance of LTD along with LTP inhibition leads to an overall synapse-inhibitory effect (reviewed in [59]).

When cultured hippocampal neurons were incubated with synthetic ADDLs, F-12-prepared soluble brain extracts, or crude human CSF, and probed with ADDL-specific antibodies a punctate binding pattern reminiscent of synaptic termini was observed [181] (Fig. 2). The antibodies used were shown to be 100-fold more sensitive to ADDLs (femtomole levels) than to monomeric A $\beta$  [27, 180, 181, 224, 225]. The ADDL-binding sites were demonstrated to coincide with dendritic spines at postsynaptic termini of excitatory synapses [181]. ADDL binding also overlapped with NMDAR subunit NR1 on highly arborized neurons positive for  $\alpha$  calcium-calmodulin kinase II [181] which accumulates in postsynaptic termini of neurons involved in memory function [181]. In addition, ADDLs specifically bound to excitatory pyramidal, but not GABAergic, neurons [180], and to neurons

positive for NMDAR subunits NR1 and NR2B [180]. Similarly, ADDLs did not bind astrocytes or inhibitory neurons expressing glutamic acid decarboxylase [180]. Preferential binding of ADDLs to excitatory synapses at postsynaptic sites was consistent with the inhibitory impact of ADDLs on NMDAR-dependent LTP [26, 223] and NMDAR-mediated phosphorylation of cAMP-response-element-binding protein [226], demonstrating that ADDLs could impact crucial receptors involved in synaptic plasticity.

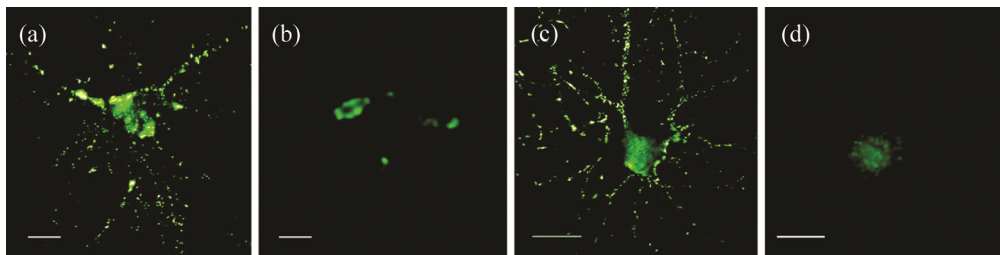


**Figure 2: Punctate ADDL-binding to neurons.** ADDLs isolated from AD brain or prepared *in vitro* show identical punctate binding to neuronal cell-surface proteins. Cultured hippocampal neurons were incubated with soluble extracts of human brain or synthetic ADDLs. Immunoreactivity against ADDLs was visualized by microscopy using M93 antibody. Soluble AD-brain proteins (a), soluble control-brain proteins (b), synthetic ADDLs (c), and synthetic ADDLs pre-treated (1 h) with oligomer-specific antibody M71 (d) are shown. Small puncta distributed along neurites, are evident for AD extracts and synthetic ADDLs, but not for control extracts or antibody-preadsorbed ADDLs (Scale bar = 10  $\mu$ m). Adopted with permission from [27].

Defective neuronal actin-regulatory machinery is an underlying factor in dendritic and synaptic dysfunctions in many neurological disorders accompanied by cognitive deficits, including AD and Down syndrome (reviewed in [213]). ADDLs were shown to affect spine shape, which, like receptor expression is a facet of spine cell biology with ramifications for signaling and plasticity [227, 228]. ADDL-induced alterations of spine morphology which resembled the morphology of immature and diseased spines associated with mental retardation and prionoses [229].

ADDL binding to neuritic spines was reported to induce expression of the activity-regulated cytoskeleton-associated protein (Arc), a synaptic immediate-early gene [181, 230]. Proper expression of Arc is essential for LTP, but its ectopic and aberrant expression causes failure of long-term memory formation [231]. ADDLs generated a rapid and sustained increase in synaptic Arc protein expression [181], which interfered with long-term memory formation [231] and was hypothesized to lead to

synapse failure and memory loss. De Felice *et al.* showed that ADDL treatment of mature primary hippocampal neurons led to reproducible and dose-dependent generation of reactive oxygen species (ROS) in the vicinity of synaptic ADDL-binding sites [182]. It was shown that ADDL binding to the NR1 subunit of NMDAR and NMDA-mediated  $\text{Ca}^{2+}$  influx led to ROS generation, further delineating the mechanisms of ADDL neurotoxicity [182]. Interestingly, ADDL treatment was shown to induce  $\tau$  hyperphosphorylation in neuroblastoma cells and rat hippocampal primary neurons before neuronal death occurred [177]. Intrahippocampal injection of an oligomer-specific antibody was sufficient to reverse the effect of amyloid and  $\tau$  pathologies, providing an additional insight into ADDL-mediated neurotoxicity [232].

Although *in vitro* experiments demonstrated that ADDLs interfered specifically with memory-associated experimental phenomena, a crucial question is whether ADDLs exist, and cause the same toxic effects, *in vivo*. Conformation-specific polyclonal [233] and monoclonal antibodies [179] shown to discriminate between ADDLs and  $\text{A}\beta$  monomers have been used to address this question. Dot-blot assays have detected ADDL immunoreactivity in transgenic mice and in AD brains which were extracted without detergents or harsh chemicals precluding extraction-induced alterations of the assembly structures [27, 225]. ADDL concentrations were 70-fold higher in AD brains compared to controls [27]. In the nontransgenic mouse brain, no ADDLs (detection limit  $<10$  fmol/ $\mu\text{g}$ ) were detected by dot-blotting brain extracts using an ADDL-specific antibody [225]. However, in brains of transgenic mice, ADDL concentrations varied from  $\sim 20$ – $250$  fmol/ $\mu\text{g}$  depending on the brain region tested [225]. Soluble brain proteins extracted in F-12 culture medium by ultracentrifugation contained ADDL immunoreactivity that correlated with presence of AD [27, 181] (reviewed in [59]). These findings support the hypothesis that ADDLs may be an important component in the amyloid cascade, as opposed to the poor correlation between insoluble amyloid deposits and cognitive impairment [59].

## **Protofibrils**

### ***Structural Characterization***

PF are  $\text{A}\beta_{40}$ - and  $\text{A}\beta_{42}$ -derived curvilinear, soluble assemblies, which were described originally by Walsh *et al.* [90] and Harper *et al.* [28]. Walsh *et al.* reported

studies using SEC, DLS, and TEM examining initial stages of A $\beta$  oligomerization and characterizing A $\beta$  intermediates during fibrillogenesis. By SEC, PF had apparent mass >100 kDa. They predominantly comprised curved, fibril-like structures of 6–8 nm in diameter and  $\leq$ 200 nm long as observed by TEM [90]. Harper *et al.* detected the same protofibrillar assemblies of A $\beta$  during polymerization by AFM [28]. They noted that A $\beta$ 40 PF, which appeared during the first week of incubation, had diameters of 3.1 nm and were 20–70 nm long [28]. The PF showed a periodic diametrical variation every 20 nm. In contrast, A $\beta$ 42 PF formed within the first day of incubation and had larger diameters (4.2 nm) than those of A $\beta$ 40. A $\beta$ 42 PF elongated overtime with diametrical periodicity similar to A $\beta$ 40 [28].

TEM examination of A $\beta$  PF with rotary shadowing [30] demonstrated flexible rods up to  $\sim$ 200 nm long, with larger diameters than those observed by regular TEM or AFM. PF appeared more beaded with a periodicity of 3–6 nm, and the proportion of small PF (<10 nm) was higher, suggesting that these smaller structures might have been overlooked using TEM with routine negative staining or that the preparations were simply different [30]. The beaded structures were shown to be typical of early PF, whereas at later time points, PF appeared smoother [234]. High-resolution AFM studies have demonstrated that A $\beta$ 40 PF had a diameter of  $\sim$ 4.3 nm, with periodicity of  $\sim$ 20 nm, and coexisted with spherical species of the same diameter [161]. Spheres similar to those have been hypothesized by us and others to be precursors which join together to form PF [32, 159].

PF have a high  $\beta$ -sheet content, a characteristic similar to that of mature amyloid fibrils [30] and are recognized by antibody WO1, which reacts with the fibrillar form of various amyloid proteins [235]. Thus, PF are the latest precursors on the pathway of fibril formation described to date. Nevertheless, apparently a substantial conformational rearrangement occurs upon maturation of PF into fibrils as evidenced by the observations that PF can be readily disassembled into LMW A $\beta$ , whereas mature fibrils do not typically disaggregate back into PF [30]. Proline substitution experiments showed that A $\beta$ 40 PF were “less structured” in the region Glu<sup>22</sup>–Gly<sup>29</sup> compared to mature fibrils [235]. Hydrogen–deuterium exchange data demonstrated that the C-terminal Met<sup>35</sup>–Val<sup>40</sup> and the N-terminal Asp<sup>1</sup>–Phe<sup>19</sup> regions of A $\beta$ 40 were highly exposed to solvent both in fibrils and PF. In contrast, the Phe<sup>20</sup>–Leu<sup>34</sup> segment was highly protected from hydrogen–

deuterium exchange in fibrils but much less so in PF [78]. The  $\beta$ -structure ( $\beta$ -sheet and  $\beta$ -turn) content of PF was similar to that of fibrils as assessed by CD studies [90]. Collectively, these data suggested that the  $\beta$ -sheet elements comprising the amyloid fibrils were already present in PF. These elements could be expanded into adjacent residues and other elements, such as lateral association of filaments, may contribute to the maturation of amyloid fibrils.

### ***Biological Activity***

Initial studies to assess the biological activity of PF were performed in cultured primary rat cortical neurons over a time scale of minutes to hours, presumably before PF convert to fibrils [30]. In these experiments, compromise of cell viability by SEC-isolated PF was evaluated using the 3-(4,5-dimethylthiazol-2-yl)-2,5-diphenyltetrazolium bromide (MTT) assay [236]. It was found that PF and fibrils altered the normal physiology of cultured neurons, whereas LMW A $\beta$  did not [30]. To explore and compare the toxic effects of LMW A $\beta$ , PF, and fibrils further, Hartley *et al.* used rat cerebral primary mixed cultures (containing neurons, astrocytes, and microglia) and showed that PF caused neuronal injury and altered electrophysiological activities, ultimately causing cell death [30]. Although LMW A $\beta$  caused a rapid but transient increase in excitatory post-synaptic currents (EPSCs), PF or fibrils ( $\sim 3 \mu\text{M}$ ) invariably produced rapid and sustained increases in electrical activity, six-fold greater than that induced by LMW A $\beta$  [30]. Similarly, PF and fibrils significantly increased the frequency of action potentials and augmented the frequency and size of membrane depolarization compared to LMW A $\beta$  preparation [29]. Substantial neuron loss (80% as opposed to 10% non-treated cells) was observed consistently using the lactate dehydrogenase assay [237] and immunostaining against neuron-specific, microtubule-associated protein-2, after 5 days exposure to LMW and protofibrillar A $\beta$  [29]. It was hypothesized that LMW A $\beta$  could either convert to PF that cause the neurotoxicity or it could induce neurotoxicity by a mechanism independent of PF [29]. Relevant to this hypothesis, it was initially shown that human brain-derived A $\beta$  dimers inhibited LTP, enhanced LTD, and reduced dendritic spine density in rodent hippocampal neurons [193]. However, it was found later that covalently stabilized A $\beta$  dimers readily formed relatively stable PFs, which mediated the above-mentioned toxic activities (see Table 1) [174].

Important insight into the clinical relevance of PF came from investigation of a family in Northern Sweden, members of which carry a mutation in the *app* gene that leads to a single amino acid substitution in the A $\beta$  region, E22G (dubbed the Arctic mutation) [188]. Surprisingly, even though carriers of this mutation have decreased plasma levels of A $\beta$ 40 and A $\beta$ 42 compared to non-carriers, they develop early-onset AD [188]. *In vitro* fibrillization studies showed that A $\beta$  containing the E22G substitution formed PF faster and in larger quantities than wild-type A $\beta$ , suggesting that PF may be the main disease-causing agents in carriers of the Arctic mutation [188]. These findings, along with the observations of PF formation by most other amyloidogenic proteins, have positioned PF as a likely primary pathogenic assembly state and an important target for drug development efforts for amyloidosis [238].

Concentrations of 4-hydroxy-2-nonenal (HNE), a metabolite of oxidative stress resulting from fatty-acid peroxidation, and of HNE-derived lipid peroxidation products, have been shown to increase in AD [239]. HNE has been shown to modify A $\beta$  by 1,4 conjugation to primary amino groups and Schiff base formation, which could result in putative covalent intermolecular cross-linking of A $\beta$  monomers [240]. A $\beta$ 40 prepared after a 285-h incubation with HNE predominantly had a PF-like, curved morphology when examined by AFM, whereas preparations formed in the absence of HNE comprised straight fibrils predominantly [240]. Both the long, straight fibrils formed in the absence of HNE and the curved fibrillar aggregates formed in the presence of HNE were rich in  $\beta$ -sheet structure, based on their CD spectra. In the presence of HNE, accelerated formation of protofibrillar A $\beta$ 40 species was observed, whereas generation of mature straight fibrils even upon extended incubations was inhibited [240]. These data suggested that HNE could cause accumulation of toxic A $\beta$  PF by preventing their maturation to the less toxic fibrils [239]. Similarly, docosahexaenoic acid was shown to stabilize soluble A $\beta$ 42 PF and hinder their conversion to insoluble fibrils, thus leading to a sustained A $\beta$ -induced neurotoxicity measured using cultured PC12 cells [241]. These observations suggest that toxic effects of PF could be promoted by molecular interactions that prevented downstream fibril formation.

## A $\beta$ \*56

Lesné and colleagues have identified an oligomeric A $\beta$  species, termed A $\beta$ \*56, that caused cognitive deficits in middle-aged transgenic *Tg(APP<sup>SWE</sup>)2576Kahs* (*Tg2576*) mice [31]. The *Tg2576* mice express high levels of a human APP variant, which carries a familial AD-linked double mutation originating in a Swedish lineage (K670N, M671L) [242, 243]. A $\beta$  concentrations in these mice increase rapidly at 6 months of age, and abundant amyloid plaques are apparent between 9–12 months [242]. *Tg2576* mice recapitulate many other neurological features of AD, including neuroinflammation and oxidative stresses, dystrophic neurites, and significant cognitive deficits (reviewed in [242]). However, other important features, such as neurofibrillary tangles and significant neuron loss are not found in this model [244].

Because in these and other APP transgenic mice administration of A $\beta$ -specific antibodies has been shown to rapidly ameliorate memory decline, and because memory deficits were thought to precede plaques, Lesné *et al.* reasoned that a particular A $\beta$  species could promote cognitive decline preceding plaque maturation [31]. They found that insoluble A $\beta$  accumulated over 7 months without noticeable spatial memory decline. In contrast, certain soluble and extracellular A $\beta$  species, which migrated as LMW bands in SDS-PAGE/Western blots, correlated strongly with memory deficits at 6 months of age, suggesting that these oligomers, particularly those with apparent gel mobility of A $\beta$  dodecamers, were important neurotoxins in this model. Based on these data, it was proposed that similar species could be causing AD [31]. In support of this hypothesis, when pathophysiologically relevant concentrations of A $\beta$ \*56 (8.5 pmol) were administered into the lateral cerebral ventricles of healthy young rats pre-trained in the Morris water maze, the rats developed defective long-term spatial memory. These are important findings supporting the central role of oligomeric A $\beta$  in the disease mechanism of AD.

The structural characterization of A $\beta$ \*56 as a putative dodecamer should be interpreted cautiously because the apparent electrophoretic migration of this oligomer, corresponding to 56 kDa, may not represent accurately its *in vivo* mass given the artifactual effects of SDS [63], which was included in the initial steps of

the extraction protocol. Of note, Jacobsen *et al.* have found that cognitive deficits in *Tg2756* mice occurred before the reported time of appearance of A $\beta$ \*56 [245].

Longitudinal water-maze spatial training was reported to reduce A $\beta$  and  $\tau$  neuropathology transiently but significantly, and improve later learning performance in a triple transgenic (3 $\times$ Tg) murine model of AD [246]. The 3 $\times$ Tg-AD mice harbor human APP containing the Swedish mutations (KM670/671NL), human  $\tau$  containing the frontotemporal dementia-associated mutation, P301L, and a human presenilin 1 gene (*PSEN1*) containing the AD-linked mutation, PS1M146V [246]. The improvement in performance in 3 $\times$ Tg-AD mice occurred at 6–12 months and depended strongly on spatial training [246]. To achieve this effect, pre-training was required before development of overt neuropathology, presumably because it delayed A $\beta$  redistribution to extracellular plaques and reduced the concentration of A $\beta$  oligomers, including one with an apparent SDS-PAGE mobility similar to A $\beta$ \*56 [246]. These findings suggest that A $\beta$ \*56 is a neurotoxic form of A $\beta$  that may be important in the etiology of AD. Currently, the structural relationships of this species to PF and ADDLs are unknown, although under certain conditions, ADDLs also display electrophoretic migration corresponding to a dodecamer [27].

### A $\beta$ Pores

A $\beta$  pores are channel-like structures believed to disrupt cell membranes and cellular ionic homeostasis [247]. In lipid bilayers *in vitro*, A $\beta$  was shown to form uniform pore-like structures with 8–12 nm outer and 2 nm inner diameters [247, 248]. These are thought to serve as Ca<sup>2+</sup> channels and thus have been hypothesized to cause excitotoxicity and mediate A $\beta$ -induced neurotoxicity in AD [249, 250]. Reports of various models including artificial phospholipid membrane bilayers, excised neuronal membrane patches, whole-cell patch-clamp experiments, and phospholipid vesicles support a channel-forming property of A $\beta$  [247, 250-262]. In these studies, imaging techniques [247, 254, 256, 257], electrophysiological experiments [250, 251, 253-255, 257, 258, 261, 262], or cation-sensitive dyes [257] were used to assess channel-like properties of A $\beta$ . However, other studies have reported general disruption of the plasma membrane homeostasis without channel formation [263-265]. In a study by Kaye *et al.* the effect of spherical A $\beta$ 42 oligomers on membrane conductivity was assessed using planar lipid bilayers [265]. It was found that these A $\beta$ 42 oligomers specifically

increased the conductance of the bilayer in a concentration-dependent manner whereas no increase in conductance was observed for LMW A $\beta$  species (monomer or dimer) or for A $\beta$  fibrils [265]. The increase in membrane conductance in response to spherical oligomers occurred in the absence of evidence for discrete ion-channel or pore formation [265]. It was postulated that soluble oligomers enhanced movement of ions through the lipid bilayer by a channel-independent mechanism [265]. High sensitivity recording has indicated that there was little change in the noise level of the current trace as the current increased from 0 to ~100 pA after oligomer addition.

A $\beta$ 42 was reported to be more prone to forming channels than A $\beta$ 40 [18]. High-resolution examination of individual A $\beta$ 42 channel-like structures revealed two subunit arrangements: rectangular and hexagonal structures, putatively comprising tetramers and hexamers, respectively [247]. The disease-associated mutant E22G form of A $\beta$ 40 was shown to form pore-like structures akin to those formed by A $\beta$ 42 [36, 266]. Treatment of the hypothalamic neuronal cells GT1-7 with A $\beta$ 40 has led to simultaneous formation of Ca<sup>2+</sup> channels and increased intracellular Ca<sup>2+</sup> concentration ([Ca<sup>2+</sup>]<sub>i</sub>) as determined by fluorometric measurements, suggesting that A $\beta$ 40 also could disrupt biological and artificial membranes, possibly *via* formation of pores [252, 267].

### **Paranuclei**

Using PICUP followed by SDS-PAGE analysis, A $\beta$ 40 and A $\beta$ 42 were shown to form distinct oligomer size distributions, suggesting that the two A $\beta$  alloforms oligomerized through distinct pathways [32]. In those experiments, A $\beta$ 42 preferentially formed pentamer/hexamer units termed paranuclei, which self-associated into larger assemblies, including dodecamers and octadecamers [32]. In contrast, A $\beta$ 40 formed a roughly equimolar, quasi-equilibrium mixture of monomers, dimers, trimers, and tetramers [103].

A systematic study using PICUP assessed oligomerization of 34 A $\beta$  alloforms [34], including those containing familial AD-linked amino acid substitutions, N-terminal truncations found in AD plaques, and modifications that altered the charge, hydrophobicity, or conformation of A $\beta$  [34]. C-terminal length was found

to be the most important structural determinant in early oligomerization, and the side-chain of Ile<sup>41</sup> in A $\beta$ 42 was found to be important both for effective formation of paranuclei and for their self-association [34]. Thus, A $\beta$ 41 and longer alloforms formed abundant paranuclei whereas A $\beta$ 40 and shorter alloforms did not [32]. The side-chain of Ala<sup>42</sup>, and the C-terminal carboxyl group, affected paranucleus self-association [34]. In a related study, oxidation of Met<sup>35</sup> in A $\beta$ 42 was found to preclude paranucleus formation and led to generation of oligomers indistinguishable from those produced by A $\beta$ 40 [33]. These data demonstrated that modification of even a single atom could induce dramatic effects on A $\beta$  paranucleus formation and downstream assembly, providing important insights into mechanisms of A $\beta$  assembly into neurotoxic oligomers potentially relevant to AD pathogenesis. As discussed above, the difference in toxicity between A $\beta$ 40 and A $\beta$ 42 [268] correlates with observations that certain oligomeric A $\beta$  forms, such as paranuclei and ADDLs, are produced by A $\beta$ 42 only, emphasizing strong correlation of the latter to the pathogenic process of AD.

### **$\beta$ amy Balls**

$\beta$ amy balls are A $\beta$ 40-derived structures that form spontaneously when high concentrations of A $\beta$ 40 (60–600  $\mu$ M) are incubated in phosphate-buffered saline at 30°C for 8–13 days [39].  $\beta$ amy balls, have diameters of 20–200  $\mu$ m and were shown to be composed of birefringent 6–10-nm diameter A $\beta$  fibrils with random orientation [39]. Although such high A $\beta$  concentrations used to generate  $\beta$ amy balls are unlikely to occur *in vivo* [22, 269], it was argued that these concentrations could possibly occur locally at microfoci circumscribing the amyloid plaques in AD brain [39]. Interestingly, *in vivo* extracellular retinal deposits called drusen have an apparent similarity to  $\beta$ amy balls. Drusen are A $\beta$ -containing macromolecular assemblies and are a pathologic sign in age-related macular degeneration [270]. However, these structures have larger diameters and unlike  $\beta$ amy balls, which are produced from synthetic A $\beta$ 40 *in vitro* in the absence of other proteins, the retinal deposits contain other A $\beta$ -binding proteins [270].

### **Amylospheroids**

Amylospheroids, were described as A $\beta$ 40- and A $\beta$ 42-derived assemblies with 10–15-nm diameters [35]. A $\beta$ 40 amylospheroids formed by incubating 350  $\mu$ M of the

peptide in phosphate-buffered saline under slow rotation for 5–7 days at 37°C [35]. A $\beta$ 42 amylospheroids were produced by incubating 0.01–1  $\mu$ M peptide in the same buffer for 8–10 h at 4°C [35]. Indeed, it was observed that A $\beta$ 42 amylospheroids, which formed faster and at substantially lower concentration than those of A $\beta$ 40, were also more toxic than A $\beta$ 40 amylospheroids [35], correlating with the higher toxicity and pathogenicity of A $\beta$ 42 in AD compared to A $\beta$ 40. Although these A $\beta$ 42 assemblies are spherical [35], they are morphologically distinct from ADDLs in their diameter (2.5 nm by AFM [95] vs. 10 nm by TEM, respectively).

Using antibodies reactive to amylospheroids, Noguchi *et al.* reported immunoisolation of neurotoxic, 10–15-nm, spherical A $\beta$  assemblies, from brains affected by AD or dementia with Lewy bodies, which they termed native amylospheroids [198]. The amount of native amylospheroids correlated with disease severity. These native amylospheroids were non-reactive with antibody A11, had a high mass (>100 kDa), and induced degeneration of human neurons *in vitro*. Amylospheroid-induced neuronal degeneration was reverted only by anti-amylospheroid antibodies. Immunospecificity of the antibodies for amylospheroids was suggested to be indicative of their tertiary surface topology distinct from those of other reported assemblies, including dimers, ADDLs, or A11-reactive assemblies [198]. Amylospheroid-specific polyclonal antibodies were generated in immunized rabbits (rpASD1;  $K_d = 5$  pM) and monoclonal antibodies in hamsters (haASD1;  $K_d = 0.5$  pM). These antibodies reacted with epitopes distinct from those on dimers, A11-reactive 12-mers, or fibrils [198]. Amylospheroids bound neuronal presynaptic target(s) and demonstrated a mode of toxicity independent of NMDAR-mediated synaptic transmission [198].

### **Globulomers**

Globulomers are A $\beta$ 42 oligomers produced by incubating 400  $\mu$ M A $\beta$ 42 in phosphate-buffered saline in the presence of 0.2% SDS at 37°C for 6 h [89]. These species also have been produced by incubation of A $\beta$ 42 with lauric, oleic, or arachidonic acids [89], suggesting that they are generated by interaction of A $\beta$ 42 with micelles of SDS or fatty acids. A $\beta$ 42 globulomers were neurotoxic to rat brain slices and antibodies generated against globulomers detected

immunoreactive epitopes in tissue sections [89]. Similar globular structures of A $\beta$ 40 were reported to form after 18 h incubation in 25 mM 2-morpholinoethanesulfonic acid buffer (pH 4.5) in a "hanging-drop" environment [271]. Hanging-drop environment is used extensively for protein crystallization and provides a static, low-convection environment with a markedly increased hydrophobic air–buffer interfacial area compared to that of the microfuge-tube environment [271].

### Toxic Fibrillar Oligomers of A $\beta$

Based on reactivity of antibodies specific for epitopes generically associated with distinct aggregation states of different amyloid assemblies, at least two types of oligomeric amyloid assemblies were proposed: fibrillar and non-fibrillar oligomers [38]. Accordingly, monomers of amyloidogenic proteins aggregate to form non-fibrillar oligomers reactive with polyclonal antibody A11, but not OC. Non-fibrillar oligomers are transient intermediates that may undergo further aggregation and form fibrils ultimately. On the other hand, amyloidogenic proteins also can self-associate into fibrillar oligomers that are reactive with OC, but not A11. These fibrillar oligomers likely represent fibril nuclei or seeds which can elongate by recruiting additional monomers [38]. Interestingly, in the presence of Zn<sup>2+</sup>, A $\beta$ 40 was found to form toxic, fibrillar oligomers that upon incubation self-associated into large, non-fibrillar structures and lost their toxicity [164]. The OC antibody has been generated in rabbits immunized with A $\beta$  fibrils [189], suggesting that A $\beta$ -derived fibrillar oligomers share surface structural features with A $\beta$  fibrils. Furthermore, fibrillar oligomers are similar to fibrils in terms of their ability to seed formation of additional fibrillar oligomers, but not A $\beta$  fibrils [191], suggesting that they likely have a lattice distinct from the fibrils.

James *et al.* recently characterized a particular preparation of toxic A $\beta$ 42-derived fibrillar oligomers (TABFOs) [190]. This TABFO preparation had similar morphology and OC reactivity to fibrillar oligomers reported previously [191]. To prepare TABFOs, recombinant wild-type A $\beta$ 42 was dissolved in HFIP initially. After removing HFIP by evaporation, A $\beta$ 42 was resuspended in dilute ammonium hydroxide, which prevents fibrillation and allows formation of TABFOs. TABFOs were stable in SEC, which was the final purification step. TABFOs converted into

fibrils in phosphate-buffered saline. TABFO-derived fibrils had typical amyloid features by TEM and ThT fluorescence and contained significant  $\beta$ -structure and negligible  $\alpha$ -helical content by CD spectroscopy [190]. Structural studies showing the fibril-like cross- $\beta$  structure of TABFOs may explain the reactivity of the antibody OC with fibrillar oligomers and mature amyloid fibrils [38].

Functionally, TABFOs were found to be toxic to neurons and HeLa cells by MTT assays at  $\geq 2.25 \mu\text{g/mL}$  ( $0.5 \mu\text{M}$  of  $\text{A}\beta_{42}$  monomer equivalent). It was proposed that TABFO toxicity may be related to their potential to form membrane pores. Pore formation has been implicated in the toxicity of  $\text{A}\beta$  oligomers [36, 272].

### **OLIGOMERS OF DISEASE-RELATED AMYLOIDOGENIC PROTEINS OTHER THAN $\text{A}\beta$**

Over twenty human amyloidoses are caused by aberrant protein folding and aggregation [273-275]. As  $\text{A}\beta$  often is considered an archetypal protein in studies of these diseases, the discoveries of toxic non-fibrillar  $\text{A}\beta$  assemblies and their centrality in AD have led to a search for similar assemblies of other amyloidosis-related proteins. To date, at least 24 different proteins have been identified as causative agents of amyloidoses [276]. In essentially all cases, such assemblies have been found and had adverse biological effects similar to those of  $\text{A}\beta$  oligomers [5, 7, 11, 277]. Because this review focuses on non-fibrillar assemblies of  $\text{A}\beta$ , we do not intend to cover assemblies of other amyloidogenic proteins in detail, but rather to highlight a few examples and discuss current features that are common to all or most of these assemblies.

The structures reported for amyloidogenic protein oligomers, in general, have been similar to those described for  $\text{A}\beta$ , namely PF, annular (pore-like) PF, and spherical oligomers. In several cases, annular PF have been the predominant structures found. However, as discussed elsewhere [63], it is important to note that in many cases the term PF has been used even though the morphologies of the assemblies under study were distinct from those originally defined as PF.

One of the most studied amyloidogenic proteins is  $\alpha$ -synuclein, the function of which is not clear although it is believed to be part of the ubiquitin system that

marks proteins for proteasomal degradation [278, 279].  $\alpha$ -Synuclein is the predominant component in Lewy bodies, the pathological hallmarks in PD brain, and has been implicated in other degenerative disorders (synucleinopathies), including dementia with Lewy bodies and multiple system atrophy [280]. Similar to A $\beta$ ,  $\alpha$ -synuclein belongs to a growing family of “intrinsically unstructured” proteins [281, 282], a characteristic that perhaps renders these proteins more prone to undergoing amyloidogenic assembly. Mutant  $\alpha$ -synuclein alloforms linked to familial PD were found to oligomerize faster than the wild-type protein, whereas the rate of fibril formation did not correlate with the presence of disease-causing mutations [283]. Non-fibrillar assemblies of both wild-type and mutant  $\alpha$ -synuclein included spherical oligomers, protofibrillar structures, and most abundantly, annular PF [266, 284]. The latter morphology suggested that the mechanism whereby  $\alpha$ -synuclein induces toxicity is pore formation in cell membranes. In agreement with this idea, protofibrillar  $\alpha$ -synuclein was found to permeabilize synthetic vesicles [285]. Interestingly, this effect was increased by the familial PD-linked mutants A30P and A53T [286], but not by the mutant E46K [287]. Thus, although pore formation may be involved in  $\alpha$ -synuclein-induced toxicity, other mechanisms also have been implicated, but these are not well-understood [288].

Two amyloidogenic proteins involved in sugar metabolism are insulin and IAPP. Insulin aggregation is not associated with disease but has been studied by multiple groups as a convenient *in vitro* model [289-292]. Biophysical investigation of insulin fibrillogenesis has identified oligomeric populations with conformations distinct from those of natively folded insulin dimer and hexamer [293]. Taking advantage of the relative stability of insulin oligomers and using special instrumentation, Robinson and co-workers have provided one of the first examples of mass spectrometric investigation of amyloidogenic protein oligomers, and demonstrated the power of this experimental approach for studying the effects of pH and metal ion binding on oligomerization [294]. In a study combining structural characterization and cytotoxicity experiments, Grudzielanek *et al.* found no toxicity for low-order insulin oligomers, whereas substantial toxicity was measured for high-order,  $\beta$ -sheet-rich aggregates that displayed either fibrillar or amorphous morphology [295].

In contrast to insulin, IAPP aggregation is believed to be causative in T2D. IAPP is a 37-residue peptide hormone produced in pancreatic  $\beta$ -cells and co-secreted with insulin. Early stages of T2D are characterized by insulin resistance followed by increased insulin and IAPP secretion. Elevated IAPP concentrations lead to its assembly into toxic oligomers and insoluble aggregates [14]. Oligomeric and protofibrillar IAPP were shown to interact with synthetic membranes [296], a characteristic that decreases with further aggregation, providing a clue for the mechanism of IAPP toxicity [297]. The interaction with biological membranes may induce a transient  $\alpha$ -helical conformation in IAPP, presumably facilitating penetration of the oligomers into the membrane resulting in solute leakage across the membrane [298, 299]. Strong evidence for the neurotoxic role of IAPP oligomers in T2D was given in a study in which rifampicin, an inhibitor of IAPP fibril, but not oligomer formation, did not protect pancreatic  $\beta$ -cells against apoptosis induced by either endogenously expressed or externally applied IAPP [300]. More recent data have suggested that *in vivo*, toxic IAPP oligomers are formed intracellularly and therefore, oligomer-specific antibodies do not prevent cell death *in vitro* and *in vivo* [301].

Numerous other examples have demonstrated the important roles of oligomers of amyloidogenic proteins as disease-causing agents. Before the focus in the amyloid field shifted from fibrils to oligomers, it had been known that although no sequence similarity was found among amyloidogenic proteins, the fibril structures of all were highly similar, characterized by fibrillar morphology with periodic helical twist and cross- $\beta$  structures [302, 303]. The realization that the precursor oligomers may be the proximate disease-causing agents in the amyloidoses related to these proteins raised the question whether oligomer structures also were similar. High-resolution microscopic studies of oligomeric structures, mostly by TEM and AFM, have demonstrated that in most cases the morphologies observed were spherical, annular, or protofibrillar (worm-like). Conformational studies of oligomers have been difficult because the oligomers typically are metastable and exist in mixtures. Structural insight has been offered by Glabe and co-workers who developed antibodies that showed specificity for oligomers of proteins with unrelated sequences but did not bind the monomeric or fibrillar forms of these proteins [304]. The first polyclonal antibody, A11, and similar antibodies

developed in follow-up studies showed remarkable ability to bind to oligomers formed by proteins as diverse as A $\beta$ ,  $\alpha$ -synuclein, IAPP, lysozyme, insulin, poly Q, and prion fragments [304]. These observations strongly suggested that a predominant mechanism whereby these oligomers injure cells is through permeabilization of the plasma membrane because toxic oligomers sharing a common structure formed by both intracellular and extracellular proteins [264, 265]. As discussed above, oligomers may interact with membranes by several mechanisms, including pore-formation and shallow penetration under the surface resulting in thinning of the membrane and a net increase in its permeability. Further delineation of the specific mechanisms governing these interactions requires additional studies and will be highly important for designing reagents that block them.

### **NON-FIBRILLAR ASSEMBLIES OF DISEASE-UNRELATED PROTEINS**

In his 1972 Nobel-Prize acceptance speech, Anfinsen stated that “the native conformation [of proteins] is determined by the totality of inter-atomic interactions and hence by the amino acid sequence, in a given environment” which does not always favor the normally functional and folded state of proteins. Consistent with Anfinsen's theory, the conformational-change hypothesis postulates that one of 17 normally soluble and functional human proteins could undergo structural alterations under partially denaturing conditions leading to self-assembly and amyloid fibril formation [305]. Besides disease-associated amyloid-forming proteins, and proteins that naturally form non-pathological, functional amyloid-like fibrils (reviewed in [306]), disease-unrelated proteins [307] and artificially designed peptides [308-310] have been found to form amyloid under particular non-native conditions. To the best of our knowledge, the ability of disease-unrelated peptides and proteins to form amyloid fibrils was first reported by Guijarro *et al.* [311] and Litvinovich *et al.* [312]. The src-homology 3 (SH3) domain of bovine phosphatidyl inositol 3-kinase (PI3K), an 85-residue,  $\beta$ -structured protein, was shown to aggregate slowly and form amyloid fibrils under acidic pH [311]. Thenceforth, the disease-unrelated SH3 domain has served as an excellent model for systematic studies examining structural properties of amyloid fibrils and molecular mechanisms of amyloid formation [313-316]. The PI3K-SH3 was shown to adopt a compact denatured state under acidic conditions before

formation of amyloid fibrils [317]. Limited proteolysis studies showed that PI3K-SH3 at low pH had a partially folded conformation [318] and progressively displayed enhanced susceptibility to proteolysis, suggesting that the protein became more unfolded in the early stages of aggregation [318]. In contrast, the amyloid fibrils that formed over longer periods of time were resistant to proteolysis [318]. It was suggested that the protein aggregates formed initially were relatively dynamic and this flexibility allowed for the particular interactions leading to formation of the highly ordered fibrils [318].

After Litvinovich *et al.* demonstrated formation of amyloid-like fibrils by self-association of murine fibronectin type III module [312], others reported that similar conversions in a number of disease-unrelated proteins could be induced *in vitro* by a deliberate, rational choice of excipient conditions [317, 319]. Examples (reviewed in [307]) include human apolipoprotein CII, ADA2H, amphotericin, stefin B and endostatin, murine V1 domain, equine acylphosphatase (AcP) and apomyoglobin, monellin (*Dioscoreophyllum camminsii*), and yeast phosphoglycerate kinase. Fezoui *et al.* reported *de novo* design of a monomeric  $\alpha$ -helix-turn- $\alpha$ -helix peptide ( $\alpha\alpha$ ) which converted to  $\beta$ -sheet-rich amyloid-type, protease-resistant, 6–10 -nm fibrils at 37°C in a neutral aqueous buffer [308]. Formation of fibrils from full-length proteins requires solution conditions that partially or completely disrupt the native structure of the protein, but not completely disturb hydrogen bonds [317]. It was observed that proteins with as few as four residues, and amino-acid homopolymers that are unable to fold into stable globular structures, form fibrils readily [307, 320, 321]. Therefore, it has been suggested that the ability to form amyloid fibrils could be a generic property of polypeptide chains [307].

In one study of non-fibrillar assemblies of disease-unrelated proteins, tapping-mode AFM was used to follow the process of HypF-N aggregation which was induced by incubating the protein in the presence of trifluoroethanol (TFE) [322]. HypF-N was shown to aggregate hierarchically through a number of distinct steps with morphologically different intermediates [322]. Initially, globular assemblies appeared, which subsequently self-assembled into beaded chains, similar to those found for amyloidogenic proteins [323-325]. Subsequently, these organized into crescents, large annular and ribbon-like structures (Fig. 3), and eventually

assembled into mature fibrils of different sizes [322]. The globule height was measured to be 2.8–3.0 nm [322]. Although HypF-N and AcP are similarly prone to conversion from a predominantly  $\alpha$ -helical conformation to one rich in  $\beta$ -sheet, HypF-N aggregation rate was found to be dramatically higher ( $\sim 1,000$ -fold) than AcP, possibly due to the higher hydrophobicity and lower net charge of HypF-N compared to AcP [326].

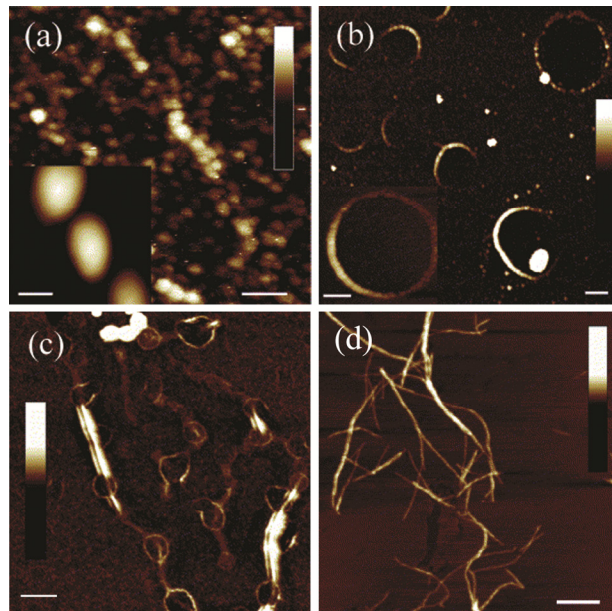


**Figure 3: Hierarchical aggregation process of HypF-N.** (a) Tapping AFM images taken under liquid (height data, scan size 670 nm, Z range 20 nm) of HypF-N globular aggregates observed a few hours after the onset of the aggregation process in the presence of 30% TFE. Scale bar = 100 nm. Inset, STM image (height data, scan size 42 nm, Z range 15 nm) of globular aggregates obtained under the same conditions, but diluted 1:50 prior to deposition onto the substrate; the globules are apparently asymmetric and tend to form a defined mutual orientation. Scale bar = 10 nm. (b) HypF-N crescents and a ring observed after 3 days of incubation in 30% TFE (scan size 5.3  $\mu\text{m}$ , Z range 45 nm). Inset, high resolution image of a ring (scan size 1.9  $\mu\text{m}$ , Z range 120 nm), revealing its globular components, taken after 5 days of incubation in 30% TFE. Scale bars = 400 nm. (c) Tapping-mode AFM image taken in air (height data) after three days of incubation in 30% TFE showing the co-existence of annular structures with thin and wide ribbon-like fibrils. Scan size 4.8  $\mu\text{m}$ , Z range 40 nm. Scale = 500 nm. (d) Tapping-mode AFM images taken in air (height data) of mature fibrils obtained in 30% TFE showing supercoiled fibrils obtained after eight days (scan size 3.6  $\mu\text{m}$ , Z range 80 nm). Adopted with permission from [322].

In contrast to fibrils of disease-causing amyloidogenic proteins, those formed by disease-unrelated proteins did not cause cytotoxicity in cell-culture experiments.

For example, fibrils formed by the aforementioned  $\alpha$  peptide displayed no neurotoxicity, even though they were morphologically indistinguishable from A $\beta$  and IAPP fibrils, which were toxic [308]. It was therefore unexpected that the non-fibrillar assemblies of PI3K-SH3 and HypF-N were shown to be highly toxic to PC12 cells and murine fibroblasts *in vitro* [327]. The extent of cellular injury caused by the cytotoxic oligomers was comparable to that of A $\beta$ 42 oligomers, whereas the corresponding fibrils of both PI3K-SH3 and HypF-N were benign.

Early non-fibrillar HypF-N assemblies were shown to permeabilize artificial phospholipid membranes more efficiently than mature fibrils, indicating that this disease-unrelated protein displayed the same toxic properties as non-fibrillar assemblies of pathological peptides and proteins [322]. Further investigation of the cellular effects of HypF-N oligomers revealed that they entered the cytoplasm and caused an acute rise in ROS levels and  $[Ca^{2+}]_i$ , leading to cell death [328]. In a study where murine fibroblasts and endothelial cells were treated with non-fibrillar HypF-N assemblies, the two cell types underwent two different death mechanisms—fibroblasts exposed for 24 h to 10  $\mu$ M HypF-N oligomers underwent necrosis, whereas endothelial cells treated similarly sustained apoptosis [329]. A similar study comparing cytotoxic effects of non-fibrillar and fibrillar HypF-N assemblies using a panel of normal and pathological cell-lines showed that cells were variably affected by the same amount of non-fibrillar aggregates, whereas mature fibrils showed little or no toxicity [330]. This difference in the extent of compromise of cell viability was significantly related to the cell-membrane cholesterol content and to different cellular  $Ca^{2+}$ -buffering and antioxidant capacities of the various cell types [330]. Recently, it has been shown that microinjection into rat brain nucleus basalis magnocellularis of PI3K-SH3 or HypF-N assemblies, but not the corresponding mature fibrils, compromised neuronal viability dose-dependently [8]. Taken together, these data clearly demonstrate that the non-fibrillar assemblies of disease-unrelated proteins are highly toxic whereas the corresponding mature fibrils are not [8]. The toxic effect of the oligomers may arise when these assemblies assume a “misfolded” conformation which may expose hydrophobic residues that are natively entombed within the core structure. Such aggregation-prone regions may interact with membranes and other cellular components modifying their structural/functional homeostasis.

Dobson and co-workers have proposed that evolutionary mechanisms may have been in force to ensure propagation of proteins that resist aggregation for efficient function [331]. However, genetic, environmental, and metabolic factors that decrease the solubility or increase the concentration of susceptible proteins *in vivo* may act against those forces and induce protein misfolding disorders including neurodegenerative diseases [331].

The fact that aggregates of some disease-unrelated proteins could function similarly to those formed by amyloidogenic, disease-related peptides and proteins, has profound implications for understanding the mechanistic fundamentals of abnormal protein deposition in amyloidoses. These observations facilitate investigation and discovery of the general mechanistic features underlying protein misfolding and aggregation [307] and help defining likely targets for drug design.

### **CRYSTALLOGRAPHIC STUDIES OF AMYLOID OLIGOMER MODELS**

The dynamic, polymorphic, transient, and non-crystalline behaviors of oligomeric amyloid species have precluded determination of their structures at atomic resolution. However, recent X-ray crystallographic studies have provided structural details of oligomers of peptides derived from amyloidogenic protein sequences, shedding light on oligomer structures [332-335]. In one study, nanobodies were used to trap and characterize intermediates of  $\beta_2$ -microglobulin ( $\beta_2m$ ) fibrillation for X-ray crystallographic studies [335]. A single-domain antibody that blocks fibrillogenesis of a proteolytic amyloidogenic  $\beta_2m$  fragment ( $\Delta N6\beta_2m$ ) was used to trap and crystallize  $\Delta N6\beta_2m$  for crystallography. This approach identified two extended hinge loops, which folded into a two-stranded antiparallel  $\beta$ -sheet. The  $\beta$ -strands of this sheet self-associated and stacked perpendicularly to the strand direction to form intermolecular  $\beta$ -sheets running parallel to the axis of oligomer growth, providing an elongation mechanism by a self-template growth mechanism [335].

Another study used microcrystals of a cyclic, 42-membered peptide ring consisting of two densely packed  $\beta$ -sheets. The individual  $\beta$ -strands, joined by two  $\delta$ -linked,  $\beta$ -turn-mimicking ornithine residues, were antiparallel to each other [333]. Key amyloidogenic segments of A $\beta$  and  $\tau$  were selected and incorporated

into these macrocyclic structures to model their respective oligomeric arrangements [333]. These macrocycles assembled into dimers through backbone hydrogen bonds in parallel or antiparallel  $\beta$ -strand arrangements. Tetramer formation occurred through complementary side-chain interactions, forming a variety of  $\beta$ -sheet– $\beta$ -sheet packing geometries, deviating by  $0^\circ$  to  $45^\circ$  from the typical fibrillar cross- $\beta$  arrangements [333]. Despite architectural and interfacial similarities between macrocyclic oligomers and fibrillar structures, the macrocyclic oligomers differed from fibrillar structures by an additional degree of freedom in the sheet–sheet packing. In the cross- $\beta$  structure of fibrils, the strands in opposing sheets are constrained to either parallel or antiparallel orientations. In contrast, in the oligomeric macrocycles the opposing  $\beta$ -sheet orientations ranged from orthogonal to parallel arrangements, likely accommodating additional (non-cross- $\beta$ ) sheet–sheet packing geometries, which potentially limit extension of  $\beta$ -structures into macrocyclic oligomers [333]. Further work will be needed to test whether this is a general structural phenomenon in all oligomers.

Laganowski *et al.* [336] used a Rosetta-Profile algorithm to identify amyloid-forming fragments in  $\alpha$ B-crystallin, a chaperone protein found in the ocular lens [337]. The algorithm identified polypeptide sequence fragments, which formed the steric-zipper spines of amyloid fibrils [338, 339]. The authors chose  $\alpha$ B-crystallin because it formed amyloid fibrils more slowly than A $\beta$  or IAPP, facilitating trapping of  $\alpha$ B-crystallin and studying them before fibrillation onset. After characterizing  $\alpha$ B-crystallin fragments as amyloid oligomers, they studied them by X-ray crystallography [336]. One of these fragments produced a stable cytotoxic oligomer, which was termed cylindrin. This oligomer had six antiparallel strands woven into a single sheet rolled into a nonporous barrel (Fig. 4). Each strand was composed of a sequence of 11 amino acid residues, Lys-Val-Lys-Val-Leu-Gly-Asp-Val-Ile-Glu-Val. The axial interior of the cylinder was closed by the Val triplet, forming hydrophobic interactions and excluding water molecules. The cylindrin structure was similar to a steric zipper, but it was cylindrical rather than nearly flat as in amyloid fibrils [336]. Each antiparallel pair of  $\beta$ -strands in the cylindrin sheet is out of register with neighboring pairs in contrast to  $\beta$ -strands in amyloid fibrils [340-342] or short steric zippers [77]. This indicates that an “unrolled cylindrin sheet would not be an in-register structure,

ready to bond with an identical sheet to form the steric zipper spine of an amyloid fiber” [336]. This study suggests that the transition from cylindrin to an antiparallel fibril-like structure would require crossing a high free-energy barrier.



**Figure 4: Ribbon representation of the crystal structure of cylindrin—the first model structure for amyloid oligomers.** Pairs of  $\beta$ -strands form antiparallel dimers, assembled around an axis through the barrel of the cylindrin. Figure is courtesy of Dr. David Eisenberg, UCLA.

Liu *et al.* designed  $\beta$ -sheet amyloid mimics derived from  $\beta_2m$ , IAPP,  $\tau$ , and  $A\beta$ , based on  $\beta$ -sheet mimics described by Cheng *et al.* [343]. These mimics, studied by crystallography and molecular dynamics simulations, were found to form out-of-register, antiparallel, cylindrin-like, oligomeric structures. The oligomeric structures were found to form out-of-register fibrils upon longer incubation duration [344]. Interestingly, the oligomeric structures were reactive with antibody A11 [344]. This study raises the hypothesis that oligomeric assemblies containing antiparallel, out-of-register  $\beta$ -sheets may promote distinct amyloid aggregation pathways in which the resultant fibrillar aggregates, besides being toxic themselves, may function as a source for toxic, out-of-register, cylindrin-like oligomers [344].

## **PRION-LIKE PROPAGATION AND TRANSMISSION OF MISFOLDED PROTEIN STRUCTURES**

In 1967, a heretical hypothesis was proposed to explain the transmission and infectivity mechanisms of scrapie, an ovine/caprine TSE [345, 346]. Based on this

hypothesis and other studies [347], the causal infectious agents of TSEs were identified to be misfolded forms of the prion protein (PrP<sup>Sc</sup>), which replicate in affected individuals by converting the normal, cellular prion protein (PrP<sup>C</sup>), into more of the misfolded,  $\beta$ -sheet-rich isoform, PrP<sup>Sc</sup> [348]. After being debated and researched for decades, this hypothesis was confirmed finally by demonstrating that the infectious prions can be generated *in vitro*, without any genetic material, by self-template misfolding and resultant replication [349-352]. Thus, prion replication requires minute quantities of PrP<sup>Sc</sup>, which convert the host PrP<sup>C</sup> into PrP<sup>Sc</sup> autocatalytically. Thus, PrP<sup>Sc</sup> particles form a nucleus to recruit additional monomeric PrP<sup>C</sup> that undergoes a conformational transition and polymerizes as fibrillar PrP<sup>Sc</sup> [353]. Seeding of additional polymerization can occur also by fragmentation of large PrP<sup>Sc</sup> aggregates into several smaller particles that serve as seeds and cause exponential accumulation of PrP<sup>Sc</sup> [354].

This mechanism was thought to be exclusive to prion diseases, yet recent literature suggests that protein culprits in other protein-misfolding diseases, including AD and PD, also undergo a similar seeding–nucleation process. The similarity between the mechanisms of protein misfolding in TSEs and other protein-misfolding diseases has raised the hypothesis that the latter diseases may also be transmissible and the implicated proteins may behave as infectious agents [355-363]. Experiments testing this hypothesis have generated accumulating evidence showing prion-like transmission and/or propagation mechanisms in common neurodegenerative diseases though actual infectivity remains highly debated (Table 2) [364, 365]. For example, it was found that a single intrastriatal inoculation of  $\alpha$ -synuclein fibrils caused cell–cell transmission of pathologic  $\alpha$ -synuclein and formation of Lewy-body pathology in anatomically interconnected regions in transgenic [366] and wild-type non-transgenic mice [367]. Lewy-body-like pathology resulted in progressive loss of dopaminergic neurons in the *substantia nigra pars compacta*, but not in the adjacent ventral tegmental area, and was accompanied by reduced dopamine levels culminating in motor deficits [367]. The possibility that AD pathology may be transmitted akin to prions was studied in transgenic mice expressing the human amyloid protein injected intracerebrally with dilute brain homogenates from AD patients [368-372]. In these experiments, pre-formed A $\beta$  aggregates were necessary to seed A $\beta$  accumulation as plaques in the brains of inoculated animals. In a separate

study, A $\beta$  seeds that accelerated cerebral A $\beta$  amyloidosis were characterized and shown to consist of a range of aggregated A $\beta$  species of varying sizes and sensitivities to proteinase K digestion [373]. The A $\beta$  in the brain extracts was more resistant to proteinase K than synthetic fibrillar A $\beta$ , and this proteinase-K-resistant fraction in the brain extracts was capable of inducing amyloid deposition by intracerebral injection in young transgenic mice [373]. However, induction of A $\beta$  deposition in the above studies is only an accelerated version of pathology, which otherwise would develop spontaneously due to the genetic manipulations in these animal models. This is unlike prion diseases, which onset *de novo* in humans and animals that mostly do not have a predisposition to develop the disease. On the other hand, studies in transgenic animals expressing low levels of wild-type human APP show that pathologic changes, which would not have developed otherwise during the animals' lifespans, are inducible by human brain extracts containing A $\beta$  aggregates [374, 375]. Another piece of evidence supporting the similarity between A $\beta$  and prion transmission has been the observation that pathology was induced by a peripheral route—intraperitoneal injection of transgenic mice with AD brain extracts [371]. However, because the source of the misfolded A $\beta$  used in these experiments was diseased brain homogenates, the relevance of these findings for AD transmissibility in otherwise normal individuals remains uncertain.

**Table 2:** Prion-like properties of proteins involved in protein-misfolding diseases.

Protein	Seed-Mediated Propagation of Misfolding	Intercellular Transmission	Tissue Migration	Transmissibility	Only Protein Sufficient for Infection	Protease Resistance of Aggregates	Cross-Seeding with Other Proteins
Prion protein [376]	Yes	Yes	Yes	Yes	Yes	Yes	Yes: between recombinant murine and Syrian hamster prion protein [377]
Serum amyloid A in captive cheetahs [378, 379] (reviewed in [365])	Seeded aggregates cause polymerization of native protein <i>in vitro</i> .	No, amyloid formation occurs interstitially.	No, diffuse simultaneous deposition in many tissues	Yes, but only in cheetahs [378, 379].	Amyloid fibrils can cause infection on the background of an inflammatory predisposition in host [380, 381].	Yes.	Yes: fibrils of medin (AMed amyloidosis) [382] <i>in vitro</i> ; apolipoprotein A-II amyloid (AApoAII) and protein A amyloid (AA) both cross-seed and cross-compete

Protein	Seed-Mediated Propagation of Misfolding	Intercellular Transmission	Tissue Migration	Transmissibility	Only Protein Sufficient for Infection	Protease Resistance of Aggregates	Cross-Seeding with Other Proteins
							in amyloid formation in a murine model [383].
Amyloid $\beta$ -protein ( $A\beta$ )	Seeded polymerization of native protein by aggregates <i>in vitro</i> [384, 385] and <i>in vivo</i> [368, 369, 371-374].	Aggregation takes place extracellularly; however, oligomeric assemblies of $A\beta$ are transmitted amongst neurons with distinct connections, leading to transfer of cytotoxicity <i>in vitro</i> [386].	Defined spatiotemporal pattern of lesion propagation and progression during pathogenesis may be explained by cell-cell transmission of oligomers through axonal transport between different brain regions [387-389].	Transmission in murine models by intracerebral or intraperitoneal inoculation of preformed aggregates [368, 369, 371, 372, 375].	Natural transmission of AD is undocumented. Experimental evidence indicates transmission in mice or rats with a genetic predisposition to pathogenesis [368, 369, 371-374].	Yes [373, 390].	Yes: with tau and $\alpha$ -synuclein [391, 392].
Microtubule-associated protein tau	Seeded polymerization of native protein by aggregates has been documented <i>in vitro</i> [393].	Extracellular aggregates are taken up by cells <i>in vitro</i> and <i>in vivo</i> in transgenic mice by intracerebral inoculation [393-398].	Outward pattern of lesion propagation from transentorhinal cortex in AD may explain transmission of misfolding through axonal transport between different brain regions [389, 399].	Transmission in mice with a genetic predisposition by intracerebral inoculation of preformed aggregates [393-398].	Natural transmission of tauopathies is undocumented.	No evidence to date	Yes. Cross-seeding occurs with $\alpha$ -synuclein, $A\beta$ , and IAPP [392, 395, 400].
Superoxide dismutase 1 (SOD-1) [360]	Native and mutant SOD-1 variants co-associate, forming aggregates and fibrils under non-denaturing conditions [401, 402] in familial ALS [403], in transgenic models [404], and in	Mutant SOD-1 aggregates enter neurons efficiently by macropinocytosis and seed aggregation of the normally soluble SOD-1 [362, 407].	Motor neuron degeneration initiates focally and spreads to contiguous regions with disease progression, providing indirect evidence for tissue spreading of pathology [408, 409].	Undocumented	Possible because intercellular misfolding progression was blocked by antibodies against misfolded SOD-1 (reviewed in [365])	Misfolded protein is highly susceptible to proteases [406].	Seeds of S100A6, an EF-hand $Ca^{2+}$ -binding protein, promote SOD-1 aggregation [410].

Protein	Seed-Mediated Propagation of Misfolding	Intercellular Transmission	Tissue Migration	Transmissibility	Only Protein Sufficient for Infection	Protease Resistance of Aggregates	Cross-Seeding with Other Proteins
	cell-culture systems [362, 405, 406].						
$\alpha$ -Synuclein [358]	Seeded polymerization of aggregation <i>in vitro</i> [411], in cell cultures [412] and <i>in vivo</i> [413].	$\alpha$ -Synuclein misfolding is transferred to transplanted stem cell grafts in patients with PD [414, 415], murine [413, 416], and rat models [417]. Endocytosis likely mediates uptake of $\alpha$ -synuclein <i>in vivo</i> , and transferred $\alpha$ -synuclein causes seeded aggregation of endogenous $\alpha$ -synuclein in recipient neurons [417]. Lipid peroxidation product, HNE, induces $\alpha$ -synuclein oligomerization and promotes cell-cell transfer of seeding-capable assemblies [418].	Contiguous, progressive spread of PD lesions from brainstem to cortex [419-423] provides indirect evidence for tissue migration of misfolding.	Undocumented	Undocumented	Cell-transmitted $\alpha$ -synuclein aggregates were shown to be sensitive to protease treatment [417].	Cross-seeding occurs with, $\gamma$ -synuclein [424], tau [392], and A $\beta$ [391].
Huntingtin	Polyglutamine peptides exceeding a critical length aggregate <i>in vitro</i> and <i>in vivo</i> [425, 426]. Brain extracts of patients and transgenic mice accelerate seeded polyglutamine amyloid formation [427].	Aggregates are internalized by cells in culture [428].	Systematic, contiguous dissemination of pathology in HD [429] has been documented.	Unlikely because genetic susceptibility in host is necessary.	No, because etiology constitutes underlying genetic mutations.	Yes.	Fibrillar aggregates of huntingtin function as a structural template to induce, <i>in vitro</i> and <i>in vivo</i> , fibrillation of TIA-1, an RNA-binding protein containing a Q/N-rich sequence [430].

Whether infectious or not, propagation of protein misfolding may be one of the mechanisms responsible for the findings that pathological changes in various neurodegenerative diseases, including AD, PD, and HD, progress temporally in a characteristic, step-wise, anatomical pattern. Neuropathological studies by Braak *et al.* and others have shown that Lewy bodies in PD and neurofibrillary tangles in AD initiate early in the course of these diseases in circumscribed brain regions while progressing in predictable topographies through anatomical connections [387, 389, 399, 422]. Similarly, in an AD mouse model, the pathology progresses from the entorhinal cortex to all of the hippocampal subregions and cortical areas through anatomical connections, such as the perforant pathway [388]. Neurodegenerative changes in HD progress simultaneously in two defined anatomical directions in the striatum [431]. Among the first affected in HD are the striatal projection neurons, particularly those expressing enkephalin [432]. Brain-imaging studies show that cortical regions processing motor, sensory, and visual functions undergo thinning in asymptomatic huntingtin gene carriers, and cortical areas that subserve more advanced functions are affected later in the course of HD [429]. This defined spatiotemporal pattern of lesion propagation and progression in neurodegenerative diseases may be explained by cell–cell transmission of misfolded proteins through axonal transport between different brain regions. Indeed, oligomeric, fluorescently tagged A $\beta$  microinjected into electrophysiologically defined primary hippocampal rat neurons were shown to transfer between differentiated neurons through direct connections [386]. With progressive accumulation of such oligomers, the acceptor cells gradually showed signs of neurite damage and cytotoxicity [386]. In this study, time-lapse imaging showed that diffuse, intracellular A $\beta$  oligomers gradually accumulated into vesicular structures corresponding to lysosomes and A $\beta$ -containing vesicles travelled in neurites at a speed of 61 nm/s, the velocity of late endosomes or lysosomes [386]. Collectively, it was postulated that macroautophagic formation of endosomes/lysosomes might have mediated intraneuritic transfer of A $\beta$  oligomers, which were then exocytosed from the donor cells and rapidly endocytosed by the acceptor cells [386]. Other mechanisms of transmission such as exosomes [433] and tunneling nanotubes [434] also have been discussed as potential means of cell–cell transmission of A $\beta$  or other amyloidogenic proteins.

The studies described above demonstrate that regional spreading of protein misfolding may play an important role in the pathogenesis and progression of many protein-misfolding diseases. Furthermore, these studies strongly indicate that at least some prion characteristics, including the molecule–molecule transmission of misfolding and cell–cell spreading of misfolded protein moieties occur in other protein-misfolding diseases. Contextually, another noteworthy phenomenon is the cross-seeding mechanism whereby misfolded aggregates of one protein may interact and promote aggregation of a different protein [391, 435].

## CONCLUSIONS

Since the amyloid-cascade hypothesis was formulated [1], intensive research has led to an exponential accumulation of data elucidating the pathogenic mechanisms of AD. In mid-December, 2012, PubMed database searches, using the queries “Alzheimer's disease”, “amyloid”, and “protein misfolding disease” returned 87,702, 53,493, and 32,184 hits, respectively. Importantly, as our understanding of the devastating *morbus* Alzheimer, and other neurodegenerative and protein-misfolding diseases has been growing, an alternative, encompassing paradigm has been emerging. This paradigm postulates that non-fibrillar protein assemblies rather than mature amyloidogenic fibrils likely are the key neurotoxins responsible for most of the pathogenic mechanisms in protein-misfolding and neurodegenerative diseases, including AD. Accordingly, oligomeric species with different degrees of structural order are thought to mediate various pathogenic mechanisms that may lead to cytotoxicity and cell loss eventuating in organic and systemic morbidity. It is thought that histopathological progression of neurodegenerative lesions and symptom development likely occur by dissemination of protein-misfolding through connected brain regions. With the progressive use of classical techniques, and the advent of novel, sophisticated methodologies, several different forms of non-fibrillar assemblies of A $\beta$  and those of other amyloidogenic proteins have been described. This has led to considerable progress in the elucidation of structural and functional features and fundamentals of the assembly of these proteins at the molecular level. Overall, it is postulated that some of the non-fibrillar amyloidogenic assemblies are on path to fibrillogenesis. The resulting protein fibrils are thought to be the end-stage sinks for the toxic non-fibrillar species. Fibrillar assemblies accumulate progressively

into intra- and/or extracellular proteinaceous amyloid aggregates generating the disease-specific lesions *in vivo*. However, recent crystallographic studies of disease-related model peptides, having shed light on the structures of oligomeric amyloid assemblies, may have reignited the counter-argument that out-of-register, antiparallel amyloid fibrils may be cytotoxic in their own right [344].

In AD research, various forms of non-fibrillar A $\beta$  assemblies, including activated monomeric conformers, ADDLs, PF, cell-derived dimers and trimers, and annular assemblies have been described (Table 1). In many cases, the structural and functional interrelationships amongst these assemblies are still elusive and their atomically resolved structural relationships with out-of-register, antiparallel “cylindrins” are yet to be examined. Nevertheless, some have been shown to be pathogenic through one or several common pathways, suggesting that they may share structural features and possibly mechanisms of action. Understanding these intricate structure–function correlations will decipher a complex and interconnected array of pathogenic mechanisms.

Global research efforts have established a framework for understanding the fundamentals of A $\beta$  assembly [7, 10, 11]. A remaining challenge is to assess how these fundamental structural principles are linked to cellular and tissular microenvironments during progression of AD. Many experimental conditions have been used to study the structure and function of non-fibrillar assemblies, but it is difficult to regenerate and scrutinize the actual *in vivo* milieus and conditions in which protein assembly, oligomerization, fibrillization, and deposition occur. Similarly, it is extremely difficult to assess all the possible interactions these assemblies may have with various cellular components and organelles. A multitude of detrimental mechanisms, including disruption of cellular metabolism, synapse structure and function deregulation, membrane damage, ionic imbalance, oxidative/inflammatory stress, apoptotic, and other cytotoxic effects, have been shown to be mediated by non-fibrillar A $\beta$  assemblies, emphasizing that a single therapeutic approach likely will be insufficient to prevent or treat AD progression. By inference, this likely is true also for other amyloidoses. The intricacy of the pathogenic mechanisms in these diseases calls for rational diagnostic and therapeutic approaches that would target not only a single assembly or a single mechanism, but a multitude of assemblies and mechanisms. It is important to

design and discover therapeutic agents that could target various assemblies that potentially become active early or are continuously active throughout the course of disease. Successful targeting of non-fibrillar assemblies *in vitro* and in animal models could have crucial diagnostic and prognostic implications for amyloid-related diseases.

## ACKNOWLEDGEMENTS

We acknowledge Mr. Sean M. Spring for conducting the experiment described in Fig. 1. The work was supported by funding from the Jim Easton Consortium for Alzheimer's Drug Discovery and Biomarker Development at UCLA, Team Parkinson/Parkinson Alliance, grant 20095024 from the RJG Foundation, a grant from the Cure Alzheimer's Fund, and a UCLA Alzheimer's Disease Research Center Pilot Award (from NIH/NIA P50AG016570).

## CONFLICT OF INTEREST

The authors confirm that this chapter content has no conflict of interest.

## DISCLOSURE

This chapter is an update of our previous publication in CAR "Structure–Function Relationships of Pre-Fibrillar Protein Assemblies in Alzheimer's Disease and Related Disorders" published in 'CAR', Volume 5, Number 3, June, pp. 319 to 341.

## ABBREVIATIONS

$\alpha\alpha$	=	$\alpha$ -helix-turn- $\alpha$ -helix
$\beta_2m$	=	$\beta_2$ -microglobulin
AcP	=	Acylphosphatase
AD	=	Alzheimer's disease
ADDLs	=	A $\beta$ -derived diffusible ligands

AFM	= Atomic-force microscopy
APF	= Annular A $\beta$ 42-derived protofibrils
APP	= Amyloid $\beta$ -protein precursor
Arc	= Activity-regulated cytoskeleton-associated protein
A $\beta$	= Amyloid $\beta$ -protein
[Ca <sup>2+</sup> ] <sub>i</sub>	= Intracellular Ca <sup>2+</sup> concentration
CD	= Circular dichroism
CSF	= Cerebrospinal fluid
DLS	= Dynamic light scattering
EPSC	= Excitatory post-synaptic current
FAIMS	= Field-asymmetric ion-mobility spectrometry
FTIR	= Fourier-transform infrared spectroscopy
HD	= Huntington's disease
HFIP	= 1,1,1,3,3,3-hexafluoro-2-isopropanol
HNE	= 4-hydroxy-2-nonenal
HPLC	= High-performance liquid chromatography
HypF-N	= Hydrogenase maturation-factor
IAPP	= Islet amyloid polypeptide
IMS-MS	= Ion-mobility spectrometry-mass spectrometry
LMW	= Low molecular weight

LTD	=	Long-term depression
LTP	=	Long-term potentiation
MALDI	=	Matrix-assisted laser-desorption ionization
MALLS	=	Multi-angle laser light scattering
MPL	=	Mass-per-length
MTT	=	3-(4,5-Dimethylthiazol-2-yl)-2,5-diphenyltetrazolium bromide
nAChR	=	Nicotinic acetylcholine receptor
NMDA	=	<i>N</i> -methyl-D-aspartate
NMDAR(s)	=	NMDA receptor(s)
PD	=	Parkinson's disease
PF	=	Protofibrils
PI3K	=	Phosphatidyl inositol 3-kinase
PICUP	=	Photo-induced cross-linking of unmodified proteins
PrP <sup>C</sup>	=	Cellular prion protein
PrP <sup>Sc</sup>	=	Misfolded prion protein
ROS	=	Reactive oxygen species
SDS	=	Sodium dodecyl sulfate
SEC	=	Size-exclusion chromatography
SH3	=	Src-homology 3
SPPS	=	Solid-phase peptide synthesis

STEM	= Scanning transmission electron microscopy
STM	= Scanning tunneling microscopy
SOD1	= Superoxide dismutase 1
T2D	= Type-2 diabetes mellitus
TABFOs	= Toxic A $\beta$ 42-derived fibrillar oligomers
TEM	= Transmission electron microscopy
TFE	= Trifluoroethanol
ThT	= Thioflavin T
TSE	= Transmissible spongiform encephalopathies

## REFERENCES

- [1] Hardy JA, Higgins GA. Alzheimer's disease: the amyloid cascade hypothesis. *Science* 1992; 256: 184-5.
- [2] Terry RD, Masliah E, Salmon DP, *et al.* Physical basis of cognitive alterations in Alzheimer's disease: synapse loss is the major correlate of cognitive impairment. *Ann Neurol* 1991; 30: 572-80.
- [3] Mucke L, Masliah E, Yu GQ, *et al.* High-level neuronal expression of A $\beta$ <sub>1-42</sub> in wild-type human amyloid protein precursor transgenic mice: synaptotoxicity without plaque formation. *J Neurosci* 2000; 20: 4050-8.
- [4] Klein WL, Krafft GA, Finch CE. Targeting small A $\beta$  oligomers: the solution to an Alzheimer's disease conundrum? *Trends Neurosci* 2001; 24: 219-24.
- [5] Kirkitadze MD, Bitan G, Teplow DB. Paradigm shifts in Alzheimer's disease and other neurodegenerative disorders: the emerging role of oligomeric assemblies. *J Neurosci Res* 2002; 69: 567-77.
- [6] Hardy J, Selkoe DJ. The amyloid hypothesis of Alzheimer's disease: progress and problems on the road to therapeutics. *Science* 2002; 297: 353-6.
- [7] Caughey B, Lansbury PT. Protofibrils, pores, fibrils, and neurodegeneration: separating the responsible protein aggregates from the innocent bystanders. *Annu Rev Neurosci* 2003; 26: 267-98.
- [8] Baglioni S, Casamenti F, Bucciantini M, *et al.* Prefibrillar amyloid aggregates could be generic toxins in higher organisms. *J Neurosci* 2006; 26: 8160-7.
- [9] Lansbury PT, Lashuel HA. A century-old debate on protein aggregation and neurodegeneration enters the clinic. *Nature* 2006; 443: 774-9.
- [10] Haass C, Selkoe DJ. Soluble protein oligomers in neurodegeneration: lessons from the Alzheimer's amyloid  $\beta$ -peptide. *Nat Rev Mol Cell Biol* 2007; 8: 101-12.

- [11] Ferreira ST, Vieira MN, De Felice FG. Soluble protein oligomers as emerging toxins in Alzheimer's and other amyloid diseases. *IUBMB life* 2007; 59: 332-45.
- [12] Fleming Outeiro T, Tetzlaff J. Mechanisms of disease II: cellular protein quality control. *Semin Pediatr Neurol* 2007; 14: 15-25.
- [13] Agorogiannis EI, Agorogiannis GI, Papadimitriou A, Hadjigeorgiou GM. Protein misfolding in neurodegenerative diseases. *Neuropathol Appl Neurobiol* 2004; 30: 215-24.
- [14] Marzban L, Park K, Verchere CB. Islet amyloid polypeptide and type 2 diabetes. *Exp Gerontol* 2003; 38: 347-51.
- [15] Lachmann HJ, Hawkins PN. Systemic amyloidosis. *Curr Opin Pharmacol* 2006; 6: 214-20.
- [16] FINDER VH, GLOCKSHUBER R. Amyloid- $\beta$  aggregation. *Neurodegener Dis* 2007; 4: 13-27.
- [17] Teplow DB. Structural and kinetic features of amyloid  $\beta$ -protein fibrillogenesis. *Amyloid* 1998; 5: 121-42.
- [18] Lashuel HA, Lansbury PT, Jr. Are amyloid diseases caused by protein aggregates that mimic bacterial pore-forming toxins? *Q Rev Biophys* 2006; 39: 167-201.
- [19] Taylor BM, Sarver RW, Fici G, *et al.* Spontaneous aggregation and cytotoxicity of the  $\beta$ -amyloid A $\beta$ <sub>1-40</sub>: a kinetic model. *J Protein Chem* 2003; 22: 31-40.
- [20] Roher AE, Palmer KC, Yurewicz EC, Ball MJ, Greenberg BD. Morphological and biochemical analyses of amyloid plaque core proteins purified from Alzheimer disease brain tissue. *J Neurochem* 1993; 61: 1916-26.
- [21] Enya M, Morishima-Kawashima M, Yoshimura M, *et al.* Appearance of sodium dodecyl sulfate-stable amyloid  $\beta$ -protein (A $\beta$ ) dimer in the cortex during aging. *Am J Pathol* 1999; 154: 271-9.
- [22] Vigo-Pelfrey C, Lee D, Keim P, Lieberburg I, Schenk DB. Characterization of  $\beta$ -amyloid peptide from human cerebrospinal fluid. *J Neurochem* 1993; 61: 1965-8.
- [23] Podlisny MB, Ostaszewski BL, Squazzo SL, *et al.* Aggregation of secreted amyloid  $\beta$ -protein into sodium dodecyl sulfate-stable oligomers in cell culture. *J Biol Chem* 1995; 270: 9564-70.
- [24] Walsh DM, Klyubin I, Fadeeva JV, *et al.* Naturally secreted oligomers of amyloid  $\beta$  protein potently inhibit hippocampal long-term potentiation *in vivo*. *Nature* 2002; 416: 535-9.
- [25] Walsh DM, Tseng BP, Rydel RE, Podlisny MB, Selkoe DJ. The oligomerization of amyloid  $\beta$ -protein begins intracellularly in cells derived from human brain. *Biochemistry* 2000; 39: 10831-9.
- [26] Lambert MP, Barlow AK, Chromy BA, *et al.* Diffusible, nonfibrillar ligands derived from A $\beta$ <sub>1-42</sub> are potent central nervous system neurotoxins. *Proc Natl Acad Sci USA* 1998; 95: 6448-53.
- [27] Gong Y, Chang L, Viola KL, *et al.* Alzheimer's disease-affected brain: presence of oligomeric A $\beta$  ligands (ADDLs) suggests a molecular basis for reversible memory loss. *Proc Natl Acad Sci USA* 2003; 100: 10417-22.
- [28] Harper JD, Wong SS, Lieber CM, Lansbury PT. Observation of metastable A $\beta$  amyloid protofibrils by atomic force microscopy. *Chem Biol* 1997; 4: 119-25.
- [29] Hartley DM, Walsh DM, Ye CP, *et al.* Protofibrillar intermediates of amyloid  $\beta$ -protein induce acute electrophysiological changes and progressive neurotoxicity in cortical neurons. *J Neurosci* 1999; 19: 8876-84.
- [30] Walsh DM, Hartley DM, Kusumoto Y, *et al.* Amyloid  $\beta$ -protein fibrillogenesis. Structure and biological activity of protofibrillar intermediates. *J Biol Chem* 1999; 274: 25945-52.

- [31] Lesné S, Koh MT, Kotilinek L, *et al.* A specific amyloid- $\beta$  protein assembly in the brain impairs memory. *Nature* 2006; 440: 352-7.
- [32] Bitan G, Kirkitadze MD, Lomakin A, *et al.* Amyloid  $\beta$ -protein (A $\beta$ ) assembly: A $\beta$ 40 and A $\beta$ 42 oligomerize through distinct pathways. *Proc Natl Acad Sci USA* 2003; 100: 330-5.
- [33] Bitan G, Tarus B, Vollers SS, *et al.* A molecular switch in amyloid assembly: Met35 and amyloid  $\beta$ -protein oligomerization. *J Am Chem Soc* 2003; 125: 15359-65.
- [34] Bitan G, Vollers SS, Teplow DB. Elucidation of primary structure elements controlling early amyloid  $\beta$ -protein oligomerization. *J Biol Chem* 2003; 278: 34882-9.
- [35] Hoshi M, Sato M, Matsumoto S, *et al.* Spherical aggregates of  $\beta$ -amyloid (amylospheroid) show high neurotoxicity and activate tau protein kinase I/glycogen synthase kinase-3 $\beta$ . *Proc Natl Acad Sci USA* 2003; 100: 6370-5.
- [36] Lashuel HA, Hartley D, Petre BM, Walz T, Lansbury PT, Jr. Neurodegenerative disease: amyloid pores from pathogenic mutations. *Nature* 2002; 418: 291.
- [37] Lashuel HA, Hartley DM, Petre BM, *et al.* Mixtures of wild-type and a pathogenic (E22G) form of A $\beta$ 40 *in vitro* accumulate protofibrils, including amyloid pores. *J Mol Biol* 2003; 332: 795-808.
- [38] Glabe CG. Structural classification of toxic amyloid oligomers. *J Biol Chem* 2008; 283: 29639-43.
- [39] Westlind-Danielsson A, Arnerup G. Spontaneous *in vitro* formation of supramolecular  $\beta$ -amyloid structures, "betaamy balls", by  $\beta$ -amyloid 1-40 peptide. *Biochemistry* 2001; 40: 14736-43.
- [40] Merrifield B. Concept and early development of solid-phase peptide synthesis. *Methods Enzymol* 1997; 289: 3-13.
- [41] Kim YS, Moss JA, Janda KD. Biological tuning of synthetic tactics in solid-phase synthesis: application to A $\beta$ (1-42). *J Org Chem* 2004; 69: 7776-8.
- [42] Sharpe S, Yau WM, Tycko R. Expression and purification of a recombinant peptide from the Alzheimer's  $\beta$ -amyloid protein for solid-state NMR. *Protein Expr Purif* 2005; 42: 200-10.
- [43] Lee EK, Hwang JH, Shin DY, Kim DI, Yoo YJ. Production of recombinant amyloid- $\beta$  peptide 42 as an ubiquitin extension. *Protein Expr Purif* 2005; 40: 183-9.
- [44] Dobeli H, Draeger N, Huber G, *et al.* A biotechnological method provides access to aggregation competent monomeric Alzheimer's 1-42 residue amyloid peptide. *Biotechnology (NY)* 1995; 13: 988-93.
- [45] Carrotta R, Di Carlo M, Manno M, *et al.* Toxicity of recombinant  $\beta$ -amyloid prefibrillar oligomers on the morphogenesis of the sea urchin *Paracentrotus lividus*. *FASEB J* 2006; 20: 1916-7.
- [46] Tickler AK, Barrow CJ, Wade JD. Improved preparation of amyloid- $\beta$  peptides using DBU as  $N^{\alpha}$ -Fmoc deprotection reagent. *J Pept Sci* 2001; 7: 488-94.
- [47] Zarándi M, Soós K, Fülöp L, *et al.* Synthesis of A $\beta$ [1-42] and its derivatives with improved efficiency. *J Pept Sci* 2007; 13: 94-9.
- [48] Tickler AK, Clippingdale AB, Wade JD. Amyloid- $\beta$  as a "difficult sequence" in solid phase peptide synthesis. *Protein Pept Lett* 2004; 11: 377-84.
- [49] García-Martín F, Quintanar-Audelo M, García-Ramos Y, *et al.* ChemMatrix, a poly(ethylene glycol)-based support for the solid-phase synthesis of complex peptides. *J Comb Chem* 2006; 8: 213-20.

- [50] Bacsa B, Bosze S, Kappe CO. Direct solid-phase synthesis of the  $\beta$ -amyloid (1–42) peptide using controlled microwave heating. *J Org Chem* 2010; 75: 2103-6.
- [51] Sohma Y, Sasaki M, Hayashi Y, Kimura T, Kiso Y. Design and synthesis of a novel water-soluble A $\beta$ 1–42 isopeptide: an efficient strategy for the preparation of Alzheimer's disease-related peptide, A $\beta$ 1–42, via *O-N* intramolecular acyl migration reaction. *Tetrahedron Lett* 2004; 45: 5965-68.
- [52] Sohma Y, Taniguchi A, Yoshiya T, *et al.* 'Click peptide': a novel '*O*-acyl isopeptide method' for peptide synthesis and chemical biology-oriented synthesis of amyloid  $\beta$  peptide analogues. *J Pept Sci* 2006; 12: 823-8.
- [53] Macao B, Hoyer W, Sandberg A, *et al.* Recombinant amyloid  $\beta$ -peptide production by coexpression with an affibody ligand. *BMC Biotechnol* 2008; 8: 82.
- [54] Cornista JC, Koga Y, Takano K, Kanaya S. Amyloidogenicity and pitrilysin sensitivity of a lysine-free derivative of amyloid  $\beta$ -peptide cleaved from a recombinant fusion protein. *J Biotechnol* 2006; 122: 186-97.
- [55] Yonemoto IT, Wood MR, Balch WE, Kelly JW. A general strategy for the bacterial expression of amyloidogenic peptides using BCL-XL-1/2 fusions. *Protein Sci* 2009; 18: 1978-86.
- [56] Garai K, Crick SL, Mustafi SM, Frieden C. Expression and purification of amyloid- $\beta$  peptides from *Escherichia coli*. *Protein Expr Purif* 2009; 66: 107-12.
- [57] Bockhorn JJ, Lazar KL, Gasser AJ, *et al.* Novel semisynthetic method for generating full length  $\beta$ -amyloid peptides. *Biopolymers* 2010; 94: 511-20.
- [58] Teplow DB. Preparation of amyloid  $\beta$ -protein for structural and functional studies. *Methods Enzymol* 2006; 413: 20-33.
- [59] Klein WL, Stine WB, Jr., Teplow DB. Small assemblies of unmodified amyloid  $\beta$ -protein are the proximate neurotoxin in Alzheimer's disease. *Neurobiol Aging* 2004; 25: 569-80.
- [60] Howlett DR, Jennings KH, Lee DC, *et al.* Aggregation state and neurotoxic properties of Alzheimer  $\beta$ -amyloid peptide. *Neurodegeneration* 1995; 4: 23-32.
- [61] Simmons LK, May PC, Tomaselli KJ, *et al.* Secondary structure of amyloid  $\beta$  peptide correlates with neurotoxic activity *in vitro*. *Mol Pharmacol* 1994; 45: 373-9.
- [62] Soto C, Castaño EM, Kumar RA, Beavis RC, Frangione B. Fibrillogenesis of synthetic amyloid- $\beta$  peptides is dependent on their initial secondary structure. *Neurosci Lett* 1995; 200: 105-8.
- [63] Bitan G, Fradinger EA, Spring SM, Teplow DB. Neurotoxic protein oligomers—what you see is not always what you get. *Amyloid* 2005; 12: 88-95.
- [64] Zeeb M, Balbach J. Protein folding studied by real-time NMR spectroscopy. *Methods* 2004; 34: 65-74.
- [65] Benilova I, Karran E, De Strooper B. The toxic A $\beta$  oligomer and Alzheimer's disease: an emperor in need of clothes. *Nat Neurosci* 2012; 15: 349-57.
- [66] Bitan G, Teplow DB. Rapid photochemical cross-linking—a new tool for studies of metastable, amyloidogenic protein assemblies. *Acc Chem Res* 2004; 37: 357-64.
- [67] Li H, Rahimi F, Sinha S, *et al.* Amyloids and Protein Aggregation—Analytical Methods. *Encyclopedia of Analytical Chemistry*: John Wiley & Sons, Ltd; 2009.
- [68] Lee JP, Stimson ER, Ghilardi JR, *et al.* <sup>1</sup>H NMR of A $\beta$  amyloid peptide congeners in water solution. Conformational changes correlate with plaque competence. *Biochemistry* 1995; 34: 5191-200.

- [69] Zhang S, Iwata K, Lachenmann MJ, *et al.* The Alzheimer's peptide A $\beta$  adopts a collapsed coil structure in water. *J Struct Biol* 2000; 130: 130-41.
- [70] Yan Y, Wang C. A $\beta$ 42 is more rigid than A $\beta$ 40 at the C terminus: implications for A $\beta$  aggregation and toxicity. *J Mol Biol* 2006; 364: 853-62.
- [71] Riek R, Güntert P, Döbeli H, Wipf B, Wüthrich K. NMR studies in aqueous solution fail to identify significant conformational differences between the monomeric forms of two Alzheimer peptides with widely different plaque-competence, A $\beta$ (1-40)<sup>ox</sup> and A $\beta$ (1-42)<sup>ox</sup>. *Eur J Biochem* 2001; 268: 5930-6.
- [72] Hou L, Shao H, Zhang Y, *et al.* Solution NMR studies of the A $\beta$ (1-40) and A $\beta$ (1-42) peptides establish that the Met35 oxidation state affects the mechanism of amyloid formation. *J Am Chem Soc* 2004; 126: 1992-2005.
- [73] Sgourakis NG, Yan Y, McCallum SA, Wang C, Garcia AE. The Alzheimer's peptides A $\beta$ 40 and 42 adopt distinct conformations in water: a combined MD/NMR study. *J Mol Biol* 2007; 368: 1448-57.
- [74] Lazo ND, Grant MA, Condrón MC, Rigby AC, Teplow DB. On the nucleation of amyloid  $\beta$ -protein monomer folding. *Protein Sci* 2005; 14: 1581-96.
- [75] Bemporad F, Chiti F. Protein misfolded oligomers: experimental approaches, mechanism of formation, and structure-toxicity relationships. *Chem Biol* 2012; 19: 315-27.
- [76] MacArthur MW, Driscoll PC, Thornton JM. NMR and crystallography—complementary approaches to structure determination. *Trends Biotechnol* 1994; 12: 149-53.
- [77] Sawaya MR, Sambashivan S, Nelson R, *et al.* Atomic structures of amyloid cross- $\beta$  spines reveal varied steric zippers. *Nature* 2007; 447: 453-7.
- [78] Kheterpal I, Chen M, Cook KD, Wetzel R. Structural differences in A $\beta$  amyloid protofibrils and fibrils mapped by hydrogen exchange–mass spectrometry with on-line proteolytic fragmentation. *J Mol Biol* 2006; 361: 785-95.
- [79] Laemmli UK. Cleavage of structural proteins during the assembly of the head of bacteriophage T4. *Nature* 1970; 227: 680-5.
- [80] Khan JM, Qadeer A, Chaturvedi SK, *et al.* SDS can be utilized as an amyloid inducer: a case study on diverse proteins. *PLoS One* 2012; 7: e29694.
- [81] Gudiksen KL, Gitlin I, Whitesides GM. Differentiation of proteins based on characteristic patterns of association and denaturation in solutions of SDS. *Proc Natl Acad Sci USA* 2006; 103: 7968-72.
- [82] Leffers KW, Schell J, Jansen K, *et al.* The structural transition of the prion protein into its pathogenic conformation is induced by unmasking hydrophobic sites. *J Mol Biol* 2004; 344: 839-53.
- [83] Kawooya JK, Emmons TL, Gonzalez-DeWhitt PA, Camp MC, D'Andrea SC. Electrophoretic mobility of Alzheimer's amyloid- $\beta$  peptides in urea–sodium dodecyl sulfate–polyacrylamide gel electrophoresis. *Anal Biochem* 2003; 323: 103-13.
- [84] Montserret R, McLeish MJ, Böckmann A, Geourjon C, Penin F. Involvement of electrostatic interactions in the mechanism of peptide folding induced by sodium dodecyl sulfate binding. *Biochemistry* 2000; 39: 8362-73.
- [85] Yamamoto S, Hasegawa K, Yamaguchi I, *et al.* Low concentrations of sodium dodecyl sulfate induce the extension of  $\beta_2$ -microglobulin-related amyloid fibrils at a neutral pH. *Biochemistry* 2004; 43: 11075-82.

- [86] Rangachari V, Moore BD, Reed DK, *et al.* Amyloid- $\beta$ (1–42) rapidly forms protofibrils and oligomers by distinct pathways in low concentrations of sodium dodecylsulfate. *Biochemistry* 2007; 46: 12451-62.
- [87] Rangachari V, Reed DK, Moore BD, Rosenberry TL. Secondary structure and interfacial aggregation of amyloid- $\beta$ (1–40) on sodium dodecyl sulfate micelles. *Biochemistry* 2006; 45: 8639-48.
- [88] Piening N, Weber P, Hogen T, *et al.* Photo-induced crosslinking of prion protein oligomers and prions. *Amyloid* 2006; 13: 67-77.
- [89] Barghorn S, Nimmrich V, Striebinger A, *et al.* Globular amyloid  $\beta$ -peptide<sub>1–42</sub> oligomer—a homogenous and stable neuropathological protein in Alzheimer's disease. *J Neurochem* 2005; 95: 834-47.
- [90] Walsh DM, Lomakin A, Benedek GB, Condron MM, Teplow DB. Amyloid  $\beta$ -protein fibrillogenesis. Detection of a protofibrillar intermediate. *J Biol Chem* 1997; 272: 22364-72.
- [91] Mori H, Takio K, Ogawara M, Selkoe DJ. Mass spectrometry of purified amyloid  $\beta$  protein in Alzheimer's disease. *J Biol Chem* 1992; 267: 17082-6.
- [92] Wahlström A, Hugonin L, Perálvarez-Marín A, Jarvet J, Gräslund A. Secondary structure conversions of Alzheimer's A $\beta$ (1–40) peptide induced by membrane-mimicking detergents. *FEBS J* 2008; 275: 5117-28.
- [93] Yang M, Teplow DB. Amyloid  $\beta$ -protein monomer folding: free-energy surfaces reveal alloform-specific differences. *J Mol Biol* 2008; 384: 450-64.
- [94] Reed MN, Hofmeister JJ, Jungbauer L, *et al.* Cognitive effects of cell-derived and synthetically derived A $\beta$  oligomers. *Neurobiol Aging* 2011; 32: 1784-94.
- [95] Hepler RW, Grimm KM, Nahas DD, *et al.* Solution state characterization of amyloid  $\beta$ -derived diffusible ligands. *Biochemistry* 2006; 45: 15157-67.
- [96] Rahimi F, Bitan G. Overview of Fibrillar and Oligomeric Assemblies of Amyloidogenic Proteins In: Rahimi F, Bitan G, editors. *Non-fibrillar Amyloidogenic Protein Assemblies—Common Cytotoxins Underlying Degenerative Diseases*. Netherlands: Springer Netherlands; 2012. p. 1–36.
- [97] Fancy DA, Kodadek T. Chemistry for the analysis of protein-protein interactions: rapid and efficient cross-linking triggered by long wavelength light. *Proc Natl Acad Sci USA* 1999; 96: 6020-4.
- [98] Bitan G. Structural study of metastable amyloidogenic protein oligomers by photo-induced cross-linking of unmodified proteins. *Methods Enzymol* 2006; 413: 217-36.
- [99] Lopes DH, Sinha S, Rosensweig C, Bitan G. Application of photochemical cross-linking to the study of oligomerization of amyloidogenic proteins. *Methods Mol Biol* 2012; 849: 11-21.
- [100] Rahimi F, Maiti P, Bitan G. Photo-induced cross-linking of unmodified proteins (PICUP) applied to amyloidogenic peptides. *Journal of visualized experiments: JoVE* 2009.
- [101] Hayden EY, Teplow DB. Continuous flow reactor for the production of stable amyloid protein oligomers. *Biochemistry* 2012.
- [102] Squires TM, Brady JF. A simple paradigm for active and nonlinear microrheology. *Physics of Fluids* 2005; 17: 073101.
- [103] Bitan G, Lomakin A, Teplow DB. Amyloid  $\beta$ -protein oligomerization: prenucleation interactions revealed by photo-induced cross-linking of unmodified proteins. *J Biol Chem* 2001; 276: 35176-84.

- [104] Nichols MR, Moss MA, Reed DK, *et al.* Growth of  $\beta$ -amyloid(1–40) protofibrils by monomer elongation and lateral association. Characterization of distinct products by light scattering and atomic force microscopy. *Biochemistry* 2002; 41: 6115-27.
- [105] Kheterpal I, Lashuel HA, Hartley DM, *et al.* A $\beta$  protofibrils possess a stable core structure resistant to hydrogen exchange. *Biochemistry* 2003; 42: 14092-8.
- [106] Bitan G, Teplow DB. Preparation of aggregate-free, low molecular weight amyloid- $\beta$  for assembly and toxicity assays. *Methods Mol Biol* 2005; 299: 3-9.
- [107] Urbanke C, Witte G, Curth U. Sedimentation velocity method in the analytical ultracentrifuge for the study of protein-protein interactions. *Methods Mol Biol* 2005; 305: 101-14.
- [108] Mok YF, Howlett GJ. Sedimentation velocity analysis of amyloid oligomers and fibrils. *Methods Enzymol* 2006; 413: 199-217.
- [109] Lebowitz J, Lewis MS, Schuck P. Modern analytical ultracentrifugation in protein science: a tutorial review. *Protein Sci* 2002; 11: 2067-79.
- [110] Huang TH, Yang DS, Plaskos NP, *et al.* Structural studies of soluble oligomers of the Alzheimer  $\beta$ -amyloid peptide. *J Mol Biol* 2000; 297: 73-87.
- [111] Philo JS. Is any measurement method optimal for all aggregate sizes and types? *AAPS J* 2006; 8: E564-71.
- [112] Einstein A. On the motion of small particles suspended in liquids at rest required by the molecular-kinetic theory of heat. *Annalen der Physik* 1905; 17: 549-60.
- [113] Sutherland W. A dynamical theory of diffusion for non-electrolytes and the molecular mass of albumin. *Philos Mag* 1905; 9: 781-85.
- [114] Lomakin A, Benedek GB, Teplow DB. Monitoring protein assembly using quasielastic light scattering spectroscopy. *Methods Enzymol* 1999; 309: 429-59.
- [115] Wyatt P. Light scattering and the absolute characterization of macromolecules. *Anal Chim Acta* 1993; 272: 1-40.
- [116] Oliva A, Llabrés M, Fariña JB. Applications of multi-angle laser light-scattering detection in the analysis of peptides and proteins. *Curr Drug Discov Technol* 2004; 1: 229-42.
- [117] Tomski SJ, Murphy RM. Kinetics of aggregation of synthetic  $\beta$ -amyloid peptide. *Arch Biochem Biophys* 1992; 294: 630-8.
- [118] Shen CL, Scott GL, Merchant F, Murphy RM. Light scattering analysis of fibril growth from the amino-terminal fragment  $\beta$ (1–28) of  $\beta$ -amyloid peptide. *Biophys J* 1993; 65: 2383-95.
- [119] Lomakin A, Chung DS, Benedek GB, Kirschner DA, Teplow DB. On the nucleation and growth of amyloid  $\beta$ -protein fibrils: detection of nuclei and quantitation of rate constants. *Proc Natl Acad Sci USA* 1996; 93: 1125-9.
- [120] Murphy RM, Pallitto MM. Probing the kinetics of  $\beta$ -amyloid self-association. *J Struct Biol* 2000; 130: 109-22.
- [121] Ward RV, Jennings KH, Jepras R, *et al.* Fractionation and characterization of oligomeric, protofibrillar and fibrillar forms of  $\beta$ -amyloid peptide. *Biochem J* 2000; 348 Pt 1: 137-44.
- [122] Lomakin A, Teplow DB. Quasielastic light scattering study of amyloid  $\beta$ -protein fibril formation. *Protein Pept Lett* 2006; 13: 247-54.
- [123] Lomakin A, Teplow DB, Benedek GB. Quasielastic light scattering for protein assembly studies. *Methods Mol Biol* 2005; 299: 153-74.
- [124] Kanu AB, Dwivedi P, Tam M, Matz L, Hill HH, Jr. Ion mobility-mass spectrometry. *J Mass Spectrom* 2008; 43: 1-22.

- [125] Tang K, Li F, Shvartsburg AA, Strittmatter EF, Smith RD. Two-dimensional gas-phase separations coupled to mass spectrometry for analysis of complex mixtures. *Anal Chem* 2005; 77: 6381-8.
- [126] Bernstein SL, Wyttenbach T, Baumketner A, *et al.* Amyloid  $\beta$ -protein: monomer structure and early aggregation states of A $\beta$ 42 and its Pro<sup>19</sup> alloform. *J Am Chem Soc* 2005; 127: 2075-84.
- [127] Shvartsburg AA, Li F, Tang K, Smith RD. Characterizing the structures and folding of free proteins using 2-D gas-phase separations: observation of multiple unfolded conformers. *Anal Chem* 2006; 78: 3304-15.
- [128] Greenfield NJ. Using circular dichroism spectra to estimate protein secondary structure. *Nat Protoc* 2006; 1: 2876-90.
- [129] Whitmore L, Wallace BA. Protein secondary structure analyses from circular dichroism spectroscopy: methods and reference databases. *Biopolymers* 2008; 89: 392-400.
- [130] Kirkitadze MD, Condrón MM, Teplow DB. Identification and characterization of key kinetic intermediates in amyloid  $\beta$ -protein fibrillogenesis. *J Mol Biol* 2001; 312: 1103-19.
- [131] Gursky O, Aleshkov S. Temperature-dependent  $\beta$ -sheet formation in  $\beta$ -amyloid A $\beta$ <sub>1-40</sub> peptide in water: uncoupling  $\beta$ -structure folding from aggregation. *Biochim Biophys Acta* 2000; 1476: 93-102.
- [132] Lim KH, Collver HH, Le YT, Nagchowdhuri P, Kenney JM. Characterizations of distinct amyloidogenic conformations of the A $\beta$ (1-40) and (1-42) peptides. *Biochem Biophys Res Commun* 2007; 353: 443-9.
- [133] Hou L, Kang I, Marchant RE, Zagorski MG. Methionine 35 oxidation reduces fibril assembly of the amyloid A $\beta$ (1-42) peptide of Alzheimer's disease. *J Biol Chem* 2002; 277: 40173-6.
- [134] Ahting U, Thieffry M, Engelhardt H, *et al.* Tom40, the pore-forming component of the protein-conducting TOM channel in the outer membrane of mitochondria. *J Cell Biol* 2001; 153: 1151-60.
- [135] Hetényi C, Szabó Z, Klement E, *et al.* Pentapeptide amides interfere with the aggregation of  $\beta$ -amyloid peptide of Alzheimer's disease. *Biochem Biophys Res Commun* 2002; 292: 931-6.
- [136] Lin SY, Chu HL. Fourier transform infrared spectroscopy used to evidence the prevention of  $\beta$ -sheet formation of amyloid  $\beta$ (1-40) peptide by a short amyloid fragment. *Int J Biol Macromol* 2003; 32: 173-7.
- [137] Kakio A, Yano Y, Takai D, *et al.* Interaction between amyloid  $\beta$ -protein aggregates and membranes. *J Pept Sci* 2004; 10: 612-21.
- [138] Brzyska M, Trzesniewska K, Gers T, Elbaum D. Discrete conformational changes as regulators of the hydrolytic properties of beta-amyloid (1-40). *FEBS J* 2006; 273: 5598-611.
- [139] Mastrangelo IA, Ahmed M, Sato T, *et al.* High-resolution atomic force microscopy of soluble A $\beta$ 42 oligomers. *J Mol Biol* 2006; 358: 106-19.
- [140] Kim YS, Liu L, Axelsen PH, Hochstrasser RM. 2D IR provides evidence for mobile water molecules in  $\beta$ -amyloid fibrils. *Proc Natl Acad Sci USA* 2009; 106: 17751-6.
- [141] Woys AM, Almeida AM, Wang L, *et al.* Parallel  $\beta$ -sheet vibrational couplings revealed by 2D IR spectroscopy of an isotopically labeled macrocycle: quantitative benchmark for the interpretation of amyloid and protein infrared spectra. *J Am Chem Soc* 2012; 134: 19118-28.

- [142] Middleton CT, Marek P, Cao P, *et al.* Two-dimensional infrared spectroscopy reveals the complex behaviour of an amyloid fibril inhibitor. *Nat Chem* 2012; 4: 355-60.
- [143] De Carlo S, Harris JR. Negative staining and cryo-negative staining of macromolecules and viruses for TEM. *Micron* 2011; 42: 117-31.
- [144] Harris JR. Negative staining of thinly spread biological particulates. *Methods Mol Biol* 1999; 117: 13-30.
- [145] Sherratt MJ, Meadows RS, Graham HK, Kielty CM, Holmes DF. ECM macromolecules: rotary shadowing and transmission electron microscopy. *Methods Mol Biol* 2009; 522: 175-81.
- [146] Jonic S, Vénien-Bryan C. Protein structure determination by electron cryo-microscopy. *Curr Opin Pharmacol* 2009; 9: 636-42.
- [147] Nybo M, Svehag SE, Holm Nielsen E. An ultrastructural study of amyloid intermediates in A $\beta$ <sub>1-42</sub> fibrillogenesis. *Scand J Immunol* 1999; 49: 219-23.
- [148] Modler AJ, Gast K, Lutsch G, Damaschun G. Assembly of amyloid protofibrils *via* critical oligomers—a novel pathway of amyloid formation. *J Mol Biol* 2003; 325: 135-48.
- [149] Roher AE, Chaney MO, Kuo YM, *et al.* Morphology and toxicity of A $\beta$ -(1-42) dimer derived from neuritic and vascular amyloid deposits of Alzheimer's disease. *J Biol Chem* 1996; 271: 20631-5.
- [150] Selenica ML, Wang X, Ostergaard-Pedersen L, Westlind-Danielsson A, Grubb A. Cystatin C reduces the *in vitro* formation of soluble A $\beta$ <sub>1-42</sub> oligomers and protofibrils. *Scand J Clin Lab Invest* 2007; 67: 179-90.
- [151] Wood SJ, Maleeff B, Hart T, Wetzel R. Physical, morphological and functional differences between pH 5.8 and 7.4 aggregates of the Alzheimer's amyloid peptide A $\beta$ . *J Mol Biol* 1996; 256: 870-7.
- [152] Lührs T, Ritter C, Adrian M, *et al.* 3D structure of Alzheimer's amyloid- $\beta$ (1-42) fibrils. *Proc Natl Acad Sci USA* 2005; 102: 17342-7.
- [153] Engel A, Colliex C. Application of scanning transmission electron microscopy to the study of biological structure. *Curr Opin Biotechnol* 1993; 4: 403-11.
- [154] Lashuel HA, Wall JS. Molecular electron microscopy approaches to elucidating the mechanisms of protein fibrillogenesis. *Methods Mol Biol* 2005; 299: 81-101.
- [155] Goldsbury C, Frey P, Olivieri V, Aebi U, Müller SA. Multiple assembly pathways underlie amyloid- $\beta$  fibril polymorphisms. *J Mol Biol* 2005; 352: 282-98.
- [156] Goldsbury CS, Wirtz S, Müller SA, *et al.* Studies on the *in vitro* assembly of A $\beta$ <sub>1-40</sub>: implications for the search for A $\beta$  fibril formation inhibitors. *J Struct Biol* 2000; 130: 217-31.
- [157] Petkova AT, Leapman RD, Guo Z, *et al.* Self-propagating, molecular-level polymorphism in Alzheimer's  $\beta$ -amyloid fibrils. *Science* 2005; 307: 262-5.
- [158] Wall JS, Simon MN, Lin BY, Vinogradov SN. Mass mapping of large globin complexes by scanning transmission electron microscopy. *Methods Enzymol* 2008; 436: 487-501.
- [159] Blackley HK, Sanders GH, Davies MC, *et al.* *In-situ* atomic force microscopy study of  $\beta$ -amyloid fibrillization. *J Mol Biol* 2000; 298: 833-40.
- [160] Kowalewski T, Holtzman DM. *In situ* atomic force microscopy study of Alzheimer's  $\beta$ -amyloid peptide on different substrates: new insights into mechanism of  $\beta$ -sheet formation. *Proc Natl Acad Sci USA* 1999; 96: 3688-93.

- [161] Harper JD, Wong SS, Lieber CM, Lansbury PT, Jr. Assembly of A $\beta$  amyloid protofibrils: an *in vitro* model for a possible early event in Alzheimer's disease. *Biochemistry* 1999; 38: 8972-80.
- [162] Arimon M, Díez-Pérez I, Kogan MJ, *et al.* Fine structure study of A $\beta$ 1-42 fibrillogenesis with atomic force microscopy. *FASEB J* 2005; 19: 1344-6.
- [163] Wang Z, Zhou C, Wang C, *et al.* AFM and STM study of  $\beta$ -amyloid aggregation on graphite. *Ultramicroscopy* 2003; 97: 73-9.
- [164] Solomonov I, Korkotian E, Born B, *et al.* Zn<sup>2+</sup>-A $\beta$ 40 complexes form metastable quasi-spherical oligomers that are cytotoxic to cultured hippocampal neurons. *J Biol Chem* 2012.
- [165] Hansma PK, Elings VB, Marti O, Bracker CE. Scanning tunneling microscopy and atomic force microscopy: application to biology and technology. *Science* 1988; 242: 209-16.
- [166] Shivji AP, Brown F, Davies MC, *et al.* Scanning tunnelling microscopy studies of  $\beta$ -amyloid fibril structure and assembly. *FEBS Lett* 1995; 371: 25-8.
- [167] Losic D, Martin LL, Mechler A, Aguilar MI, Small DH. High resolution scanning tunnelling microscopy of the  $\beta$ -amyloid protein (A $\beta$ 1-40) of Alzheimer's disease suggests a novel mechanism of oligomer assembly. *J Struct Biol* 2006; 155: 104-10.
- [168] Stratman NC, Castle CK, Taylor BM, *et al.* Isoform-specific interactions of human apolipoprotein E to an intermediate conformation of human Alzheimer amyloid-beta peptide. *Chem Phys Lipids* 2005; 137: 52-61.
- [169] Sun XD, Mo ZL, Taylor BM, Epps DE. A slowly formed transient conformer of A $\beta$ <sup>1-40</sup> is toxic to inward channels of dissociated hippocampal and cortical neurons of rats. *Neurobiol Dis* 2003; 14: 567-78.
- [170] Xia W, Zhang J, Kholodenko D, *et al.* Enhanced production and oligomerization of the 42-residue amyloid  $\beta$ -protein by Chinese hamster ovary cells stably expressing mutant presenilins. *J Biol Chem* 1997; 272: 7977-82.
- [171] Li S, Hong S, Shepardson NE, *et al.* Soluble oligomers of amyloid  $\beta$  protein facilitate hippocampal long-term depression by disrupting neuronal glutamate uptake. *Neuron* 2009; 62: 788-801.
- [172] Cleary JP, Walsh DM, Hofmeister JJ, *et al.* Natural oligomers of the amyloid- $\beta$  protein specifically disrupt cognitive function. *Nat Neurosci* 2005; 8: 79-84.
- [173] Shankar GM, Bloodgood BL, Townsend M, *et al.* Natural oligomers of the Alzheimer amyloid- $\beta$  protein induce reversible synapse loss by modulating an NMDA-type glutamate receptor-dependent signaling pathway. *J Neurosci* 2007; 27: 2866-75.
- [174] O'Nuallain B, Freir DB, Nicoll AJ, *et al.* Amyloid  $\beta$ -protein dimers rapidly form stable synaptotoxic protofibrils. *J Neurosci* 2010; 30: 14411-9.
- [175] Oda T, Wals P, Osterburg HH, *et al.* Clusterin (apoJ) alters the aggregation of amyloid  $\beta$ -peptide (A $\beta$ <sub>1-42</sub>) and forms slowly sedimenting A $\beta$  complexes that cause oxidative stress. *Exp Neurol* 1995; 136: 22-31.
- [176] Klein WL. A $\beta$  toxicity in Alzheimer's disease: globular oligomers (ADDLs) as new vaccine and drug targets. *Neurochem Int* 2002; 41: 345-52.
- [177] De Felice FG, Wu D, Lambert MP, *et al.* Alzheimer's disease-type neuronal tau hyperphosphorylation induced by A $\beta$  oligomers. *Neurobiol Aging* 2007.
- [178] Chromy BA, Nowak RJ, Lambert MP, *et al.* Self-assembly of A $\beta$ (1-42) into globular neurotoxins. *Biochemistry* 2003; 42: 12749-60.
- [179] Lambert MP, Velasco PT, Chang L, *et al.* Monoclonal antibodies that target pathological assemblies of A $\beta$ . *J Neurochem* 2007; 100: 23-35.
- [180] Lacor PN, Buniel MC, Furlow PW, *et al.* A $\beta$  oligomer-induced aberrations in synapse composition, shape, and density provide a molecular basis for loss of connectivity in Alzheimer's disease. *J Neurosci* 2007; 27: 796-807.

- [181] Lacor PN, Buniel MC, Chang L, *et al.* Synaptic targeting by Alzheimer's-related amyloid  $\beta$  oligomers. *J Neurosci* 2004; 24: 10191-200.
- [182] De Felice FG, Velasco PT, Lambert MP, *et al.* A $\beta$  oligomers induce neuronal oxidative stress through an *N*-methyl-D-aspartate receptor-dependent mechanism that is blocked by the Alzheimer drug memantine. *J Biol Chem* 2007; 282: 11590-601.
- [183] Zempel H, Thies E, Mandelkow E, Mandelkow EM. A $\beta$  oligomers cause localized Ca<sup>2+</sup> elevation, missorting of endogenous Tau into dendrites, Tau phosphorylation, and destruction of microtubules and spines. *J Neurosci* 2010; 30: 11938-50.
- [184] White JA, Manelli AM, Holmberg KH, Van Eldik LJ, Ladu MJ. Differential effects of oligomeric and fibrillar amyloid- $\beta$  1-42 on astrocyte-mediated inflammation. *Neurobiol Dis* 2005; 18: 459-65.
- [185] Wang X, Perry G, Smith MA, Zhu X. Amyloid- $\beta$ -derived diffusible ligands cause impaired axonal transport of mitochondria in neurons. *Neurodegener Dis* 2010; 7: 56-9.
- [186] Ye C, Walsh DM, Selkoe DJ, Hartley DM. Amyloid  $\beta$ -protein induced electrophysiological changes are dependent on aggregation state: *N*-methyl-D-aspartate (NMDA) *versus* non-NMDA receptor/channel activation. *Neurosci Lett* 2004; 366: 320-5.
- [187] Ye CP, Selkoe DJ, Hartley DM. Protofibrils of amyloid  $\beta$ -protein inhibit specific K<sup>+</sup> currents in neocortical cultures. *Neurobiol Dis* 2003; 13: 177-90.
- [188] Nilsberth C, Westlind-Danielsson A, Eckman CB, *et al.* The 'Arctic' APP mutation (E693G) causes Alzheimer's disease by enhanced A $\beta$  protofibril formation. *Nat Neurosci* 2001; 4: 887-93.
- [189] Kaye R, Canto I, Breydo L, *et al.* Conformation dependent monoclonal antibodies distinguish different replicating strains or conformers of prefibrillar A $\beta$  oligomers. *Mol Neurodegener* 2010; 5: 57.
- [190] Stroud JC, Liu C, Teng PK, Eisenberg D. Toxic fibrillar oligomers of amyloid- $\beta$  have cross- $\beta$  structure. *Proc Natl Acad Sci USA* 2012; 109: 7717-22.
- [191] Wu JW, Breydo L, Isas JM, *et al.* Fibrillar oligomers nucleate the oligomerization of monomeric amyloid  $\beta$  but do not seed fibril formation. *J Biol Chem* 2010; 285: 6071-9.
- [192] Sandberg A, Luheshi LM, Söllvander S, *et al.* Stabilization of neurotoxic Alzheimer amyloid- $\beta$  oligomers by protein engineering. *Proc Natl Acad Sci USA* 2010; 107: 15595-600.
- [193] Shankar GM, Li S, Mehta TH, *et al.* Amyloid- $\beta$  protein dimers isolated directly from Alzheimer's brains impair synaptic plasticity and memory. *Nat Med* 2008; 14: 837-42.
- [194] Jin M, Shepardson N, Yang T, *et al.* Soluble amyloid  $\beta$ -protein dimers isolated from Alzheimer cortex directly induce Tau hyperphosphorylation and neuritic degeneration. *Proc Natl Acad Sci USA* 2011; 108: 5819-24.
- [195] Hu NW, Smith IM, Walsh DM, Rowan MJ. Soluble amyloid- $\beta$  peptides potently disrupt hippocampal synaptic plasticity in the absence of cerebrovascular dysfunction *in vivo*. *Brain* 2008; 131: 2414-24.
- [196] Lasagna-Reeves CA, Glabe CG, Kaye R. Amyloid- $\beta$  annular protofibrils evade fibrillar fate in Alzheimer disease brain. *J Biol Chem* 2011; 286: 22122-30.
- [197] Kaye R, Pensalfini A, Margol L, *et al.* Annular protofibrils are a structurally and functionally distinct type of amyloid oligomer. *J Biol Chem* 2009; 284: 4230-7.
- [198] Noguchi A, Matsumura S, Dezawa M, *et al.* Isolation and characterization of patient-derived, toxic, high mass amyloid  $\beta$ -protein (A $\beta$ ) assembly from Alzheimer disease brains. *J Biol Chem* 2009; 284: 32895-905.

- [199] Matsumura S, Shinoda K, Yamada M, *et al.* Two distinct amyloid  $\beta$ -protein (A $\beta$ ) assembly pathways leading to oligomers and fibrils identified by combined fluorescence correlation spectroscopy, morphology, and toxicity analyses. *J Biol Chem* 2011; 286: 11555-62.
- [200] Cooper JA, Buhle EL, Jr., Walker SB, Tsong TY, Pollard TD. Kinetic evidence for a monomer activation step in actin polymerization. *Biochemistry* 1983; 22: 2193-202.
- [201] Shen CL, Murphy RM. Solvent effects on self-assembly of  $\beta$ -amyloid peptide. *Biophys J* 1995; 69: 640-51.
- [202] Lee S, Fernandez EJ, Good TA. Role of aggregation conditions in structure, stability, and toxicity of intermediates in the A $\beta$  fibril formation pathway. *Protein Sci* 2007; 16: 723-32.
- [203] Chimon S, Ishii Y. Capturing intermediate structures of Alzheimer's  $\beta$ -amyloid, A $\beta$ (1-40), by solid-state NMR spectroscopy. *J Am Chem Soc* 2005; 127: 13472-3.
- [204] Koudinov AR, Berezov TT, Koudinova NV. The levels of soluble amyloid  $\beta$  in different high density lipoprotein subfractions distinguish Alzheimer's and normal aging cerebrospinal fluid: implication for brain cholesterol pathology? *Neurosci Lett* 2001; 314: 115-8.
- [205] Koudinov AR, Koudinova NV, Kumar A, Beavis RC, Ghiso J. Biochemical characterization of Alzheimer's soluble amyloid Beta protein in human cerebrospinal fluid: association with high density lipoproteins. *Biochem Biophys Res Commun* 1996; 223: 592-7.
- [206] Kawarabayashi T, Shoji M, Younkin LH, *et al.* Dimeric amyloid  $\beta$  protein rapidly accumulates in lipid rafts followed by apolipoprotein E and phosphorylated tau accumulation in the Tg2576 mouse model of Alzheimer's disease. *J Neurosci* 2004; 24: 3801-9.
- [207] Morishima-Kawashima M, Ihara Y. The presence of amyloid  $\beta$ -protein in the detergent-insoluble membrane compartment of human neuroblastoma cells. *Biochemistry* 1998; 37: 15247-53.
- [208] Townsend M, Shankar GM, Mehta T, Walsh DM, Selkoe DJ. Effects of secreted oligomers of amyloid  $\beta$ -protein on hippocampal synaptic plasticity: a potent role for trimers. *J Physiol* 2006; 572: 477-92.
- [209] Walsh DM, Klyubin I, Fadeeva JV, Rowan MJ, Selkoe DJ. Amyloid- $\beta$  oligomers: their production, toxicity and therapeutic inhibition. *Biochem Soc Trans* 2002; 30: 552-7.
- [210] Walsh DM, Townsend M, Podlisny MB, *et al.* Certain inhibitors of synthetic amyloid  $\beta$ -peptide (A $\beta$ ) fibrillogenesis block oligomerization of natural A $\beta$  and thereby rescue long-term potentiation. *J Neurosci* 2005; 25: 2455-62.
- [211] Walsh DM, Selkoe DJ. A $\beta$  Oligomers – a decade of discovery. *J Neurochem* 2007.
- [212] Dudai Y. Molecular bases of long-term memories: a question of persistence. *Curr Opin Neurobiol* 2002; 12: 211-6.
- [213] Kojima N, Shirao T. Synaptic dysfunction and disruption of postsynaptic drebrin-actin complex: a study of neurological disorders accompanied by cognitive deficits. *Neurosci Res* 2007; 58: 1-5.
- [214] Calabrese B, Shaked GM, Tabarean IV, *et al.* Rapid, concurrent alterations in pre- and postsynaptic structure induced by naturally-secreted amyloid- $\beta$  protein. *Mol Cell Neurosci* 2007; 35: 183-93.
- [215] Shrestha BR, Vitolo OV, Joshi P, *et al.* Amyloid  $\beta$  peptide adversely affects spine number and motility in hippocampal neurons. *Mol Cell Neurosci* 2006; 33: 274-82.

- [216] McLaurin J, Golomb R, Jurewicz A, Antel JP, Fraser PE. Inositol stereoisomers stabilize an oligomeric aggregate of Alzheimer amyloid  $\beta$  peptide and inhibit A $\beta$ -induced toxicity. *J Biol Chem* 2000; 275: 18495-502.
- [217] Townsend M, Cleary JP, Mehta T, *et al.* Orally available compound prevents deficits in memory caused by the Alzheimer amyloid- $\beta$  oligomers. *Ann Neurol* 2006; 60: 668-76.
- [218] Snyder EM, Nong Y, Almeida CG, *et al.* Regulation of NMDA receptor trafficking by amyloid- $\beta$ . *Nat Neurosci* 2005; 8: 1051-8.
- [219] Calero M, Rostagno A, Matsubara E, *et al.* Apolipoprotein J (clusterin) and Alzheimer's disease. *Microsc Res Tech* 2000; 50: 305-15.
- [220] Stine WB, Jr., Dahlgren KN, Krafft GA, LaDu MJ. *In vitro* characterization of conditions for amyloid- $\beta$  peptide oligomerization and fibrillogenesis. *J Biol Chem* 2003; 278: 11612-22.
- [221] Whitlock JR, Heynen AJ, Shuler MG, Bear MF. Learning induces long-term potentiation in the hippocampus. *Science* 2006; 313: 1093-7.
- [222] Martin SJ, Grimwood PD, Morris RG. Synaptic plasticity and memory: an evaluation of the hypothesis. *Annu Rev Neurosci* 2000; 23: 649-711.
- [223] Wang HW, Pasternak JF, Kuo H, *et al.* Soluble oligomers of  $\beta$  amyloid (1-42) inhibit long-term potentiation but not long-term depression in rat dentate gyrus. *Brain Res* 2002; 924: 133-40.
- [224] Fong DK, Rao A, Crump FT, Craig AM. Rapid synaptic remodeling by protein kinase C: reciprocal translocation of NMDA receptors and calcium/calmodulin-dependent kinase II. *J Neurosci* 2002; 22: 2153-64.
- [225] Chang L, Bakhos L, Wang Z, Venton DL, Klein WL. Femtomole immunodetection of synthetic and endogenous amyloid- $\beta$  oligomers and its application to Alzheimer's disease drug candidate screening. *J Mol Neurosci* 2003; 20: 305-13.
- [226] Tong L, Balazs R, Thornton PL, Cotman CW.  $\beta$ -Amyloid peptide at sublethal concentrations downregulates brain-derived neurotrophic factor functions in cultured cortical neurons. *J Neurosci* 2004; 24: 6799-809.
- [227] Harris KM, Kater SB. Dendritic spines: cellular specializations imparting both stability and flexibility to synaptic function. *Annu Rev Neurosci* 1994; 17: 341-71.
- [228] Carlisle HJ, Kennedy MB. Spine architecture and synaptic plasticity. *Trends Neurosci* 2005; 28: 182-7.
- [229] Fiala JC, Spacek J, Harris KM. Dendritic spine pathology: cause or consequence of neurological disorders? *Brain Res Brain Res Rev* 2002; 39: 29-54.
- [230] Tzingounis AV, Nicoll RA. Arc/Arg3.1: linking gene expression to synaptic plasticity and memory. *Neuron* 2006; 52: 403-7.
- [231] Guzowski JF, Lyford GL, Stevenson GD, *et al.* Inhibition of activity-dependent arc protein expression in the rat hippocampus impairs the maintenance of long-term potentiation and the consolidation of long-term memory. *J Neurosci* 2000; 20: 3993-4001.
- [232] Oddo S, Caccamo A, Tran L, *et al.* Temporal profile of amyloid- $\beta$  (A $\beta$ ) oligomerization in an *in vivo* model of Alzheimer disease. A link between A $\beta$  and tau pathology. *J Biol Chem* 2006; 281: 1599-604.
- [233] Lambert MP, Viola KL, Chromy BA, *et al.* Vaccination with soluble A $\beta$  oligomers generates toxicity-neutralizing antibodies. *J Neurochem* 2001; 79: 595-605.
- [234] Seilheimer B, Bohrmann B, Bondolfi L, *et al.* The toxicity of the Alzheimer's  $\beta$ -amyloid peptide correlates with a distinct fiber morphology. *J Struct Biol* 1997; 119: 59-71.
- [235] Williams AD, Segal M, Chen M, *et al.* Structural properties of A $\beta$  protofibrils stabilized by a small molecule. *Proc Natl Acad Sci USA* 2005; 102: 7115-20.
- [236] Mosmann T. Rapid colorimetric assay for cellular growth and survival: application to proliferation and cytotoxicity assays. *J Immunol Methods* 1983; 65: 55-63.

- [237] Korzeniewski C, Callewaert DM. An enzyme-release assay for natural cytotoxicity. *J Immunol Methods* 1983; 64: 313-20.
- [238] Haass C, Steiner H. Protofibrils, the unifying toxic molecule of neurodegenerative disorders? *Nat Neurosci* 2001; 4: 859-60.
- [239] Sayre LM, Zelasko DA, Harris PL, *et al.* 4-Hydroxynonenal-derived advanced lipid peroxidation end products are increased in Alzheimer's disease. *J Neurochem* 1997; 68: 2092-7.
- [240] Siegel SJ, Bieschke J, Powers ET, Kelly JW. The oxidative stress metabolite 4-hydroxynonenal promotes Alzheimer protofibril formation. *Biochemistry* 2007; 46: 1503-10.
- [241] Johansson AS, Garlind A, Berglind-Dehlin F, *et al.* Docosahexaenoic acid stabilizes soluble amyloid- $\beta$  protofibrils and sustains amyloid- $\beta$ -induced neurotoxicity *in vitro*. *FEBS J* 2007; 274: 990-1000.
- [242] Eriksen JL, Janus CG. Plaques, tangles, and memory loss in mouse models of neurodegeneration. *Behav Genet* 2007; 37: 79-100.
- [243] Codita A, Winblad B, Mohammed AH. Of mice and men: more neurobiology in dementia. *Curr Opin Psychiatry* 2006; 19: 555-63.
- [244] Cole GM, Frautschy SA. Alzheimer's amyloid story finds its star. *Trends Mol Med* 2006; 12: 395-6.
- [245] Jacobsen JS, Wu CC, Redwine JM, *et al.* Early-onset behavioral and synaptic deficits in a mouse model of Alzheimer's disease. *Proc Natl Acad Sci USA* 2006; 103: 5161-6.
- [246] Billings LM, Green KN, McGaugh JL, LaFerla FM. Learning decreases A $\beta$ \*56 and tau pathology and ameliorates behavioral decline in 3 $\times$ Tg-AD mice. *J Neurosci* 2007; 27: 751-61.
- [247] Lin H, Bhatia R, Lal R. Amyloid  $\beta$  protein forms ion channels: implications for Alzheimer's disease pathophysiology. *FASEB J* 2001; 15: 2433-44.
- [248] Quist A, Doudevski I, Lin H, *et al.* Amyloid ion channels: a common structural link for protein-misfolding disease. *Proc Natl Acad Sci USA* 2005; 102: 10427-32.
- [249] Arispe N, Pollard HB, Rojas E. Giant multilevel cation channels formed by Alzheimer disease amyloid  $\beta$ -protein [A $\beta$ P-(1-40)] in bilayer membranes. *Proc Natl Acad Sci USA* 1993; 90: 10573-7.
- [250] Arispe N, Rojas E, Pollard HB. Alzheimer disease amyloid  $\beta$  protein forms calcium channels in bilayer membranes: blockade by tromethamine and aluminum. *Proc Natl Acad Sci USA* 1993; 90: 567-71.
- [251] Kawahara M, Arispe N, Kuroda Y, Rojas E. Alzheimer's disease amyloid  $\beta$ -protein forms Zn<sup>2+</sup>-sensitive, cation-selective channels across excised membrane patches from hypothalamic neurons. *Biophys J* 1997; 73: 67-75.
- [252] Kawahara M, Kuroda Y. Molecular mechanism of neurodegeneration induced by Alzheimer's  $\beta$ -amyloid protein: channel formation and disruption of calcium homeostasis. *Brain Res Bull* 2000; 53: 389-97.
- [253] Sanderson KL, Butler L, Ingram VM. Aggregates of a  $\beta$ -amyloid peptide are required to induce calcium currents in neuron-like human teratocarcinoma cells: relation to Alzheimer's disease. *Brain Res* 1997; 744: 7-14.
- [254] Rhee SK, Quist AP, Lal R. Amyloid  $\beta$  protein-(1-42) forms calcium-permeable, Zn<sup>2+</sup>-sensitive channel. *J Biol Chem* 1998; 273: 13379-82.

- [255] Hirakura Y, Lin MC, Kagan BL. Alzheimer amyloid A $\beta$ 1–42 channels: effects of solvent, pH, and Congo Red. *J Neurosci Res* 1999; 57: 458-66.
- [256] Lin H, Zhu YJ, Lal R. Amyloid  $\beta$  protein (1–40) forms calcium-permeable, Zn<sup>2+</sup>-sensitive channel in reconstituted lipid vesicles. *Biochemistry* 1999; 38: 11189-96.
- [257] Bhatia R, Lin H, Lal R. Fresh and globular amyloid  $\beta$  protein (1–42) induces rapid cellular degeneration: evidence for A $\beta$ P channel-mediated cellular toxicity. *FASEB J* 2000; 14: 1233-43.
- [258] Kourie JI, Henry CL, Farrelly P. Diversity of amyloid  $\beta$  protein fragment [1–40]-formed channels. *Cell Mol Neurobiol* 2001; 21: 255-84.
- [259] Kagan BL, Hirakura Y, Azimov R, Azimova R, Lin MC. The channel hypothesis of Alzheimer's disease: current status. *Peptides* 2002; 23: 1311-5.
- [260] Lin MC, Kagan BL. Electrophysiologic properties of channels induced by A $\beta$ 25–35 in planar lipid bilayers. *Peptides* 2002; 23: 1215-28.
- [261] Bahadi R, Farrelly PV, Kenna BL, *et al.* Cu<sup>2+</sup>-induced modification of the kinetics of A $\beta$ (1–42) channels. *Am J Physiol Cell Physiol* 2003; 285: C873-80.
- [262] Alarcón JM, Brito JA, Hermosilla T, *et al.* Ion channel formation by Alzheimer's disease amyloid  $\beta$ -peptide (A $\beta$ 40) in unilamellar liposomes is determined by anionic phospholipids. *Peptides* 2006; 27: 95-104.
- [263] Sokolov Y, Kozak JA, Kayed R, *et al.* Soluble amyloid oligomers increase bilayer conductance by altering dielectric structure. *J Gen Physiol* 2006; 128: 637-47.
- [264] Demuro A, Mina E, Kayed R, *et al.* Calcium dysregulation and membrane disruption as a ubiquitous neurotoxic mechanism of soluble amyloid oligomers. *J Biol Chem* 2005; 280: 17294-300.
- [265] Kayed R, Sokolov Y, Edmonds B, *et al.* Permeabilization of lipid bilayers is a common conformation-dependent activity of soluble amyloid oligomers in protein misfolding diseases. *J Biol Chem* 2004; 279: 46363-6.
- [266] Lashuel HA, Petre BM, Wall J, *et al.*  $\alpha$ -Synuclein, especially the Parkinson's disease-associated mutants, forms pore-like annular and tubular protofibrils. *J Mol Biol* 2002; 322: 1089-102.
- [267] Kawahara M, Kuroda Y. Intracellular calcium changes in neuronal cells induced by Alzheimer's  $\beta$ -amyloid protein are blocked by estradiol and cholesterol. *Cell Mol Neurobiol* 2001; 21: 1-13.
- [268] Dahlgren KN, Manelli AM, Stine WB, Jr., *et al.* Oligomeric and fibrillar species of amyloid- $\beta$  peptides differentially affect neuronal viability. *J Biol Chem* 2002; 277: 32046-53.
- [269] Scheuner D, Eckman C, Jensen M, *et al.* Secreted amyloid  $\beta$ -protein similar to that in the senile plaques of Alzheimer's disease is increased *in vivo* by the presenilin 1 and 2 and APP mutations linked to familial Alzheimer's disease. *Nat Med* 1996; 2: 864-70.
- [270] Anderson DH, Talaga KC, Rivest AJ, *et al.* Characterization of  $\beta$  amyloid assemblies in drusen: the deposits associated with aging and age-related macular degeneration. *Exp Eye Res* 2004; 78: 243-56.
- [271] Moore RA, Hayes SF, Fischer ER, Priola SA. Amyloid formation *via* supramolecular peptide assemblies. *Biochemistry* 2007; 46: 7079-87.
- [272] Zhu YJ, Lin H, Lal R. Fresh and nonfibrillar amyloid  $\beta$  protein(1–40) induces rapid cellular degeneration in aged human fibroblasts: evidence for A $\beta$ P-channel-mediated cellular toxicity. *FASEB J* 2000; 14: 1244-54.

- [273] Buxbaum J. The amyloidoses. *Mt Sinai J Med* 1996; 63: 16-23.
- [274] Buxbaum JN. The systemic amyloidoses. *Curr Opin Rheumatol* 2004; 16: 67-75.
- [275] Gambetti P, Russo C. Human brain amyloidoses. *Nephrol Dial Transplant* 1998; 13 Suppl 7: 33-40.
- [276] Bellotti V, Nuvolone M, Giorgetti S, *et al.* The workings of the amyloid diseases. *Ann Med* 2007; 39: 200-7.
- [277] Glabe CG. Common mechanisms of amyloid oligomer pathogenesis in degenerative disease. *Neurobiol Aging* 2006; 27: 570-5.
- [278] Layfield R, Cavey JR, Lowe J. Role of ubiquitin-mediated proteolysis in the pathogenesis of neurodegenerative disorders. *Ageing Res Rev* 2003; 2: 343-56.
- [279] Betarbet R, Sherer TB, Greenamyre JT. Ubiquitin-proteasome system and Parkinson's diseases. *Exp Neurol* 2005; 191 Suppl 1: S17-27.
- [280] Murray IVJ, Lee VMY, Trojanowski JQ. Synucleinopathies: A pathological and molecular review. *Clin Neurosci Res* 2001; 1: 445-55.
- [281] Tompa P. Intrinsically unstructured proteins. *Trends Biochem Sci* 2002; 27: 527-33.
- [282] Dyson HJ, Wright PE. Intrinsically unstructured proteins and their functions. *Nat Rev Mol Cell Biol* 2005; 6: 197-208.
- [283] Conway KA, Lee SJ, Rochet JC, *et al.* Acceleration of oligomerization, not fibrillization, is a shared property of both  $\alpha$ -synuclein mutations linked to early-onset Parkinson's disease: implications for pathogenesis and therapy. *Proc Natl Acad Sci USA* 2000; 97: 571-6.
- [284] Ding TT, Lee SJ, Rochet JC, Lansbury PT, Jr. Annular  $\alpha$ -synuclein protofibrils are produced when spherical protofibrils are incubated in solution or bound to brain-derived membranes. *Biochemistry* 2002; 41: 10209-17.
- [285] Volles MJ, Lee SJ, Rochet JC, *et al.* Vesicle permeabilization by protofibrillar  $\alpha$ -synuclein: implications for the pathogenesis and treatment of Parkinson's disease. *Biochemistry* 2001; 40: 7812-9.
- [286] Volles MJ, Lansbury PT, Jr. Vesicle permeabilization by protofibrillar  $\alpha$ -synuclein is sensitive to Parkinson's disease-linked mutations and occurs by a pore-like mechanism. *Biochemistry* 2002; 41: 4595-602.
- [287] Fredenburg RA, Rospigliosi C, Meray RK, *et al.* The impact of the E46K mutation on the properties of  $\alpha$ -synuclein in its monomeric and oligomeric states. *Biochemistry* 2007; 46: 7107-18.
- [288] Takeda A, Hasegawa T, Matsuzaki-Kobayashi M, *et al.* Mechanisms of neuronal death in synucleinopathy. *J Biomed Biotechnol* 2006; 2006: 19365.
- [289] Murali J, Jayakumar R. Spectroscopic studies on native and protofibrillar insulin. *J Struct Biol* 2005; 150: 180-9.
- [290] Dzwolak W, Lokszejn A, Galinska-Rakoczy A, *et al.* Conformational indeterminism in protein misfolding: chiral amplification on amyloidogenic pathway of insulin. *J Am Chem Soc* 2007; 129: 7517-22.
- [291] Dzwolak W, Lokszejn A, Smirnovas V. New insights into the self-assembly of insulin amyloid fibrils: an H-D exchange FT-IR study. *Biochemistry* 2006; 45: 8143-51.
- [292] Grudzielanek S, Smirnovas V, Winter R. The effects of various membrane physical-chemical properties on the aggregation kinetics of insulin. *Chem Phys Lipids* 2007; 149: 28-39.
- [293] Ahmad A, Uversky VN, Hong D, Fink AL. Early events in the fibrillation of monomeric insulin. *J Biol Chem* 2005; 280: 42669-75.

- [294] Nettleton EJ, Tito P, Sunde M, *et al.* Characterization of the oligomeric states of insulin in self-assembly and amyloid fibril formation by mass spectrometry. *Biophys J* 2000; 79: 1053-65.
- [295] Grudzielanek S, Velkova A, Shukla A, *et al.* Cytotoxicity of insulin within its self-assembly and amyloidogenic pathways. *J Mol Biol* 2007; 370: 372-84.
- [296] Anguiano M, Nowak RJ, Lansbury PT, Jr. Protofibrillar islet amyloid polypeptide permeabilizes synthetic vesicles by a pore-like mechanism that may be relevant to type II diabetes. *Biochemistry* 2002; 41: 11338-43.
- [297] Porat Y, Kolusheva S, Jelinek R, Gazit E. The human islet amyloid polypeptide forms transient membrane-active prefibrillar assemblies. *Biochemistry* 2003; 42: 10971-7.
- [298] Jayasinghe SA, Langen R. Lipid membranes modulate the structure of islet amyloid polypeptide. *Biochemistry* 2005; 44: 12113-9.
- [299] Knight JD, Hebda JA, Miranker AD. Conserved and cooperative assembly of membrane-bound  $\alpha$ -helical states of islet amyloid polypeptide. *Biochemistry* 2006; 45: 9496-508.
- [300] Meier JJ, Kaye R, Lin CY, *et al.* Inhibition of human IAPP fibril formation does not prevent  $\beta$ -cell death: evidence for distinct actions of oligomers and fibrils of human IAPP. *Am J Physiol Endocrinol Metab* 2006; 291: E1317-24.
- [301] Lin CY, Gurlo T, Kaye R, *et al.* Toxic human islet amyloid polypeptide (h-IAPP) oligomers are intracellular, and vaccination to induce anti-toxic oligomer antibodies does not prevent h-IAPP-induced  $\beta$ -cell apoptosis in h-IAPP transgenic mice. *Diabetes* 2007; 56: 1324-32.
- [302] Serpell LC. Alzheimer's amyloid fibrils: structure and assembly. *Biochim Biophys Acta* 2000; 1502: 16-30.
- [303] Eisenberg D, Nelson R, Sawaya MR, *et al.* The structural biology of protein aggregation diseases: Fundamental questions and some answers. *Acc Chem Res* 2006; 39: 568-75.
- [304] Kaye R, Head E, Thompson JL, *et al.* Common structure of soluble amyloid oligomers implies common mechanism of pathogenesis. *Science* 2003; 300: 486-9.
- [305] Kelly JW. The alternative conformations of amyloidogenic proteins and their multi-step assembly pathways. *Curr Opin Struct Biol* 1998; 8: 101-6.
- [306] Chiti F, Dobson CM. Protein misfolding, functional amyloid, and human disease. *Annu Rev Biochem* 2006; 75: 333-66.
- [307] Stefani M, Dobson CM. Protein aggregation and aggregate toxicity: new insights into protein folding, misfolding diseases and biological evolution. *J Mol Med* 2003; 81: 678-99.
- [308] Fezoui Y, Hartley DM, Walsh DM, *et al.* A *de novo* designed helix-turn-helix peptide forms nontoxic amyloid fibrils. *Nat Struct Biol* 2000; 7: 1095-9.
- [309] Wang C, Huang L, Wang L, Hong Y, Sha Y. One-dimensional self-assembly of a rational designed  $\beta$ -structure peptide. *Biopolymers* 2007; 86: 23-31.
- [310] Kammerer RA, Steinmetz MO. *De novo* design of a two-stranded coiled-coil switch peptide. *J Struct Biol* 2006; 155: 146-53.
- [311] Guijarro JI, Sunde M, Jones JA, Campbell ID, Dobson CM. Amyloid fibril formation by an SH3 domain. *Proc Natl Acad Sci USA* 1998; 95: 4224-8.
- [312] Litvinovich SV, Brew SA, Aota S, *et al.* Formation of amyloid-like fibrils by self-association of a partially unfolded fibronectin type III module. *J Mol Biol* 1998; 280: 245-58.
- [313] Jiménez JL, Guijarro JI, Orlova E, *et al.* Cryo-electron microscopy structure of an SH3 amyloid fibril and model of the molecular packing. *EMBO J* 1999; 18: 815-21.

- [314] Zurdo J, Guijarro JI, Dobson CM. Preparation and characterization of purified amyloid fibrils. *J Am Chem Soc* 2001; 123: 8141-2.
- [315] Zurdo J, Guijarro JI, Jiménez JL, Saibil HR, Dobson CM. Dependence on solution conditions of aggregation and amyloid formation by an SH3 domain. *J Mol Biol* 2001; 311: 325-40.
- [316] Carulla N, Caddy GL, Hall DR, *et al.* Molecular recycling within amyloid fibrils. *Nature* 2005; 436: 554-8.
- [317] Chiti F, Bucciantini M, Capanni C, *et al.* Solution conditions can promote formation of either amyloid protofilaments or mature fibrils from the HypF N-terminal domain. *Protein Sci* 2001; 10: 2541-7.
- [318] Polverino de Laureto P, Taddei N, Frare E, *et al.* Protein aggregation and amyloid fibril formation by an SH3 domain probed by limited proteolysis. *J Mol Biol* 2003; 334: 129-41.
- [319] Chiti F, Webster P, Taddei N, *et al.* Designing conditions for *in vitro* formation of amyloid protofilaments and fibrils. *Proc Natl Acad Sci USA* 1999; 96: 3590-4.
- [320] Tjernberg L, Hosia W, Bark N, Thyberg J, Johansson J. Charge attraction and  $\beta$  propensity are necessary for amyloid fibril formation from tetrapeptides. *J Biol Chem* 2002; 277: 43243-6.
- [321] López De La Paz M, Goldie K, Zurdo J, *et al.* *De novo* designed peptide-based amyloid fibrils. *Proc Natl Acad Sci USA* 2002; 99: 16052-7.
- [322] Relini A, Torrassa S, Rolandi R, *et al.* Monitoring the process of HypF fibrillization and liposome permeabilization by protofibrils. *J Mol Biol* 2004; 338: 943-57.
- [323] Parbhu A, Lin H, Thimm J, Lal R. Imaging real-time aggregation of amyloid beta protein (1-42) by atomic force microscopy. *Peptides* 2002; 23: 1265-70.
- [324] Poirier MA, Li H, Macosko J, *et al.* Huntingtin spheroids and protofibrils as precursors in polyglutamine fibrilization. *J Biol Chem* 2002; 277: 41032-7.
- [325] Conway KA, Harper JD, Lansbury PT, Jr. Fibrils formed *in vitro* from  $\alpha$ -synuclein and two mutant forms linked to Parkinson's disease are typical amyloid. *Biochemistry* 2000; 39: 2552-63.
- [326] Calamai M, Taddei N, Stefani M, Ramponi G, Chiti F. Relative influence of hydrophobicity and net charge in the aggregation of two homologous proteins. *Biochemistry* 2003; 42: 15078-83.
- [327] Bucciantini M, Giannoni E, Chiti F, *et al.* Inherent toxicity of aggregates implies a common mechanism for protein misfolding diseases. *Nature* 2002; 416: 507-11.
- [328] Bucciantini M, Calloni G, Chiti F, *et al.* Prefibrillar amyloid protein aggregates share common features of cytotoxicity. *J Biol Chem* 2004; 279: 31374-82.
- [329] Bucciantini M, Rigacci S, Berti A, *et al.* Patterns of cell death triggered in two different cell lines by HypF-N prefibrillar aggregates. *FASEB J* 2005; 19: 437-9.
- [330] Cecchi C, Pensalfini A, Baglioni S, *et al.* Differing molecular mechanisms appear to underlie early toxicity of prefibrillar HypF-N aggregates to different cell types. *FEBS J* 2006; 273: 2206-22.
- [331] Tartaglia GG, Pechmann S, Dobson CM, Vendruscolo M. Life on the edge: a link between gene expression levels and aggregation rates of human proteins. *Trends Biochem Sci* 2007; 32: 204-6.
- [332] Calabrese MF, Eakin CM, Wang JM, Miranker AD. A regulatable switch mediates self-association in an immunoglobulin fold. *Nat Struct Mol Biol* 2008; 15: 965-71.
- [333] Liu C, Sawaya MR, Cheng PN, *et al.* Characteristics of amyloid-related oligomers revealed by crystal structures of macrocyclic  $\beta$ -sheet mimics. *J Am Chem Soc* 2011; 133: 6736-44.

- [334] Streltsov VA, Varghese JN, Masters CL, Nuttall SD. Crystal structure of the amyloid- $\beta$  p3 fragment provides a model for oligomer formation in Alzheimer's disease. *J Neurosci* 2011; 31: 1419-26.
- [335] Domanska K, Vanderhaegen S, Srinivasan V, *et al.* Atomic structure of a nanobody-trapped domain-swapped dimer of an amyloidogenic  $\beta$ 2-microglobulin variant. *Proc Natl Acad Sci USA* 2011; 108: 1314-9.
- [336] Laganowsky A, Liu C, Sawaya MR, *et al.* Atomic view of a toxic amyloid small oligomer. *Science* 2012; 335: 1228-31.
- [337] Ecroyd H, Carver JA. Crystallin proteins and amyloid fibrils. *Cell Mol Life Sci* 2009; 66: 62-81.
- [338] Thompson MJ, Sievers SA, Karanicolas J, *et al.* The 3D profile method for identifying fibril-forming segments of proteins. *Proc Natl Acad Sci USA* 2006; 103: 4074-8.
- [339] Goldschmidt L, Teng PK, Riek R, Eisenberg D. Identifying the amyloids, proteins capable of forming amyloid-like fibrils. *Proc Natl Acad Sci USA* 2010; 107: 3487-92.
- [340] Greenwald J, Riek R. Biology of amyloid: structure, function, and regulation. *Structure* 2010; 18: 1244-60.
- [341] Benzinger TL, Gregory DM, Burkoth TS, *et al.* Propagating structure of Alzheimer's  $\beta$ -amyloid<sub>(10-35)</sub> is parallel  $\beta$ -sheet with residues in exact register. *Proc Natl Acad Sci USA* 1998; 95: 13407-12.
- [342] Tycko R. Solid-state NMR studies of amyloid fibril structure. *Annu Rev Phys Chem* 2011; 62: 279-99.
- [343] Cheng PN, Liu C, Zhao M, Eisenberg D, Nowick JS. Amyloid  $\beta$ -sheet mimics that antagonize protein aggregation and reduce amyloid toxicity. *Nat Chem* 2012; 4: 927-33.
- [344] Liu C, Zhao M, Jiang L, *et al.* Out-of-register  $\beta$ -sheets suggest a pathway to toxic amyloid aggregates. *Proc Natl Acad Sci USA* 2012.
- [345] Griffith JS. Self-replication and scrapie. *Nature* 1967; 215: 1043-4.
- [346] Prusiner SB. Novel proteinaceous infectious particles cause scrapie. *Science* 1982; 216: 136-44.
- [347] Prusiner SB, Bolton DC, Groth DF, *et al.* Further purification and characterization of scrapie prions. *Biochemistry* 1982; 21: 6942-50.
- [348] Prusiner SB. Prions. *Proc Natl Acad Sci USA* 1998; 95: 13363-83.
- [349] Legname G, Baskakov IV, Nguyen HO, *et al.* Synthetic mammalian prions. *Science* 2004; 305: 673-6.
- [350] Castilla J, Saá P, Hetz C, Soto C. *In vitro* generation of infectious scrapie prions. *Cell* 2005; 121: 195-206.
- [351] Deleault NR, Harris BT, Rees JR, Supattapone S. Formation of native prions from minimal components *in vitro*. *Proc Natl Acad Sci USA* 2007; 104: 9741-6.
- [352] Wang F, Wang X, Yuan CG, Ma J. Generating a prion with bacterially expressed recombinant prion protein. *Science* 2010; 327: 1132-5.
- [353] Lansbury PT, Jr., Caughey B. The chemistry of scrapie infection: implications of the 'ice 9' metaphor. *Chem Biol* 1995; 2: 1-5.
- [354] Saborio GP, Permanne B, Soto C. Sensitive detection of pathological prion protein by cyclic amplification of protein misfolding. *Nature* 2001; 411: 810-3.
- [355] Soto C. Transmissible proteins: expanding the prion heresy. *Cell* 2012; 149: 968-77.
- [356] Goedert M, Clavaguera F, Tolnay M. The propagation of prion-like protein inclusions in neurodegenerative diseases. *Trends Neurosci* 2010; 33: 317-25.

- [357] Westermark GT, Westermark P. Prion-like aggregates: infectious agents in human disease. *Trends Mol Med* 2010; 16: 501-7.
- [358] Angot E, Steiner JA, Hansen C, Li JY, Brundin P. Are synucleinopathies prion-like disorders? *Lancet Neurol* 2010; 9: 1128-38.
- [359] Prusiner SB. Cell biology. A unifying role for prions in neurodegenerative diseases. *Science* 2012; 336: 1511-3.
- [360] Kanouchi T, Ohkubo T, Yokota T. Can regional spreading of amyotrophic lateral sclerosis motor symptoms be explained by prion-like propagation? *J Neurol Neurosurg Psychiatry* 2012; 83: 739-45.
- [361] Münch C, Bertolotti A. Self-propagation and transmission of misfolded mutant SOD1: prion or prion-like phenomenon? *Cell Cycle* 2011; 10: 1711.
- [362] Münch C, O'Brien J, Bertolotti A. Prion-like propagation of mutant superoxide dismutase-1 misfolding in neuronal cells. *Proc Natl Acad Sci USA* 2011; 108: 3548-53.
- [363] Lee SJ, Desplats P, Sigurdson C, Tsigelny I, Masliah E. Cell-to-cell transmission of non-prion protein aggregates. *Nat Rev Neurol* 2010; 6: 702-6.
- [364] Lee SJ, Lim HS, Masliah E, Lee HJ. Protein aggregate spreading in neurodegenerative diseases: problems and perspectives. *Neurosci Res* 2011; 70: 339-48.
- [365] Guest WC, Silverman JM, Pokrishevsky E, *et al.* Generalization of the prion hypothesis to other neurodegenerative diseases: an imperfect fit. *J Toxicol Environ Health Part A* 2011; 74: 1433-59.
- [366] Luk KC, Kehm VM, Zhang B, *et al.* Intracerebral inoculation of pathological  $\alpha$ -synuclein initiates a rapidly progressive neurodegenerative  $\alpha$ -synucleinopathy in mice. *J Exp Med* 2012; 209: 975-86.
- [367] Luk KC, Kehm V, Carroll J, *et al.* Pathological  $\alpha$ -synuclein transmission initiates parkinson-like neurodegeneration in nontransgenic mice. *Science* 2012; 338: 949-53.
- [368] Kane MD, Lipinski WJ, Callahan MJ, *et al.* Evidence for seeding of  $\beta$ -amyloid by intracerebral infusion of Alzheimer brain extracts in  $\beta$ -amyloid precursor protein-transgenic mice. *J Neurosci* 2000; 20: 3606-11.
- [369] Meyer-Luehmann M, Coomaraswamy J, Bolmont T, *et al.* Exogenous induction of cerebral  $\beta$ -amyloidogenesis is governed by agent and host. *Science* 2006; 313: 1781-4.
- [370] Watts JC, Giles K, Grillo SK, *et al.* Bioluminescence imaging of A $\beta$  deposition in bigenic mouse models of Alzheimer's disease. *Proc Natl Acad Sci USA* 2011; 108: 2528-33.
- [371] Eisele YS, Obermüller U, Heilbronner G, *et al.* Peripherally applied A $\beta$ -containing inoculates induce cerebral  $\beta$ -amyloidosis. *Science* 2010; 330: 980-2.
- [372] Eisele YS, Bolmont T, Heikenwalder M, *et al.* Induction of cerebral  $\beta$ -amyloidosis: intracerebral *versus* systemic A $\beta$  inoculation. *Proc Natl Acad Sci USA* 2009; 106: 12926-31.
- [373] Langer F, Eisele YS, Fritsch SK, *et al.* Soluble A $\beta$  seeds are potent inducers of cerebral  $\beta$ -amyloid deposition. *J Neurosci* 2011; 31: 14488-95.
- [374] Rosen RF, Fritz JJ, Dooyema J, *et al.* Exogenous seeding of cerebral  $\beta$ -amyloid deposition in  $\beta$ APP-transgenic rats. *J Neurochem* 2012; 120: 660-6.
- [375] Morales R, Duran-Aniotz C, Castilla J, Estrada LD, Soto C. *De novo* induction of amyloid- $\beta$  deposition *in vivo*. *Mol Psychiatry* 2012; 17: 1347-53.
- [376] Aguzzi A, Calella AM. Prions: protein aggregation and infectious diseases. *Physiol Rev* 2009; 89: 1105-52.

- [377] Makarava N, Lee CI, Ostapchenko VG, Baskakov IV. Highly promiscuous nature of prion polymerization. *J Biol Chem* 2007; 282: 36704-13.
- [378] Zhang B, Une Y, Fu X, *et al.* Fecal transmission of AA amyloidosis in the cheetah contributes to high incidence of disease. *Proc Natl Acad Sci USA* 2008; 105: 7263-8.
- [379] Caughey B, Baron GS. Are cheetahs on the run from prion-like amyloidosis? *Proc Natl Acad Sci USA* 2008; 105: 7113-4.
- [380] Lundmark K, Westermark GT, Nyström S, *et al.* Transmissibility of systemic amyloidosis by a prion-like mechanism. *Proc Natl Acad Sci USA* 2002; 99: 6979-84.
- [381] Solomon A, Richey T, Murphy CL, *et al.* Amyloidogenic potential of foie gras. *Proc Natl Acad Sci USA* 2007; 104: 10998-1001.
- [382] Larsson A, Malmström S, Westermark P. Signs of cross-seeding: aortic medin amyloid as a trigger for protein AA deposition. *Amyloid* 2011; 18: 229-34.
- [383] Yan J, Fu X, Ge F, *et al.* Cross-seeding and cross-competition in mouse apolipoprotein A-II amyloid fibrils and protein A amyloid fibrils. *Am J Pathol* 2007; 171: 172-80.
- [384] Paravastu AK, Qahwash I, Leapman RD, Meredith SC, Tycko R. Seeded growth of  $\beta$ -amyloid fibrils from Alzheimer's brain-derived fibrils produces a distinct fibril structure. *Proc Natl Acad Sci USA* 2009; 106: 7443-8.
- [385] Qiang W, Yau WM, Tycko R. Structural evolution of Iowa mutant  $\beta$ -amyloid fibrils from polymorphic to homogeneous states under repeated seeded growth. *J Am Chem Soc* 2011; 133: 4018-29.
- [386] Nath S, Agholme L, Kurudenkandy FR, *et al.* Spreading of neurodegenerative pathology *via* neuron-to-neuron transmission of  $\beta$ -amyloid. *J Neurosci* 2012; 32: 8767-77.
- [387] Braak H, Braak E. Neuropathological staging of Alzheimer-related changes. *Acta Neuropathol* 1991; 82: 239-59.
- [388] Harris JA, Devidze N, Verret L, *et al.* Transsynaptic progression of amyloid- $\beta$ -induced neuronal dysfunction within the entorhinal-hippocampal network. *Neuron* 2010; 68: 428-41.
- [389] Braak H, Braak E, Yilmazer D, *et al.* Pattern of brain destruction in Parkinson's and Alzheimer's diseases. *J Neural Transm* 1996; 103: 455-90.
- [390] Kai H, Shin RW, Ogino K, *et al.* Enhanced antigen retrieval of amyloid  $\beta$  immunohistochemistry: re-evaluation of amyloid  $\beta$  pathology in Alzheimer disease and its mouse model. *J Histochem Cytochem* 2012; 60: 761-9.
- [391] Ono K, Takahashi R, Ikeda T, Yamada M. Cross-seeding effects of amyloid  $\beta$ -protein and  $\alpha$ -synuclein. *J Neurochem* 2012; 122: 883-90.
- [392] Lasagna-Reeves CA, Castillo-Carranza DL, Guerrero-Muoz MJ, Jackson GR, Kaye R. Preparation and characterization of neurotoxic tau oligomers. *Biochemistry* 2010; 49: 10039-41.
- [393] Frost B, Jacks RL, Diamond MI. Propagation of tau misfolding from the outside to the inside of a cell. *J Biol Chem* 2009; 284: 12845-52.
- [394] Clavaguera F, Bolmont T, Crowther RA, *et al.* Transmission and spreading of tauopathy in transgenic mouse brain. *Nat Cell Biol* 2009; 11: 909-13.
- [395] Nonaka T, Watanabe ST, Iwatsubo T, Hasegawa M. Seeded aggregation and toxicity of  $\alpha$ -synuclein and tau: cellular models of neurodegenerative diseases. *J Biol Chem* 2010; 285: 34885-98.
- [396] Guo JL, Lee VM. Seeding of normal Tau by pathological Tau conformers drives pathogenesis of Alzheimer-like tangles. *J Biol Chem* 2011; 286: 15317-31.

- [397] de Calignon A, Polydoro M, Suárez-Calvet M, *et al.* Propagation of tau pathology in a model of early Alzheimer's disease. *Neuron* 2012; 73: 685-97.
- [398] Liu L, Drouet V, Wu JW, *et al.* Trans-synaptic spread of tau pathology *in vivo*. *PLoS One* 2012; 7: e31302.
- [399] Braak H, Braak E. Staging of Alzheimer's disease-related neurofibrillary changes. *Neurobiol Aging* 1995; 16: 271-8; discussion 78-84.
- [400] Guo JP, Arai T, Miklossy J, McGeer PL. A $\beta$  and tau form soluble complexes that may promote self aggregation of both into the insoluble forms observed in Alzheimer's disease. *Proc Natl Acad Sci USA* 2006; 103: 1953-8.
- [401] Hart PJ. Pathogenic superoxide dismutase structure, folding, aggregation and turnover. *Curr Opin Chem Biol* 2006; 10: 131-8.
- [402] Lang L, Kurnik M, Danielsson J, Oliveberg M. Fibrillation precursor of superoxide dismutase 1 revealed by gradual tuning of the protein-folding equilibrium. *Proc Natl Acad Sci USA* 2012; 109: 17868-73.
- [403] Kato S, Takikawa M, Nakashima K, *et al.* New consensus research on neuropathological aspects of familial amyotrophic lateral sclerosis with superoxide dismutase 1 (SOD1) gene mutations: inclusions containing SOD1 in neurons and astrocytes. *Amyotroph Lateral Scler Other Motor Neuron Disord* 2000; 1: 163-84.
- [404] Bruijn LI, Becher MW, Lee MK, *et al.* ALS-linked SOD1 mutant G85R mediates damage to astrocytes and promotes rapidly progressive disease with SOD1-containing inclusions. *Neuron* 1997; 18: 327-38.
- [405] Durham HD, Roy J, Dong L, Figlewicz DA. Aggregation of mutant Cu/Zn superoxide dismutase proteins in a culture model of ALS. *J Neuropathol Exp Neurol* 1997; 56: 523-30.
- [406] Grad LI, Guest WC, Yanai A, *et al.* Intermolecular transmission of superoxide dismutase 1 misfolding in living cells. *Proc Natl Acad Sci USA* 2011; 108: 16398-403.
- [407] Chia R, Tattum MH, Jones S, *et al.* Superoxide dismutase 1 and tgSOD1 mouse spinal cord seed fibrils, suggesting a propagative cell death mechanism in amyotrophic lateral sclerosis. *PLoS One* 2010; 5: e10627.
- [408] Ravits J, Paul P, Jorg C. Focality of upper and lower motor neuron degeneration at the clinical onset of ALS. *Neurology* 2007; 68: 1571-5.
- [409] Ravits JM, La Spada AR. ALS motor phenotype heterogeneity, focality, and spread: deconstructing motor neuron degeneration. *Neurology* 2009; 73: 805-11.
- [410] Botelho HM, Leal SS, Cardoso I, *et al.* S100A6 amyloid fibril formation is calcium-modulated and enhances superoxide dismutase-1 (SOD1) aggregation. *J Biol Chem* 2012.
- [411] Kim HJ, Chatani E, Goto Y, Paik SR. Seed-dependent accelerated fibrillation of  $\alpha$ -synuclein induced by periodic ultrasonication treatment. *J Microbiol Biotechnol* 2007; 17: 2027-32.
- [412] Danzer KM, Krebs SK, Wolff M, Birk G, Hengerer B. Seeding induced by  $\alpha$ -synuclein oligomers provides evidence for spreading of  $\alpha$ -synuclein pathology. *J Neurochem* 2009; 111: 192-203.
- [413] Hansen C, Angot E, Bergström AL, *et al.*  $\alpha$ -Synuclein propagates from mouse brain to grafted dopaminergic neurons and seeds aggregation in cultured human cells. *J Clin Invest* 2011; 121: 715-25.
- [414] Allan LE, Petit GH, Brundin P. Cell transplantation in Parkinson's disease: problems and perspectives. *Curr Opin Neurol* 2010; 23: 426-32.
- [415] Li JY, Englund E, Holton JL, *et al.* Lewy bodies in grafted neurons in subjects with Parkinson's disease suggest host-to-graft disease propagation. *Nat Med* 2008; 14: 501-3.

- [416] Desplats P, Lee HJ, Bae EJ, *et al.* Inclusion formation and neuronal cell death through neuron-to-neuron transmission of  $\alpha$ -synuclein. *Proc Natl Acad Sci USA* 2009; 106: 13010-5.
- [417] Angot E, Steiner JA, Lema Tomé CM, *et al.* Alpha-synuclein cell-to-cell transfer and seeding in grafted dopaminergic neurons *in vivo*. *PLoS One* 2012; 7: e39465.
- [418] Bae EJ, Ho DH, Park E, *et al.* Lipid peroxidation product 4-hydroxy-2-nonenal promotes seeding-capable oligomer formation and cell-to-cell transfer of  $\alpha$ -synuclein *Antioxid Redox Signal* 2012; [Epub ahead of print].
- [419] Braak H, Del Tredici K, Bratzke H, *et al.* Staging of the intracerebral inclusion body pathology associated with idiopathic Parkinson's disease (preclinical and clinical stages). *J Neurol* 2002; 249 Suppl 3: III/1-5.
- [420] Braak H, Del Tredici K, Rüb U, *et al.* Staging of brain pathology related to sporadic Parkinson's disease. *Neurobiol Aging* 2003; 24: 197-211.
- [421] Braak H, Ghebremedhin E, Rüb U, Bratzke H, Del Tredici K. Stages in the development of Parkinson's disease-related pathology. *Cell Tissue Res* 2004; 318: 121-34.
- [422] Brundin P, Li JY, Holton JL, Lindvall O, Revesz T. Research in motion: the enigma of Parkinson's disease pathology spread. *Nat Rev Neurosci* 2008; 9: 741-5.
- [423] Riess O, Krüger R, Schulz JB. Spectrum of phenotypes and genotypes in Parkinson's disease. *J Neurol* 2002; 249 Suppl 3: III/15-20.
- [424] Surgucheva I, Sharov VS, Surguchov A.  $\gamma$ -Synuclein: seeding of  $\alpha$ -synuclein aggregation and transmission between cells. *Biochemistry* 2012; 51: 4743-54.
- [425] Bhattacharyya AM, Thakur AK, Wetzel R. Polyglutamine aggregation nucleation: thermodynamics of a highly unfavorable protein folding reaction. *Proc Natl Acad Sci USA* 2005; 102: 15400-5.
- [426] Scherzinger E, Lurz R, Turmaine M, *et al.* Huntingtin-encoded polyglutamine expansions form amyloid-like protein aggregates *in vitro* and *in vivo*. *Cell* 1997; 90: 549-58.
- [427] Gupta S, Jie S, Colby DW. Protein misfolding detected early in pathogenesis of transgenic mouse model of Huntington disease using amyloid seeding assay. *J Biol Chem* 2012; 287: 9982-9.
- [428] Ren PH, Lauckner JE, Kachirskaia I, *et al.* Cytoplasmic penetration and persistent infection of mammalian cells by polyglutamine aggregates. *Nat Cell Biol* 2009; 11: 219-25.
- [429] Rosas HD, Salat DH, Lee SY, *et al.* Cerebral cortex and the clinical expression of Huntington's disease: complexity and heterogeneity. *Brain* 2008; 131: 1057-68.
- [430] Furukawa Y, Kaneko K, Matsumoto G, Kurosawa M, Nukina N. Cross-seeding fibrillation of Q/N-rich proteins offers new pathomechanism of polyglutamine diseases. *J Neurosci* 2009; 29: 5153-62.
- [431] Vonsattel JP, DiFiglia M. Huntington disease. *J Neuropathol Exp Neurol* 1998; 57: 369-84.
- [432] Deng YP, Albin RL, Penney JB, *et al.* Differential loss of striatal projection systems in Huntington's disease: a quantitative immunohistochemical study. *J Chem Neuroanat* 2004; 27: 143-64.
- [433] Bellingham SA, Guo BB, Coleman BM, Hill AF. Exosomes: vehicles for the transfer of toxic proteins associated with neurodegenerative diseases? *Front Physiol* 2012; 3: 124.
- [434] Marzo L, Gousset K, Zurzolo C. Multifaceted roles of tunneling nanotubes in intercellular communication. *Front Physiol* 2012; 3: 72.
- [435] Morales R, Green KM, Soto C. Cross currents in protein misfolding disorders: interactions and therapy. *CNS Neurol Disord Drug Targets* 2009; 8: 363-71.